

Universidad Autónoma de Madrid
Facultad de Ciencias
Departamento de Biología Molecular



Universidad Autónoma
de Madrid

Differential effects of neural stem cell therapy
in adult and middle-aged Parkinsonian mice

Doctoral Thesis

Anna Nelke

Madrid, 2019

Universidad Autónoma de Madrid
Facultad de Ciencias
Departamento de Biología Molecular



Differential effects of neural stem cell therapy
in adult and middle-aged Parkinsonian mice

Anna Nelke

Bachelor of Science in Neuroscience, Master in Molecular & Cellular Biology

Thesis Supervisors:

Marta Pérez Pereira

Alberto Martínez Serrano

Centro de Biología Molecular Severo Ochoa,
Centro mixto de la Universidad Autónoma de Madrid y del Consejo Superior de
Investigaciones Científicas (CBMSO – UAM/CSIC)

To my two favorite people, my parents

ACKNOWLEDGEMENTS

I would like to thank my thesis director, Alberto, for the opportunity to join the lab and his continued support throughout the years, and give a special thank you to my principal thesis supervisor, Marta, for her support, guidance, patience, and advice, and sharing her expertise with me. Appreciation is also due to Silvia and Bea for teaching and helping me.

I would like to express my gratitude to the UAM and CBMSO, and all of the people (and wild boars) I have crossed paths with in these two institutes. I am especially thankful to the Genomics, Confocal Microscopy, Instrumentation, Biological Safety, Cell Culture & Sterilization, Maintenance, and Bioinformatics, services at the CBMSO. A special thank you to each and every one of the IT staff for helping me solve my seemingly never-ending technology problems, and to the Animal Facility personnel, particularly Elena, Fernando, Fernando, Julia, Bea, Maca, Virginia, and José, for their help throughout my thesis. I would also like to thank Ilu and Joaquín for their contagious smiles and great conversations.

I am grateful to the following sources of funding: Campus de Excelencia UAM+CSIC fellowship, Cell Therapy Network (TerCel), and the Government of Spain.

I would like to thank Santiago Ramón y Cajal for his immeasurable contribution to neuroscience and whose pioneer work has allowed me and others to study and explore the amazing world of the brain. In addition, I am grateful to the many mice used in my thesis.

On a personal level, I would like to thank my parents, my brother, Alex, and my friends, for their constant love, patience, and support.

ABSTRACT

Parkinson's disease (PD), the second most common neurodegenerative disease in the world, is characterized by the death or impairment of dopaminergic neurons (DAn) in the substantia nigra pars compacta (SNpc) and the depletion of dopamine in the striatum (Str). Symptoms of the disease include tremors, rigidity, bradykinesia, and postural instability. Currently, there is no cure for PD, and treatments only help to reduce the symptoms of the disease, and do not repair or replace the DAn damaged or lost in PD. Cell replacement therapy (CRT) seeks to relieve both pathological and symptomatic PD manifestations, and has been shown to have beneficial effects in experimental PD models as well as in PD patients, but an apt cell line to be used in PD treatment has yet to be established. In addition, CRT clinical trials are more successful in younger PD patients with less advanced pathology. The main goal of this thesis was to study the effects of the transplantation of human neural stem cells (hNSCs), specifically hVM1 clone 32 cells, in an *in vivo* PD mouse model using 1-methyl-4-phenyl-1,2,3,6-tetrahydropyridine (MPTP) at four months post-transplant. The hypothesis was that the transplanted hNSCs could replace and take over the functions of the impaired or lost DAn by integrating in the host environment, thus rescuing nigrostriatal innervation, improving motor deficits, and exerting neurotrophic effects, in adult and middle-aged Parkinsonian mice.

Transplantation of hVM1 clone 32 cells rescued dopaminergic nigrostriatal populations in adult Parkinsonian mice, plausibly via the neurotrophic factors released by the cells, indicating that conditioned media (CM) rather than cells could be sufficient in providing beneficial effects. There were no clear behavioral changes between groups except for reduced stride length and hyperactivity in all MPTP-treated mice, both of which tended to be improved by hVM1 clone 32 cell transplant in middle-aged mice, while hyperactivity had a tendency of decreasing in adult hNSC-transplanted mice. In adult mice, hNSC transplantation rescued neuroblast neurogenesis in the subgranular zone, which was correlated with dopaminergic recovery in the Str and SNpc. Neuroinflammation did not impede nigrostriatal system restoration in adult mice. In both age groups, grafting of hVM1 clone 32 cells led to mast cell migration to the superficial cervical lymph nodes. Therefore, this thesis is a proof-of-concept study that CRT can work using hVM1 clone 32 cells in adult Parkinsonian mice and that these hNSCs exert a trophic effect, but CRT is less effective in middle-aged mice due to the increased neuroinflammation and decreased neurogenesis that occur in aged animals. This study emphasizes the importance of the age of recipient and the stage of PD progression when receiving a transplant, and proposes that a multifactorial treatment is needed for CRT or CM infusion in older PD patients.

RESUMEN

La enfermedad de Parkinson (EP), la segunda enfermedad neurodegenerativa más común en el mundo, se caracteriza por la muerte o el daño de neuronas dopaminérgicas (nDA) en la sustancia negra parte compacta (SNpc) y la disminución de dopamina en el estriado (Str). Los síntomas de la EP son temblores, rigidez, bradicinesia, e inestabilidad postural. Actualmente, no hay cura para la EP, y los tratamientos solo ayudan a reducir los síntomas de la enfermedad sin recuperar ni reemplazar las nDA dañadas o perdidas en la EP. La terapia de reemplazo celular (TRC) pretende aliviar las manifestaciones patológicas y sintomáticas de la EP, quedando demostrados sus efectos beneficiosos tanto en modelos experimentales como en pacientes de la EP, pero aún no ha sido establecida una línea celular adecuada como futuro tratamiento de la EP. Además, los ensayos clínicos de TRC tienen más éxito en pacientes más jóvenes con una patología menos avanzada. El objetivo principal de esta tesis fue estudiar los efectos, cuatro meses después del trasplante, de las células madre neurales humanas (hNSCs), específicamente las células hVM1 clon 32, en un modelo *in vivo* de la EP de ratón usando 1-methyl-4-phenyl-1,2,3,6-tetrahydropyridine (MPTP). La hipótesis fue que las hNSCs trasplantadas podrían reemplazar y adquirir las funciones de las nDA dañadas o muertas, integrándose en el ambiente del receptor y así rescatando la inervación nigroestriatal, mejorando los déficits de comportamiento, y ejerciendo efectos neurotróficos, en la EP en ratones adultos y de mediana edad. El trasplante de las células hVM1 clon 32 rescató las poblaciones dopaminérgicas nigroestriadas en la EP en ratones adultos, probablemente a través de factores neurotróficos liberados por las células, indicando que el medio acondicionado (CM) en vez de las células podría ser suficiente para producir efectos beneficiosos. No había cambios determinantes en comportamiento entre grupos salvo reducción de la zancada e hiperactividad en todos los ratones tratados con MPTP; ambos tendieron a mejorar tras el trasplante de células hVM1 clon 32 en ratones de mediana edad, mientras la hiperactividad tendió a disminuir en ratones adultos trasplantados con hNSCs. En ratones adultos, el trasplante de hNSCs rescató la población neurogénica de neuroblastos en la zona subgranular, correlacionándose con la recuperación dopaminérgica en el Str y la SNpc. La neuroinflamación no impidió la restauración del sistema nigroestriado en los ratones adultos, pero en los dos grupos de edad, el trasplante de células hVM1 clon 32 se relacionó con la migración de mastocitos a los nodos linfáticos cervicales superficiales. Por tanto, esta tesis es un estudio de prueba-de-concepto que la TRC funciona usando las células hVM1 clon 32 en la EP en ratones adultos y que estas células ejercen efectos tróficos en los ratones adultos, pero TRC es menos efectivo en ratones de mediana edad debido a la neuroinflamación aumentada y la neurogénesis disminuida que suceden en animales viejos. Este estudio enfatiza la importancia de la edad del receptor y la etapa de progresión de la EP a la recepción de un trasplante, y propone que un tratamiento multifactorial es necesario para la TRC o infusión de CM en pacientes de la EP más viejos.

TABLE OF CONTENTS

TABLE OF CONTENTS

ABSTRACT	1
RESUMEN	5
ABBREVIATIONS	13
INTRODUCTION	21
<i>What is Parkinson’s disease (PD)?</i>	23
<i>Dopaminergic neuron criteria</i>	24
<i>Neurotrophic factors</i>	25
<i>Current PD treatments</i>	28
<i>Failed and potential PD treatments</i>	29
<i>Cell replacement therapy</i>	32
<i>Human ventral mesencephalic cells</i>	34
<i>Experimental PD models</i>	35
<i>Neuroinflammation</i>	37
<i>Lymph nodes</i>	40
<i>Neurogenesis</i>	40
<i>Young vs. aged in PD</i>	42
OBJECTIVES	43
MATERIALS & METHODS	47
<i>Ethics statement</i>	49
<i>Cell culture</i>	49
<i>Immunocytochemistry</i>	49
<i>Next-generation sequencing</i>	51
<i>Luminex assay</i>	51
<i>Animal experimentation</i>	51
<i>Behavioral tests</i>	53
<i>Immunohistochemistry</i>	54
<i>Western blot</i>	56
<i>Toluidine histology</i>	56
<i>Microscopy</i>	57
<i>Histological quantifications</i>	57
<i>Statistical analysis</i>	57

RESULTS.....	59
<u><i>In vitro</i> characterization of hVM1 clone 32 cell line.....</u>	61
<u>Survival, differentiation, and maturation, of engrafted hVM1 clone 32 cells</u>	68
<u>Transplantation of hVM1 clone 32 cells in adult mice.....</u>	69
<i>The effect of hVM1 clone 32 cell transplantation on nigrostriatal pathway degeneration</i>	69
<i>The effect of hVM1 clone 32 cell transplantation on behavior</i>	71
<i>The effect of hVM1 clone 32 cell transplantation on inflammation.....</i>	81
<i>The effect of hVM1 clone 32 cell transplantation on mechanisms of repair.....</i>	86
<u>Transplantation of hVM1 clone 32 cells in middle-aged mice.....</u>	91
<i>The effect of hVM1 clone 32 cell transplantation on nigrostriatal pathway degeneration</i>	91
<i>The effect of hVM1 clone 32 cell transplantation on behavior</i>	94
<i>The effect of hVM1 clone 32 cell transplantation on inflammation.....</i>	103
<i>The effect of hVM1 clone 32 cell transplantation on mechanisms of repair.....</i>	107
DISCUSSION	111
CONCLUSIONS	127
CONCLUSIONES.....	131
REFERENCES.....	135
APPENDIX I.....	153
Supplementary figure 1	155
Supplementary table 1	156
APPENDIX II.....	163
Published article	165

ABBREVIATIONS

¹⁸F-FDOPA: 3,4-dihydroxy-6-[¹⁸F]fluoro-L-phenylalanine

α-syn: Alpha-synuclein (protein)

β-DAG: beta-dystroglycan

β-III tubulin: beta-III tubulin

6-OHDA: 6-hydroxydopamine

AADC: Aromatic L-amino acid decarboxylase

AAV: Adeno-associated viral

ALP: Autophagy-lysosome pathway

ARTN: Artemin

BBB: Blood-brain barrier

BDNF: Brain-derived neurotrophic factor

BLBP: Brain lipid-binding protein

BMP: Bone morphogenetic protein

BrdU: Bromodeoxyuridine

CALB2: Calretenin

CDNF: Cerebral dopamine neurotrophic factor

CL: Contralateral

CNS: Central nervous system

CNTF: Ciliary neurotrophic factor

CM: Conditioned media (*medio acondicionado)

COMT: Catechol O-methyltransferase

CRT: Cell replacement therapy

CSA: Cyclosporine A

CSF: Cerebrospinal fluid

CX3CR1: C-X3-C motif ligand 1

DA: Dopamine

DAn: Dopaminergic neuron(s)

DAPI: 4',6-Diamidino-2-phenylindole dihydrochloride

DAT: Dopamine transporter

DBS: Deep brain stimulation

DCX: Doublecortin

DJ-1: Parkinsonism associated deglycase

DPX: Distyrene, plasticiser, and xylene

DRT: Dopamine restoring treatment

EGF: Epidermal growth factor
*EP: Enfermedad de Parkinson
FGF: Fibroblast growth factor
FKN: Fractalkine
GDNF: Glial cell-derived neurotrophic factor
GFAP: Glial fibrillary acidic protein
GFL: Glial cell-derived neurotrophic factor family of ligands
GFR α : Glial cell-derived neurotrophic factor family receptor alpha
GIRK2: G-protein-regulated inward-rectifier potassium channel 2
GPi: Globus pallidus
GSH: Glutathione
hESC: Human embryonic stem cell
hfVM: Human fetal ventral mesencephalon
Hip: Hippocampus
hiPSC: Human induced pluripotent stem cell
hMSC: Human mesenchymal stem cell
hNSC: Human neural stem cell (*célula madre neural humana)
hpNSC: Human parthenogenetic neural stem cell
hVM1: Human ventral mesencephalon
i.p.: Intraperitoneally
Iba1: ionized calcium-binding adapter molecule 1
ICC: Immunocytochemistry
IHC: Immunohistochemistry
IL: Ipsilateral
IL-6: Interleukin 6
IL-10: Interleukin 10
IL-1 β : Interleukin 1 beta
IL-8: Interleukin 8
KIT: Proto-oncogene c-Kit
LB: Lewy body
L-DOPA: Levodopa, L-3,4-dihydroxyphenylalanine
LIF: Leukemia inhibitory factor
LMX1A: LIM homeobox transcription factor 1 alpha
LMX1B: LIM homeobox transcription factor 1 beta

LN: Lymph node
LRRK2: Leucine rich repeat kinase 2
MANF: Mesencephalic astrocyte-derived neurotrophic factor
MAO-B: Monoamine oxidase B
MAP2: Microtubule-associated protein 2
MC: Mast cell
MCP-1: Monocyte chemoattractant protein 1
mfb: Medial forebrain bundle
MPTP: 1-methyl-4-phenyl-1,2,3,6-tetrahydropyridine
*nDA: Neuronas dopaminérgicas
NE: Norepinephrine
NFH: Neurofilament heavy
NFL: Neurofilament light
NES: Nestin
NeuN: RNA binding Fox-1 homolog 3
NGF: Nerve growth factor
NGS: Next-generation sequencing
NPC: Neural progenitor cell
NSAID: Nonsteroidal anti-inflammatory drug
NRP1: Neuropilin 1
NRP2: Neuropilin 2
NSC: Neural stem cell
NT-3: Neurotrophin-3
NT-4: Neurotrophin-4
NTF: Neurotrophic factor
NRTN: Neurturin
NURR1: Nuclear receptor related protein-1
OB: Olfactory bulb
OFT: Open field test
PAX6: Paired box 6
PBS: Phosphate-buffered saline
PD: Parkinson´s disease
PFA: Paraformaldehyde
PITX3: Paired-like homeodomain transcription factor 3

PLL: Polylysine
PPT: Paw print test
PSD-95: Postsynaptic density protein 95
PSPN: Persephin
RANTES: Regulated upon activation of normal T cell expressed and secreted
ROS: Reactive oxygen species
S100B: S100 β
SC: Stem cell
SCF: Stem cell factor
SGZ: Subgranular zone
SHH: Sonic hedgehog
SNCA: Alpha-synuclein (gene)
SNpc: Substantia nigra pars compacta (*sustancia nigra parte compacta)
SOX2: SRY-box 2
STMN1: Stathmin 1
STN: Subthalamic nucleus
Str: Striatum (*estriado)
SVZ: Subventricular zone
SYN1: Synapsin I
SYP: Synaptophysin
TAC: Transient amplifying cell
TBS: Tris-buffered saline
TGF- β : Tumor growth factor beta
TH: Tyrosine hydroxylase
TNF- α : Tumor necrosis factor alpha
*TRC: Terapia de reemplazo celular
Trk: Tropomyosin receptor kinase
UCH-L1: Ubiquitin carboxyl-terminal hydrolase L1
UPS: Ubiquitin-proteasome system
VEGF: Vascular endothelial growth factor
VEGFR1: Vascular endothelial growth factor receptor 1
VEGFR2: Vascular endothelial growth factor receptor 2
VEGFR3: Vascular endothelial growth factor receptor 3
VIM: Vimentin

VM: Ventral mesencephalon

VMAT2: Vesicular monoamine transporter 2

VTA: Ventral tegmental area

*Spanish abbreviations used in **RESUMEN** section

INTRODUCTION

What is Parkinson's disease (PD)?

First described by James Parkinson in 1817 as "shaking palsy," Parkinson's disease (PD) is the second most common neurodegenerative disease in the world and the most common movement disorder for which there is presently no cure. Currently it is estimated that six million people worldwide have PD and it is predicted that by 2030, around nine-ten million people will suffer from PD. Moreover, men are more likely to have PD than women (Chai, Lim, 2013, De Virgilio et al., 2016, Kalia, Lang, 2015, Lesage, Brice, 2009, Sarkar, Raymick & Imam, 2016, Stoker, Torsney & Barker, 2018, Wirdefeldt et al., 2011). Approximately 5-10% of cases of PD are genetic with some of the more common mutations occurring in genes Alpha-Synuclein (*SNCA*), leucine rich repeat kinase 2 (*LRRK2*), parkin (*PRKN*), and parkinsonism associated deglycase (*DJ-1*). The rest of PD cases are termed idiopathic or sporadic, thus having no known cause (Chai, Lim, 2013, De Virgilio et al., 2016, Kalia, Lang, 2015, Lesage, Brice, 2009, Wirdefeldt et al., 2011).

Parkinson's disease is characterized by the death or impairment of dopaminergic neurons (DAN) in the substantia nigra pars compacta (SNpc) and the depletion of dopamine (DA) in the striatum (Str). The loss of DAN in the SNpc leads to the loss of DA in the Str as DAN project to the Str (Kalia, Lang, 2015, Sarkar, Raymick & Imam, 2016, Stoker, Torsney & Barker, 2018, Wirdefeldt et al., 2011). For clarification, the Str referred to throughout this work is the dorsal Str, made up of the caudate nucleus and putamen, that receives signaling from the SNpc (Macdonald, Monchi, 2011). Another hallmark of the disease is Lewy bodies (LBs), which are protein aggregates within cells that are made up of different proteins such as alpha-synuclein (α -syn), ubiquitin, and synphilin-1 (Kalia, Lang, 2015, Sarkar, Raymick & Imam, 2016, Stoker, Torsney & Barker, 2018, Wirdefeldt et al., 2011).

The SNpc is part of the basal ganglia circuit, which is responsible for voluntary movement as well as cognition, and it supplies the Str with DA. The Str provides the input to the basal ganglia so when the Str lacks DA, it does not function properly, which leads to excitation imbalance in other parts of the basal ganglia such as the globus pallidus (GPi), thalamus, and cerebral cortex (Figure 1). It is this disorientation that causes the motor symptoms, such as tremors, rigidity, bradykinesia, and postural instability, that are observed in PD patients (Chai, Lim, 2013, De Virgilio et al., 2016, Kalia, Lang, 2015, Lesage, Brice, 2009, Sarkar, Raymick & Imam, 2016, Stoker, Torsney & Barker, 2018, Wirdefeldt et al., 2011). There are also non-motor symptoms of PD, which appear in prodromal and early stages of PD, as well as later stages of the disease, such as olfactory impairment, constipation, sleep problems, cognitive impairment, anxiety, and depression (Chaudhuri, Schapira, 2009, Kalia, Lang, 2015, Stoker, Torsney & Barker, 2018, Taylor, Greene & Miller, 2010).

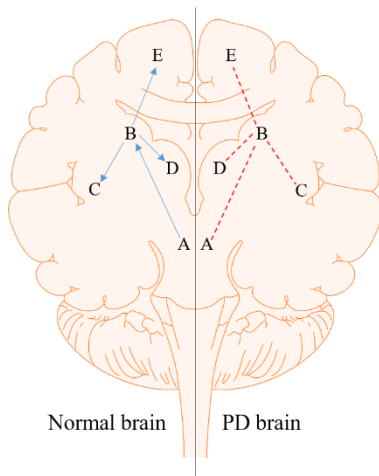


Figure 1: Diagram showing the primary pathways affected in PD. Under normal conditions, the SNpc (A), site of DAN, provides the Str (B) with DA, which sends afferents to other basal ganglia regions such as the GPi (C), thalamus (D), and cerebral cortex (E). In PD, there is a loss of DAN in the SNpc leading to a decrease in DA in the Str, which in turn affects signaling to the other basal ganglia components.

One of the major problems with PD is that by the time a patient has the described motor symptoms of the disease and is diagnosed with PD, there has already been a loss of around 80% of the brain's DA levels in the Str and at least 50% of DAN in the SNpc (Lesage, Brice, 2009, Wirdefeldt et al., 2011).

Dopaminergic neuron (DAN) criteria

One of the most common ways to quantify nigrostriatal population changes is via tyrosine hydroxylase (TH) immunostaining as TH is the rate-limiting enzyme in DA synthesis (Ang, 2006, Kriks et al., 2011, Stoker, Barker, 2016). Sonic hedgehog (SHH) and WNT, particularly WNT1/2/3a/5, signaling are involved in the differentiation and maintenance of DAN (Andersson et al., 2013, Ang, 2006, Arenas, 2014, Jovanovic et al., 2018, Kriks et al., 2011, Rafuse et al., 2005, Xia et al., 2016). Although there have been reports of bone morphogenetic protein (BMP) inhibition aiding in DAN differentiation, more recent publications have demonstrated that BMP2/5/7 actually promote the generation of DAN, and that perhaps it is the timing at which BMPs are expressed that affects DAN differentiation (Jovanovic et al., 2018, Kriks et al., 2011, Xia et al., 2016). The following table lists other genes that are implicated in the survival, maintenance, and differentiation of type A9 DAN, those found in the SNpc (Andersson et al., 2013, Ang, 2006, Blesa, Przedborski, 2014, Kriks et al., 2011, Xia et al., 2016) (Table 1). Expression studies of these genes and their proteins are used broadly in *in vitro*, *in vivo*, and human PD studies.

Category	Gene symbol	Gene name
Enzymes	<i>ALDH1</i>	aldehyde dehydrogenase
	<i>TH</i>	tyrosine hydroxylase
Receptors	<i>DRD2</i>	DA receptor D2
Transcription factors	<i>ASCL1</i>	achaete-scute homolog 1
	<i>EN1</i>	engrailed homeobox 1
	<i>EN2</i>	engrailed homeobox 2
	<i>FOXA1</i>	forkhead box A1
	<i>FOXA2</i>	forkhead box A2
	<i>LMX1A</i>	LIM homeobox transcription factor 1 alpha
	<i>LMX1B</i>	LIM homeobox transcription factor 1 beta
	<i>MSX1</i>	Msh homeobox 1
	<i>MSX2</i>	Msh homeobox 2
	<i>MYT1L</i>	myelin transcription factor 1 like
	<i>NGN2</i>	neurogenin 2
	<i>NURR1</i>	nuclear receptor related protein-1
	<i>OTX2</i>	orthodenticle homeobox 2
	<i>PAX5</i>	paired box 5
	<i>PITX2</i>	paired-like homeodomain transcription factor 2
<i>PITX3</i>	paired-like homeodomain transcription factor 3	
Transporters	<i>DAT</i>	DA transporter
	<i>SLC6A2</i>	solute carrier family 6 member 2
	<i>VMAT2</i>	vesicular monoamine transporter 2
Other	<i>GIRK2</i>	G-protein-regulated inward-rectifier potassium channel 2

Table 1: List of DAN-associated genes

Neurotrophic factors (NTFs)

Neurotrophic factors are secreted proteins that regulate neuronal survival, maintenance, proliferation, differentiation, regeneration, and migration, and are also pivotal in axonal and dendrite growth, and synaptic plasticity. They can be divided into four categories: glial cell-derived neurotrophic factor (GDNF) family of ligands (GFLs), neurotrophins, cerebral dopamine neurotrophic factor (CDNF) and mesencephalic astrocyte-derived neurotrophic factor (MANF) family, and neurotrophic cytokines (neurokines) (Allen et al., 2013, Sampaio et al., 2017, Sullivan, Toulouse, 2011, Tome et al., 2017, Xiao, Le, 2016).

The founding member of the GFLs is GDNF. It and the other GFLs, artemin (ARTN), neurturin (NRTN), and persephin (PSPN), all have very similar amino acid sequences, and are expressed in both the Str and the SNpc. All of the GFLs bind to the tyrosine kinase receptor RET, while each of them has preferential binding to a different GDNF family receptor alpha ($GFR\alpha$). The receptors $GFR\alpha1$ and $GFR\alpha2$ bind GDNF, ARTN, and NRTN, but $GFR\alpha1$ most strongly binds to GDNF while $GFR\alpha2$ most strongly binds to NRTN. Additionally, $GFR\alpha3$ only binds ARTN, and although $GFR\alpha4$ can bind all four GFLs, it binds PSPN most strongly. Out of these receptors, DAN in the SNpc only express RET and $GFR\alpha1$ (Allen et al., 2013, Baloh et al., 1998, Sullivan, Toulouse, 2011, Xiao, Le,

2016). Neurotrophic factor GDNF specifically increases the survival, proliferation, differentiation, and migration of DAN, and under control conditions GDNF increases TH levels, DAN sprouting, and DAN soma size. Furthermore, GDNF increases the expression of DAN-associated genes like *NURRI* and *PITX3*, which in turn control the expression of DAN genes *DAT*, *TH*, and *VMAT2*. The other GFLs, NTRN, ARTN, and PSPN, also promote the survival of DAN (Akerud et al., 2002, Allen et al., 2013, Sampaio et al., 2017, Sullivan, Toulouse, 2011, Tome et al., 2017, Xiao, Le, 2016).

Neurotrophins include brain-derived neurotrophic factor (BDNF), nerve growth factor (NGF), neurotrophin-3 (NT-3), and neurotrophin-4 (NT-4). All four neurotrophins are expressed in the Str and the SNpc. All neurotrophins weakly bind to the p75 neurotrophin receptor, and strongly and specifically bind to one of the neurotrophic tyrosine kinase receptors, tropomyosin receptor kinases A-C (TrkA, TrkB, and TrkC). Neurotrophic factor BDNF binds to TrkB, NGF binds to TrkA, NT-3 most strongly binds to TrkC but it can also bind to TrkA and TrkB, and NT-4, which is neurotrophin-5 in mice, binds to TrkB. Until now, only TrkB has been found on DAN in the SNpc (Allen et al., 2013, Perez-Navarro et al., 2000, Sampaio et al., 2017, Tome et al., 2017, Xiao, Le, 2016). Furthermore, BDNF regulates sensory and hippocampal neurons, but also affects some DAN, promoting neurite outgrowth. Moreover, BDNF has been shown to be especially important for synaptic plasticity, and learning and memory. For the most part, NGF is involved with sensory and cholinergic neurons, while NT-3 and NT-4 promote survival in different neuronal populations including sensory neurons, but they also participate in the survival of DAN (Allen et al., 2013, Sampaio et al., 2017, Tome et al., 2017, Xiao, Le, 2016).

Neurotrophic factors CDNF and MANF have similar amino acid sequences, and promote neuronal survival, specifically that of DAN. Both are expressed in the cerebral cortex, hippocampus (Hip), Str, and SNpc (Lindholm et al., 2007, Sullivan, Toulouse, 2011).

Neurokinins participate in the immune response and inflammation, as well as the survival, proliferation, and differentiation of neurons. They include ciliary neurotrophic factor (CNTF), interleukin 6 (IL-6), and leukemia inhibitory factor (LIF), among others (Sampaio et al., 2017, Tome et al., 2017). Neurokinin CNTF promotes the survival of DAN, and IL-6 knockout mice demonstrate DA depletion in the Str and DAN loss in the SNpc compared to WT mice (Sampaio et al., 2017, Tome et al., 2017). Proneural anti-inflammatory cytokine LIF maintains sensory neurons, promotes central nervous system (CNS) repair, participates in the differentiation and survival of astrocytes and oligodendrocytes, inhibits apoptosis, and its presence has been shown to increase the number of beta-

III tubulin-positive (β -III tubulin+) and TH+ cells *in vitro* and *in vivo* (Davis et al., 2019, Ling et al., 1998, Sampaio et al., 2017).

The fibroblast growth factor (FGF) family, specifically FGF-1, FGF-2, FGF-8, FGF-9, and FGF-20, and epidermal growth factor (EGF), have also been reported to play a role in the survival, differentiation, and protection, of DAN (Ang, 2006, Kriks et al., 2011, Tome et al., 2017, Xia et al., 2016).

The vascular endothelial growth factor (VEGF) family, which is involved in promoting angiogenesis, the development and growth of blood vessels from pre-existing blood vessels, neurogenesis, and glial proliferation, is made up of several isoforms of the factor. The family includes VEGF-A, VEGF-B, VEGF-C, among other factors; VEGF-A binds to VEGF receptor 1 (VEGFR1) and VEGF receptor 2 (VEGFR2), VEGF-B binds to VEGFR1, and VEGF-C binds to VEGFR2 or VEGF receptor 3 (VEGFR3). In addition, VEGF-A binds neuropilins 1 and 2 (NRP1 and NRP2), and VEGF-B binds NRP1. Until now, it has been understood that VEGF signals pro-angiogenic and neuroprotective effects via VEGFR2 (Caballero, Sherman & Falk, 2017, Falk et al., 2011, Shim, Madsen, 2018, Troncoso-Escudero et al., 2018). Vascular endothelial growth factor and its receptors are expressed in neurons, and VEGF has been shown to be neuroprotective for DAN *in vitro* and *in vivo* (Caballero, Sherman & Falk, 2017, Falk, Gonzalez & Sherman, 2010, Piltonen et al., 2011, Yasuhara et al., 2004). Moreover, GDNF upregulates VEGF-C expression and VEGF can upregulate GDNF expression (Piltonen et al., 2011, Yasuhara, Date, 2007).

In the SNpc of PD patients, GDNF, BDNF, NGF, and CNTF are all reduced, but the GDNF decrease in the surviving neurons in the SNpc of PD patients is twice as large as the diminution of BDNF. Additionally, one study found that CNTF, NGF, NT-3, and NT-4, levels in surviving neurons in the SNpc were not significantly different when comparing control and PD patients. In the SNpc of PD patients, VEGF-A is increased (Allen et al., 2013, Chauhan, Siegel & Lee, 2001, Falk, Gonzalez & Sherman, 2010, Sarkar, Raymick & Imam, 2016, Shim, Madsen, 2018, Xiao, Le, 2016). In addition, BDNF concentration is decreased in the Str of PD patients, and BDNF levels are correlated to the degree of DAN loss (Allen et al., 2013, Sampaio et al., 2017).

Current PD treatments

Although there is a plethora of treatments available for PD, none of them are very effective, and if they are, they are only so for a short amount of time as they only treat the symptoms of the disease. The most common ones are dopamine restoring treatments (DRTs) (Kalia, Lang, 2015, Sarkar, Raymick & Imam, 2016, Stoker, Torsney & Barker, 2018). Commonly prescribed DRTs include DA replacement drugs levodopa (L-3,4-dihydroxyphenylalanine; L-DOPA) and DA receptor agonists, as well as medications that prevent DA degradation which include catechol O-methyltransferase (COMT) and monoamine oxidase B (MAO-B) inhibitors (Contin, Martinelli, 2010, De Virgilio et al., 2016, Kalia, Lang, 2015, Sarkar, Raymick & Imam, 2016, Stoker, Torsney & Barker, 2018). The most efficient DRT, L-DOPA, is a precursor of DA. While DA cannot cross the blood-brain barrier (BBB), L-DOPA is capable of doing so and once it is in the brain, it is converted into DA by the aromatic L-amino acid decarboxylase (AADC) enzyme. Levodopa has a very short half-life which is why it is often prescribed with AADC inhibitors like carbidopa or benserazide, which is unable to cross the BBB and inhibits the breakdown of L-DOPA in the periphery, thus allowing for more L-DOPA to reach the brain (Burkhard et al., 2001, Contin, Martinelli, 2010, Sarkar, Raymick & Imam, 2016). The metabolism of L-DOPA in the periphery can also be delayed with COMT and MAO-B inhibitors. In the CNS, both of these inhibitors prevent the metabolism of DA. In addition, DA agonists are prescribed to PD patients as they mimic DA (Contin, Martinelli, 2010, Sarkar, Raymick & Imam, 2016, Stoker, Torsney & Barker, 2018). Anticholinergic drugs are another group of medications prescribed as they block the acetylcholine neurotransmitter to reduce involuntary movements like tremor seen in PD patients (Kalia, Lang, 2015, Sarkar, Raymick & Imam, 2016). The effects of all of these drugs wear off after the first few years and they all come with side effects, some of the most commonly reported ones being dyskinesias, nausea, involuntary movements, mood swings, psychosis, hallucinations, and cognitive impairment (Kalia, Lang, 2015, Sarkar, Raymick & Imam, 2016, Stoker, Barker, 2016, Stoker, Torsney & Barker, 2018).

Deep brain stimulation (DBS) is another treatment used in PD patients (Benabid et al., 2009, Kalia, Lang, 2015, Kocabicak, Temel, 2013, Sarkar, Raymick & Imam, 2016). It is defined as the unilateral or bilateral implantation of the electrodes, usually in the subthalamic nucleus (STN), a region of the basal ganglia, in order to send electrical stimulation to the STN. Sometimes the electrodes are placed in the GPi or thalamus, other regions part of the basal ganglia. Although DBS has been reported to be safe, and improve motor symptoms like dyskinesias and the quality of life of PD patients, it is well documented that it is a more successful treatment in a minority of younger PD patients with less advanced PD. Side effects of DBS include speech impairment, cognitive impairment, depression, and

suicide, in addition to the potential surgical complications (Benabid et al., 2009, Cyron, 2016, Kocabicak, Temel, 2013, Sarkar, Raymick & Imam, 2016, Stoker, Torsney & Barker, 2018).

Failed and potential PD treatments

Nowadays, it is widely accepted that PD is the result of a combination of factors, both biological and environmental. Some of the biological mechanisms thought to underlie PD are mitochondrial dysfunction, reactive oxygen species (ROS), neuroinflammation, apoptosis, protein misfolding, ubiquitin-proteasome system (UPS) and autophagy-lysosome pathway (ALP) dysfunction, and loss of NTFs. Some of the environmental factors which have been linked to an increased risk of PD are exposure to pesticides, previous head injury, rural living, and well-water use (Chai, Lim, 2013, De Virgilio et al., 2016, Kalia, Lang, 2015, Lesage, Brice, 2009, Sarkar, Raymick & Imam, 2016, Wirdefeldt et al., 2011). Drinking coffee, drinking alcohol, smoking tobacco, taking calcium channel blockers, and taking nonsteroidal anti-inflammatory drugs (NSAIDs), have all been associated with a lower risk of developing PD (De Virgilio et al., 2016, Kalia, Lang, 2015, Lesage, Brice, 2009).

There have been some failed clinical trials involving coenzyme Q10, a component of the mitochondrial electron transport chain, creatine, a source of ATP, inosine, a precursor of urate, reduced glutathione (GSH), an endogenous antioxidant, and anti-apoptotic agents TCH346 and CEP-1347. All of these treatments were tested in clinical trials and PD patients did not show any significant improvement (Kalia, Lang, 2015, Kalia, Kalia & Lang, 2015, Sarkar, Raymick & Imam, 2016).

Anti-inflammatory treatments have been shown to aid in PD treatment; examples include NSAIDs, statins, and minocycline, the latter of which is an antibiotic expected to enter a Phase III clinical trial for PD (De Virgilio et al., 2016, Sarkar, Raymick & Imam, 2016, Wirdefeldt et al., 2011). Ubiquitin carboxyl-terminal hydrolase L1 (UCH-L1) is an enzyme in neurons that when inhibited, can generate protein misfolding like the α -syn aggregates seen in PD so UCH-L1 function enhancers are being tested as therapeutic agents *in vivo* (Sarkar, Raymick & Imam, 2016). Another potential treatment to clear α -syn aggregates is immunotherapy; clinical trials testing vaccines and monoclonal antibodies to eliminate extracellular α -syn have been shown to be safe, and vaccinated PD patients showed an immune response to α -syn peptide and antibody-treated PD patients showed a decrease in α -syn levels (Kalia, Kalia & Lang, 2015, Stoker, Torsney & Barker, 2018). The UPS and ALP are very important in the breakdown and clearance of debris and harmful substances such as α -syn aggregates so one potential target is factors that enhance or disinhibit these systems (Kalia, Kalia & Lang, 2015, Sarkar, Raymick & Imam, 2016). Rapamycin, an immunosuppressant and autophagy enhancer, is currently

being studied for its effects in *in vitro* PD models (Kalia, Kalia & Lang, 2015, Stoker, Torsney & Barker, 2018). Interestingly, the most common mutations in genetic PD are in the beta-glucocerebrosidase gene that encodes an enzyme of the same name, and lead to lysosomal storage dysfunction (Kalia, Lang, 2015, Stoker, Torsney & Barker, 2018). Although most PD cases are sporadic, familial cases can help to better understand PD pathology, and there are ongoing Phase II clinical trials testing amroxol (NCT02941822 and NCT02914366) in PD patients with this genetic mutation (Stoker, Torsney & Barker, 2018, U.S. National Library of Medicine, 2019). Moreover, *SNCA*, the gene which encodes the α -syn protein, has been targeted by RNA interference in experimental PD rodent and monkey models, and via beta-2 adrenergic receptor agonists, medications already used to treat asthma and chronic obstructive pulmonary disease, which decrease *SNCA* gene transcription (Stoker, Torsney & Barker, 2018). With all of these studies targeting α -syn, it is important to remember that α -syn is expressed in the brain of healthy individuals as well. Even though its role has not been completely defined, its importance in neurotransmitter release is a strong possibility and PD rodent studies offer inconclusive evidence to whether or not lower levels of α -syn exacerbate neurodegeneration (Stoker, Torsney & Barker, 2018). Also, α -syn LBs are found in normal aging brains (Hallett et al., 2014). Based on their association with a lower risk of developing PD, caffeine and nicotine are currently being tested in phase III and phase II clinical trials, respectively (ClinicalTrials.gov Identifier: NCT01738178 and NCTC01560754) (Kalia, Kalia & Lang, 2015). Furthermore, calcium channel blockers, used to treat high blood pressure, are currently being used to treat PD (Kalia, Kalia & Lang, 2015, Kalia, Lang, 2015, Liss, Striessnig, 2019). One in particular is isradipine, which is currently in a Phase III clinical trial (ClinicalTrials.gov Identifier: NCT02168842) (U.S. National Library of Medicine, 2019); it blocks L-type Cav1.3 calcium channels thus decreasing calcium influx in DAN in the SNpc that are dependent on these specific calcium channels thereby protecting them (Kalia, Kalia & Lang, 2015, Kalia, Lang, 2015). Other drugs being tested in clinical trials in PD patients are exenatide (ClinicalTrials.gov Identifier: NCT03456687), a drug used to treat type 2 diabetes, and nilotinib (ClinicalTrials.gov Identifier: NCT03205488), used to treat chronic myelogenous leukemia (Stoker, Torsney & Barker, 2018, U.S. National Library of Medicine, 2019).

One of the ways to replace NTFs diminished by PD progression is by NTF intracerebral injection and/or gene therapy. *In vivo* studies have shown the potential of NTFs in treating PD. Intrastratial injection of GDNF promoted the survival of DAN, increased DA levels in the Str, and triggered behavioral improvement, in PD rodent and non-human primate models. Neurotrophic factors ARTN and PSPN have also been shown to rescue DAN in Parkinsonian rodents. Moreover, NTRN injected

in the Str protected nigral DAN, restored DA in the Str, and improved motor impairments, in Parkinsonian rats and monkeys. In experimental PD rodent and monkey models, BDNF inhibited DAN loss, while NGF injected in Parkinsonian mice increased DA levels in the Str. Likewise, CDNF and MANF injected in a PD rat model showed rescue of DAN, striatal DA, and behavior (Akerud et al., 2002, Lindholm et al., 2007, Sarkar, Raymick & Imam, 2016, Tome et al., 2017).

Previous clinical trials involved NRTN. This factor was injected into the Str and SNpc, depending on the trial, via an adeno-associated viral (AAV) vector. While in all trials the treatment was safe, eventually the trials ended because there was no significant improvement in PD patients (Kalia, Kalia & Lang, 2015, Sarkar, Raymick & Imam, 2016, Stoker, Torsney & Barker, 2018). More successful clinical trials have involved GDNF gene therapy. A catheter containing GDNF was injected into PD patients for two years and these patients showed motor performance improvement, increased quality of life, and an augmentation in the uptake of 3,4-dihydroxy-6-[¹⁸F]fluoro-L-phenylalanine (¹⁸F-FDOPA), which measures AADC levels, in the Str. Unfortunately, when the study was repeated, although PD patients showed an increased striatal uptake of ¹⁸F-FDOPA, used to visualize DA using PET, there were no other clinical benefits (Allen et al., 2013, Kalia, Kalia & Lang, 2015, Niethammer, Feigin & Eidelberg, 2012, Patel et al., 2005, Pretze, Wangler & Wangler, 2014, Sampaio et al., 2017). Currently, the only ongoing clinical trial involving NTFs is a study comprising the striatal injection of an AAV vector coding for GDNF in PD patients (ClinicalTrials.gov Identifier: NCT01621581) and results are pending (Kalia, Kalia & Lang, 2015). A summary of the hypothesized biological causes of PD, and their failed and potential treatments can be found in Figure 2.

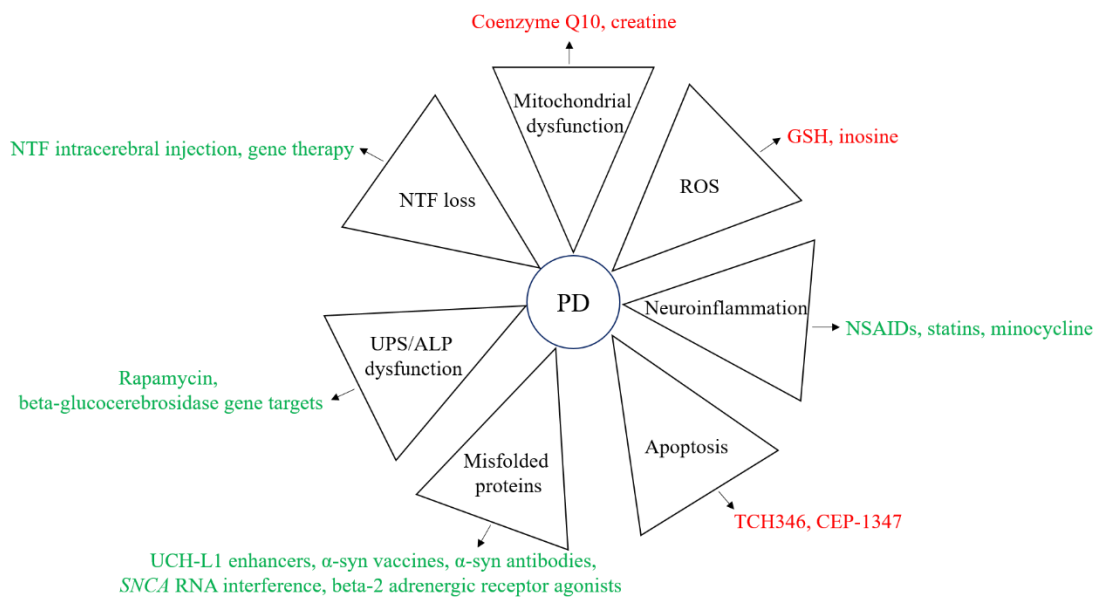


Figure 2: Summary of the hypothesized biological causes of PD and their failed (red) and potential (green) treatments.

Cell replacement therapy (CRT)

All of the aforementioned current and potential PD treatments fail to address the underlying issue, that is the loss of DAN, as they do not replace or repair the DAN lost or damaged, respectively, in PD. Moreover, none of them adequately manage all of the physical symptoms of PD and many have side effects ranging from mild to severe. Therefore, with other current treatments not fulfilling all requirements to improve the patient's life, the goal of PD treatment becomes cell replacement. In recent years, CRT has come to the forefront of science with its potential to treat diseases such as PD. Some of the different cell sources that have already been used, are being used, or will be used, in clinical trials based on their success in proof-of-concept *in vivo* Parkinsonian rodent and monkey studies include human neural stem cells (hNSCs), human fetal ventral mesencephalon (hfVM) tissue, human embryonic stem cells (hESCs), human induced pluripotent stem cells (hiPSCs), human mesenchymal stem cells (hMSCs), and human parthenogenetic neural stem cells (hpNSCs), among others (Sarkar, Raymick & Imam, 2016, Stoker, Barker, 2016, Stoker, Blair & Barker, 2017, Stoker, Torsney & Barker, 2018, U.S. National Library of Medicine, 2019, Yasuhara et al., 2017).

Up until now, there have been some promising results from clinical trials involving CRT. While PD patients transplanted with fVM grafts showed inconsistent improvement in gait, degree of muscle stiffness, and severity of dyskinesias, they had increased ¹⁸F-FDOPA uptake in the transplanted Str and there were TH+ cells in the grafts six years post-transplant (Wenning et al., 1997). Another case involved one patient transplanted with fVM cells who showed motor improvement for the first 14 years post-transplant and when he died 24 years post-transplant, some of the surviving grafted cells were TH+, although ubiquitin+ and α -syn+ LBs were found in 11% and 12% of these surviving TH+ transplanted cells, respectively (Li et al., 2016, Stoker, Barker, 2016). Another trial in PD patients found that DAT and TH were expressed in fVM transplants up to 14 years post-transplant (Hallett et al., 2014). While there have been these successes, within these same trials there were patients who showed no improvement (Stoker, Barker, 2016).

All of the different types of tissue and cells being used in clinical trials for PD have advantages and disadvantages. While hfVM grafts seem the most promising, there are huge ethical issues behind the acquisition of this tissue and the amount of tissue needed per patient, making its use impractical. By contrast, hNSCs do not have this quantity problem (Bjorklund, Lindvall, 2017, Stoker, Barker, 2016, Stoker, Blair & Barker, 2017). Furthermore, immunosuppression is needed in the PD patients treated with hESCs, hfVM, and hNSCs. In addition, hESCs pose ethical problems as they are obtained from unused embryos meant for *in vitro* fertilization (Stoker, Barker, 2016, Stoker, Blair & Barker, 2017).

While hiPSCs do not require immunosuppression and a large number of cells can be generated, there is the possibility that these cells have a genetic predisposition to PD that led to the pathogenesis in the first place (Stoker, Torsney & Barker, 2018).

In addition to each cell or tissue type having its individual drawbacks, there are concerns that have arisen about CRT in general, specifically its side effects including graft-induced dyskinesias and α -syn+ LBs found in transplanted cells (Kalia, Lang, 2015, Sarkar, Raymick & Imam, 2016). Graft-induced dyskinesias could be solved by having a purer culture as dyskinesias are usually caused by residual serotonergic neurons in the graft (Yasuhara et al., 2017). Although there have been examples of α -syn+ LBs found in the transplanted cells, some argue that this occurrence should not deter from the development of CRT as these LBs are not found in the majority of transplanted cells because only 1-5% of transplanted cells have these LBs. Also, LBs do not seem to be negatively affecting the graft as clinical improvements are still observed (Bjorklund, Lindvall, 2017, Hallett et al., 2014, Stoker, Barker, 2016). Other questions surrounding CRT include cell culture and transplantation protocol, amount of cells, location and number of grafts, migration of grafted cells, and tumor formation. Perhaps the most serious issue is that of PD patient heterogeneity, in that what works in some patients may not work in others (Sarkar, Raymick & Imam, 2016, Stoker, Barker, 2016, Stoker, Torsney & Barker, 2018, Wenning et al., 1997).

A newer, promising approach that has arisen is the merging of gene therapy and CRT. For example, NSCs transfected with NT-3 transplanted into the medial forebrain bundle (mfb) and ventral tegmental area (VTA) of Parkinsonian rats led to a reduction in the loss of SNpc DAN and behavioral amelioration (Gu et al., 2009). Another way to combine the two modalities is the encapsulation of cells that are genetically modified to secrete factors such as the NTF GDNF. This has already been shown to be beneficial in PD rodent and monkey models (Akerud et al., 2001, Yasuhara, Date, 2007, Yasuhara et al., 2017). There is one clinical trial for PD involving encapsulated cells using porcine choroid plexus cells (NTCELL®) with results pending (ClinicalTrials.gov Identifier: NCT02683629) (U.S. National Library of Medicine, 2019).

Despite the many challenges it faces, CRT is still the best known option for the future treatment of PD because it is the only one which seeks to replace the lost DAN. Whilst the search continues for an apt cell line to be used in CRT, there are others still being tested in *in vivo* studies that could one day be proven superior and tried in the clinic.

Human ventral mesencephalic (hVM1) cells

In 2009, Villa et al. described a new stable cell line of hNSCs, hVM1 (Villa et al., 2009). These cells are derived from the ventral mesencephalon (VM) of a 10 week-old aborted human fetus, and were immortalized via transduction of a retroviral vector coding for *v-myc* (LTR-*vmyc*-SV40p-Neo-LTR). Under proliferation conditions, over 96% of cells are nestin (NES)+ and over 92% of cells are vimentin (VIM)+, both markers of neural stem cells (NSCs). Under differentiation conditions, hVM1 cells display an A9 SNpc DAN phenotype and exhibit DAN markers GIRK2, LMX1A, PITX3, and TH, and neuronal markers β -III tubulin and microtubule-associated protein 2 (MAP2). However, the differentiated culture has a non-homogeneous character in that there are also astrocytes, GABAergic neurons, and serotonergic neurons, present. Furthermore, gene and protein expression studies showed an increase in dopaminergic markers such as TH and DAT and neuronal markers such as calretinin (CALB2), in differentiating cells compared to dividing cells (Villa et al., 2009). An augmentation in expression of these neural and dopaminergic cell markers indicate that the hVM1 cell line could be a source of DAN used in experimental CRT. Further studies showed that these cells have electrophysiological properties of neurons, albeit immature (Tonnesen et al., 2010). When transplanted into the right Str of three month-old female Parkinsonian rats, the hVM1 cell graft survived and integrated into the brain two and five months post-transplant. No tumors were generated and the grafted cells expressed immature neuron marker doublecortin (DCX), astrocyte marker glial fibrillary acidic protein (GFAP), and TH, two months post-transplant, which continued until month five. In addition, five months post-grafting, analysis showed that some surviving grafted cells were TH and VMAT2 double positive. In a separate study, Parkinsonian rats transplanted with hVM1 cells showed behavioral improvement four months post-transplant (Courtois et al., 2010, Ramos-Moreno, Castillo & Martinez-Serrano, 2012).

Clones were generated from the hVM1 cell line, and nine out of 70 clones were chosen to be further characterized based on their TH+ neuron generation (Ramos-Moreno et al., 2012, Villa et al., 2009). These nine clones were tested and compared for the following *in vitro* features: *v-myc* copy number, *v-myc* expression downregulation, and reduction of NSC/neural progenitor cell (NPC) markers Ki-67 and NES and augmented percentage of β -III tubulin+ and TH+ cells in differentiation conditions. The clones were also subjected to *in vivo* analysis seeking reduction of Ki-67+ cells, increased human neuron specific enolase immunostaining which marks transplant maturation, increased percentage of TH+ cells in surviving grafts, and behavioral improvement, in an experimental PD rat model two months post-transplant. Clone 30 and 32 of the hVM1 cell line were chosen as the best candidates to be used in future transplants (Ramos-Moreno et al., 2012). The differentiation of the original

polyclonal hVM1 cell line yields around 26% β -III tubulin+ cells and approximately 12% TH+ cells, when differentiated between passages 8-12 (Villa et al., 2009). Later, it was reported that these cells lose their neurogenic and dopaminergic capacity at later passages; at passage 21, they generate only 5% β -III tubulin+ cells and 1% TH+ cells, and in even higher passages, less than 1% for both (Courtois et al., 2010). Interestingly, when differentiated at passage 30, hVM1 clone 32 cells generate approximately 12.5% β -III tubulin+ cells and around 10% TH+ cells, thus strengthening the argument for their potential in experimental PD CRT (Ramos-Moreno et al., 2012). It is important to note that hVM1 cells and their clones are transplanted in an undifferentiated state as testing has shown that when in a proliferative state, and not differentiated, these cells are able to show more beneficial effects. Others have also noted the same, most notably that uncommitted cells have a better chance of incorporating into the brain and forming synapses with other cells (Redmond et al., 2007).

Experimental PD models

There exist several genetic and idiopathic PD animal models. Genetic models include SNCA, LRRK2, PRKN, and DJ-1 single transgenic mice, but DAN and DA loss is either absent or marginal with overexpression or knockout of these genes in mouse models, although LBs are observed in SNCA-overexpressing mice (Blandini, Armentero, 2012, Blesa, Przedborski, 2014). Among the most common neurotoxins used to model idiopathic PD in mice are 1-methyl-4-phenyl-1,2,3,6-tetrahydropyridine (MPTP) and 6-hydroxydopamine (6-OHDA). The neurotoxin MPTP is mostly used in mice and non-human primates, while 6-OHDA is normally used in rats. Interestingly, rats are completely resistant to MPTP. Normally injected intraperitoneally (i.p.), MPTP crosses the BBB, while 6-OHDA, which cannot cross the BBB, is stereotaxically injected, usually unilaterally in either the mfb or SNpc. The applied dose of both of these neurotoxins varies from study to study, and while a decrease of DA in the Str and DAN loss in the SNpc is replicated in both models, the speed of this decrease and the pathology by which it occurs is not the same as in PD patients (Blandini, Armentero, 2012, Blesa, Przedborski, 2014, Sarkar, Raymick & Imam, 2016). While 6-OHDA is injected directly into the brain, MPTP is injected into the periphery and therefore better mimics PD as it acts bilaterally and has a whole-body effect, especially in the light of growing evidence that PD pathology might start outside of the brain (Braak et al., 2004, Duty, Jenner, 2011, Kim et al., 2019). Neither of these *in vivo* PD models reproduces the LBs observed in PD patients. Recently, there have been attempts to reproduce the progressive DAN loss and LB formation by employing a chronic MPTP model using osmotic minipumps that continuously inject MPTP into the mice over an extended period of time, but results have not been consistent (Blandini, Armentero, 2012, Blesa, Przedborski, 2014, Duty, Jenner, 2011).

Another important aspect of PD models is the mimicking of the behavioral component of the disease. Up until now, only MPTP-treated monkeys exhibit all PD motor symptoms (tremor, rigidity, bradykinesia, and postural instability) seen in patients as well as DA and DAN loss in the Str and SNpc, respectively, but the presence of LBs is not regularly observed (Blandini, Armentero, 2012, Blesa, Przedborski, 2014, Duty, Jenner, 2011). When MPTP is administered in mice, these animals show no consistent changes in behavior and they do not reproduce all of the behavioral symptoms observed in PD patients (Blandini, Armentero, 2012, Blesa, Przedborski, 2014, Meredith, Rademacher, 2011, Rousselet et al., 2003, Zhang, Q. S. et al., 2017). Therefore, the objective is really to find tests that show differences between MPTP-treated animals and their controls in order to be able to see if PD treatments are efficient or not. The open field test (OFT) is the most commonly used test to analyze locomotor activity (Sedelis, Schwarting & Huston, 2001); the mice are placed in a roofless box and recorded. While some have reported decreased locomotor activity, there have also been studies demonstrating that the mice show no sign of changed locomotion or an increase in locomotor activity (Blandini, Armentero, 2012, Blesa, Przedborski, 2014, Sedelis, Schwarting & Huston, 2001, Taylor, Greene & Miller, 2010). The OFT can also test anxiety as control mice have a tendency to stay close to the walls of the box so MPTP-treated mice spend more time in the center of the box (Taylor, Greene & Miller, 2010). Gait changes can be measured using the paw print test (PPT), where the walking patterns of the animals are analyzed (Carvalho et al., 2013, Iancu et al., 2005). Mice lesioned with MPTP have consistently shown a decreased stride length, most significantly of the forelimbs, compared to control mice. Moreover, there are reports of motor symptoms disappearing over time. While the solution may seem to be increasing the dose of MPTP in order to increase DA and DAN loss in the Str and SNpc, respectively, higher doses of MPTP are linked to a higher mortality rate normally due to cardiotoxicity. In addition, there may be different behavioral outcomes even though the same MPTP dose is applied and the same DA and DAN diminutions are observed (Meredith, Rademacher, 2011, Sedelis, Schwarting & Huston, 2001, Taylor, Greene & Miller, 2010, Jackson-Lewis, Przedborski, 2007).

Although there is no animal model available that fully mimics PD, their contribution to a better understanding of PD pathology and to the discovery of many already available and potential treatments for PD is irrefutable (Blandini, Armentero, 2012, Blesa, Przedborski, 2014, Duty, Jenner, 2011, Meredith, Rademacher, 2011, Sarkar, Raymick & Imam, 2016, Taylor, Greene & Miller, 2010).

Neuroinflammation

Neuroinflammation, one of the characteristics of PD, is the activation of the resident CNS inflammatory cells like astrocytes and microglia and an increase in pro-inflammatory cytokines such as interleukin 1 beta (IL-1 β), IL-6, and tumor necrosis factor alpha (TNF- α), especially in the Str and SNpc (De Virgilio et al., 2016, Kalia, Lang, 2015, Troncoso-Escudero et al., 2018, Wirdefeldt et al., 2011). Under normal physiological conditions, astrocytes, the most numerous cells in the brain, maintain homeostasis, regulate the BBB, and support neurons, while microglia, the macrophages of the CNS, maintain homeostasis, participate in synapse pruning, and survey the CNS in a quiescent state, phagocytizing and removing debris. Under PD pathological conditions, microglia are the first to be activated; they become reactive and take on one of two phenotypes, either the pro-inflammatory M1 phenotype or the anti-inflammatory M2 phenotype, depending on their microenvironment. M1 microglia release ROS and pro-inflammatory cytokines like IL-1 β , IL-6, and TNF- α , to prevent tissue damage. Although they are pro-inflammatory cytokines, they have been shown to be beneficial; for example, IL-1 β and IL-6 induce neuronal growth, and it has been hypothesized that the activation of pro-inflammatory cytokines induces the activation of anti-inflammatory cytokines. In addition, reactive microglia release BDNF and GDNF (Joe et al., 2018, Phani, Loike & Przedborski, 2012, Rentzos et al., 2009, Troncoso-Escudero et al., 2018). Reactive microglia activate astrocytes, which can also take on an A1 pro-inflammatory phenotype or an A2 anti-inflammatory phenotype depending on the microenvironment (Ridet et al., 1997). A1 astrocytes form a glial scar and release pro-inflammatory cytokines which leads to neuronal death, while A2 astrocytes help to promote CNS repair by restoring homeostasis and the BBB, protecting neurons, releasing NTFs, and inhibiting excessive inflammation by controlling microglial activation via the production of anti-inflammatory cytokines. Among the NTFs produced and released by astrocytes are CNTF, FGF-2, GDNF, and NGF (Muller, Junghans & Kappler, 1995, Sofroniew, 2005, Sullivan, Toulouse, 2011).

Some cytokines and chemokines involved in neuroinflammation have more pivotal roles in PD pathology and they include IL-6, interleukin 10 (IL-10), regulated upon activation of normal T cell expressed and secreted (RANTES), eotaxin-1, monocyte chemoattractant protein 1 (MCP-1), and fractalkine (FKN). Although so far IL-6 has been classified as a pro-inflammatory cytokine, it can also take on the role of an anti-inflammatory cytokine and is released by stem cells (SCs) *in vitro* (Pawitan, 2014). Another anti-inflammatory cytokine is IL-10; secreted by SCs *in vitro* and by reactive microglia *in vivo*, IL-10 has a neuroprotective effect. It protects DAN in the SNpc, inhibits microglial proliferation in the SNpc, and inhibits microglial release of pro-inflammatory cytokines. Also, IL-10 inhibits the production of IL-1 β , IL-6, TNF- α , and RANTES (Arimoto et al., 2007,

Pawitan, 2014, Rentzos et al., 2009). Produced by microglia, RANTES is a cytokine that induces the migration of leukocytes to inflammatory regions, and is found to be increased in blood and cerebrospinal fluid (CSF) in MPTP-treated mice and monkeys as well as PD patients, compared to controls (Appay, Rowland-Jones, 2001, Arimoto et al., 2007, Fuzzati-Armentero, Cerri & Blandini, 2019). Eotaxin-1 is a cytokine that participates in the migration of mononuclear cells at sites of inflammation. Eotaxin-1 levels are increased in blood and CSF of MPTP-treated mice and monkeys (Fuzzati-Armentero, Cerri & Blandini, 2019). When RANTES and eotaxin-1 were simultaneously injected in MPTP-lesioned mice, the result was the loss of DAN in the SNpc, the loss of striatal TH+ fibers, α -syn aggregates in the SNpc, microglial activation in the SNpc, and motor impairments (Chandra et al., 2017).

Microglia also produce MCP-1, a chemokine released by SCs *in vitro* and astrocytes *in vivo*, that is expressed in neurons, astrocytes, and glial cells. It activates microglia and helps in the migration of microglia to the site of injury, promotes angiogenesis, and alters BBB permeability. It is found in the Str and SNpc, and its receptor CCR2 is expressed on neurons in the Str and on DAN in the SNpc (Arimoto et al., 2007, Banisadr et al., 2005, Conductier et al., 2010, Liu et al., 2019, Pawitan, 2014). The chemokine MCP-1 is increased in blood and CSF of PD patients compared to controls (Fuzzati-Armentero, Cerri & Blandini, 2019). *In vitro*, MCP-1 plays a role in the differentiation of DAN and affects SNpc DAN and Str DA levels, and also has cytotoxic effects (Guyon et al., 2009, Liu et al., 2019, Wang et al., 2014).

Fractalkine is produced by neurons and inhibits microglial activation by binding to its receptor, CX3CR1, which is located on microglia, and can be both membrane-bound or soluble. Essentially, FKN maintains the quiescent state of microglia, and *in vitro* it downregulates pro-inflammatory cytokine production. As microglia are the initial reactors to injury and FKN inhibits microglia, FKN controls neuroinflammation so it is no surprise that FKN is expressed at high levels in the brain (Morganti et al., 2012, Pabon et al., 2011, Thome, Standaert & Harms, 2015). Moreover, MPTP-treated mice and PD patients show increased levels of FKN in blood and CSF compared to controls (Fuzzati-Armentero, Cerri & Blandini, 2019).

Mast cells (MCs) are another type of inflammatory molecule residing in the CNS that regulate inflammation, host defense, and tissue repair, and they interact with neurons, astrocytes, and microglia. In fact, MCs can activate astrocytes and microglia. Mast cells are present in most tissues, located close to blood vessels and like astrocytes and microglia, take on a different phenotype

depending on their microenvironment. Mast cells store and release, upon activation, chymase, DA, eotaxin-1, FGF-2, histamine, interleukin 8 (IL-8), MCP-1, NGF, RANTES, serotonin, stem cell factor (SCF), TNF- α , tryptase, tumor growth factor beta (TGF- β), and VEGF, and when activated they can synthesize and release IL-1, IL-6, IL-8, IL-10, NGF, SCF, TGF- β , TNF- α , and VEGF. However, no one MC stores, synthesizes, and releases, all of these factors. In addition, human MCs express BDNF, NGF, NT-3, and TH (Kempuraj et al., 2016, Ronnberg, Calounova & Pejler, 2012, Theoharides et al., 2012). Similar to microglia, MCs express the FKN receptor, CX3CR1 (Beghdadi et al., 2011). They also express the SCF receptor, proto-oncogene c-Kit (KIT), which interacts with SCF (da Silva, Jamur & Oliver, 2014, Theoharides et al., 2012). Stem cell factor promotes mast cell survival, proliferation, maturation, and migration. It is highly expressed by neurons at sites of brain injury and is involved in NSC migration towards these sites (da Silva, Jamur & Oliver, 2014, Iemura et al., 1994, Lu et al., 2006, Norrby, 2002, Sun, Lee & Fine, 2004). The aforementioned chemokine MCP-1 is also involved in MC migration (Collington et al., 2010).

In addition, MCs are also involved in the promotion of angiogenesis by releasing the angiogenic factors chymase, FGF-2, TGF- β , and VEGF (da Silva, Jamur & Oliver, 2014, Norrby, 2002). They play a key role in transplant tolerance; for example, in MC-deficient mice there is no graft tolerance (da Silva, Jamur & Oliver, 2014, Lu et al., 2006). Furthermore, MCs are involved in the regulation of BBB permeability and can induce BBB breakage, which is thought to occur in neurodegenerative diseases like PD, thus allowing MCs and other immune cells to cross over into the CNS (Jones, Nair & Gupta, 2019, Kempuraj et al., 2016, Lindsberg, Strbian & Karjalainen-Lindsberg, 2010, Skaper, Facci & Giusti, 2014).

Although acute inflammation is thought to be neuroprotective, chronic inflammation in the CNS can be detrimental (Kempuraj et al., 2016, Rentzos et al., 2009, Troncoso-Escudero et al., 2018). One of the enigmas of neuroinflammation in PD is whether it is the neuroinflammation that causes the loss of DAN or vice-versa, or if neuroinflammation is increased in order to protect the brain upon DAN loss (Kalia, Lang, 2015, Troncoso-Escudero et al., 2018, Wirdefeldt et al., 2011). One data that supports the view that neuroinflammation exerts negative effects in PD is the fact that NSAIDs and other anti-inflammatory drugs are shown to improve PD symptoms and people who take NSAIDs are less likely to develop PD (De Virgilio et al., 2016, Kalia, Lang, 2015, Wirdefeldt et al., 2011).

Lymph nodes (LNs)

Recently, a connection between the brain and LNs was established. It was found that lymphatic vessels in the CNS carry CSF into the LNs (Aspelund et al., 2015, Louveau et al., 2015). Lymph nodes also express neuronal markers such as MAP2 and SYP, adding more evidence that the CNS and LNs communicate (Huang, J. et al., 2013, Wulfig, Gunther, 2015). In addition, in a study done in MPTP-treated mice, α -syn drained from the CNS to the LNs (Benner et al., 2008). Located in most tissues, including the LNs and CNS, MCs are capable of migrating from the brain to other tissues, including the LNs. In one study, this migration of MCs to the LNs was shown to be essential for immunosuppression (Abraham, St John, 2010, da Silva, Jamur & Oliver, 2014, Lindsberg, Strbian & Karjalainen-Lindsberg, 2010).

Neurogenesis

Neurogenesis is defined as the generation of new neurons from NSCs in the adult brain and two of the main regions of neurogenesis in the brain are the subventricular zone (SVZ), located along the lateral ventricle next to the Str, and the subgranular zone (SGZ), located in the dentate gyrus region of the Hip. In the SVZ, there reside quiescent SCs which become activated and generate transit amplifying cells (TACs) which generate neuroblasts. These neuroblasts migrate to the olfactory bulb (OB), where they mature. In the SGZ, the function is similar: quiescent SCs become activated and generate intermediate progenitor cells which divide into neuroblasts, and the neuroblasts differentiate into fully mature neurons (Apple, Solano-Fonseca & Kokovay, 2017, Daynac et al., 2016, Luo et al., 2006, van den Berge, van Strien & Hol, 2013). The general consensus is that neurogenesis occurs throughout adult life in the SVZ and SGZ, but declines with age in humans, monkeys, rats, and mice, which coincides with increased inflammation in these regions (Apple, Solano-Fonseca & Kokovay, 2017, Ben Abdallah et al., 2010, Jin et al., 2003). In rodents, bromodeoxyuridine (BrdU)-labelled proliferating cells and DCX-labelled immature neurons decrease significantly in the SVZ in middle-aged and old mice compared to young animals, and BrdU+, DCX+, and Ki-67+ cells drop to almost null in the SGZ of mice starting at seven months of age (Ben Abdallah et al., 2010, Jin et al., 2003, Luo et al., 2006).

Frequently used markers of NSCs/NPCs include brain lipid-binding protein (BLBP), GFAP, Ki-67, NES, paired box 6 (PAX6), S100 β (S100B), SRY-box 2 (SOX2), and VIM. Immature neurons express β -III tubulin, DCX, neuronal differentiation 1 (NeuroD1), stathmin 1 (STMN1), and T-box brain protein 2 (TBR2), while some common mature neuron markers are calbindin (CALB1), CALB2, MAP2, neurofilament heavy (NFH), RNA binding Fox-1 homolog 3 (NeuN), postsynaptic

density protein 95 (PSD-95), synapsin I (SYN1), and synaptophysin (SYP) (Ben Abdallah et al., 2010, Jin et al., 2004, Luo et al., 2006, Sarnat, 2013, Zhang, J., Jiao, 2015). A summary of these neural lineage markers can be found in Table 2.

NSCs/NPCs	Immature neurons/neuroblasts	Mature neurons
BLBP	β -III tubulin	CALB1
GFAP	DCX	CALB2
Ki-67	NeuroD1	MAP2
NES	STMN1	NFH
PAX6	TBR2	NeuN
S100B		PSD-95
SOX2		SYN1
VIM		SYP

Table 2: Summary of neural lineage markers

Neurogenesis is impaired by neuroinflammation, while NTFs BDNF, CNTF, EGF, FGF-2, NGF, GDNF, and VEGF, promote neurogenesis (Ekdahl et al., 2003, Pluchino et al., 2008, Shohayeb et al., 2018, Yang et al., 2008). The effect of PD on neurogenesis in patients and *in vivo* models is unclear as some studies find that PD decreases neurogenesis in the SVZ and SGZ, while others find that neurogenesis increases or doesn't change (Ermine et al., 2018, Lim, Bang & Choi, 2018, Marxreiter, Regensburger & Winkler, 2013, van den Berge, van Strien & Hol, 2013). Moreover, it has been suggested that DA controls neurogenesis in the SGZ as DA afferents make connections in the SGZ and DA receptors are located in this region (Takamura et al., 2014, Zhang, T. et al., 2016). The link between neurogenesis and PD symptomology is also interesting as migrating neuroblasts from the SVZ end up in the OB, which is important for olfaction, and olfactory dysfunction is one of the non-motor symptoms of PD. Likewise, the SGZ is located in the Hip, known for its importance in memory and learning, and cognitive dysfunction is another non-motor symptom of PD. In addition, ablation of neurogenesis in animal models leads to anxiety-like behavior, which along with depression, are other non-motor symptoms of PD (Borta, Hoglinger, 2007, Marxreiter, Regensburger & Winkler, 2013, Regensburger, Prots & Winner, 2014).

Although much of the focus in CRT is on the nigrostriatal pathway and behavioral improvement, some *in vivo* PD studies are starting to focus more on the trophic effects of the implanted cells to see if they exert any beneficial effects on neurogenesis. Several publications reported that SC transplant increased SVZ neurogenesis (Park et al., 2012, Yasuhara et al., 2006, Zuo, F. et al., 2017).

Young vs. aged in PD

Parkinson's disease is an age-associated disease, as age is the biggest risk factor for the development of PD. Very few people are diagnosed with PD before the age of 40 and it is usually diagnosed after the age of 60. Furthermore, nearly 5% of people over 65 years old have PD. Human life expectancy is increasing across the globe, and as PD prevalence increases with age, it has been predicted that by the year 2030, the cases of PD worldwide will grow by 50% (Kalia, Lang, 2015, Lesage, Brice, 2009, Sarkar, Raymick & Imam, 2016, Wirdefeldt et al., 2011). While early-stage PD symptoms include tremors, rigidity, bradykinesia, and postural instability, late-stage PD manifestations are even more serious, among them dysphagia, speech dysfunction, urinary incontinence, falling, choking, depression, dementia, and acetylcholine, glutamate, norepinephrine, and serotonin neurotransmitter imbalances (Chai, Lim, 2013, De Virgilio et al., 2016, Kalia, Lang, 2015).

Cell replacement therapy has more clinically beneficial outcomes in younger patients with less advanced PD (Stoker, Barker, 2016, Yasuhara et al., 2017). Moreover, most *in vivo* PD transplantation studies using rodents and non-human primates use adult animals, omit age specifications, and/or do not correctly categorize the animals' age group (Chaturvedi et al., 2006, Gonzalez et al., 2015, Gu et al., 2009, Jackson et al., 2017, Kriks et al., 2011, Redmond et al., 2007). By definition, an adult mouse or rat is between two and three months old. Considering the average lifespan of a mouse is two years and that of a rat is three years, the rodents used in many CRT studies extrapolate to a fairly young age in humans, much younger than 60 years old (Dutta, Sengupta, 2016, Sengupta, 2013). Therefore, although there is no doubt that progress has been made and that CRT has shown potential as a treatment for PD, it is important to have more *in vivo* studies done in older rodents in order to study what mechanisms are different from those in younger animals which lead to not so successful CRT results in older PD patients. Mice aged 10-15 months old are considered middle-aged and aged mice must be at least 18 months old (Apple, Solano-Fonseca & Kokovay, 2017, Dutta, Sengupta, 2016, Jin et al., 2003, Luo et al., 2006).

OBJECTIVES

Over the course of this thesis, the aim was to provide a comprehensive examination of an innovative strategy combining CRT and SC-driven promotion of the natural mechanisms of endogenous repair as a therapeutic approach for PD.

The hypothesis was the following: transplanted hNSCs can replace and take over the functions of the lost or impaired DAN by integrating in the host environment, thus rescuing nigrostriatal innervation, improving motor deficits, and exerting neurotrophic effects, in both adult and middle-aged Parkinsonian mice.

With this, the objectives of this thesis were to:

1. Characterize the hNSC line hVM1 clone 32 *in vitro* prior to transplantation studies by confirming DAN features of the cells which make them suitable for CRT, and by identifying factors secreted by the cells with potential beneficial effects in *in vivo* settings.
2. Study the survival, differentiation, and maturation, of engrafted hVM1 clone 32 cells in adult and middle-aged Parkinsonian mice.
3. Determine the nigrostriatal pathway degeneration in adult and middle-aged Parkinsonian mice and how this relates to functional behavior, and the effect of hVM1 clone 32 transplantation on both of these aspects.
4. Explore the effect of hVM1 clone 32 transplantation on inflammation in adult and middle-aged Parkinsonian mice, by studying astrogliosis and microgliosis in the CNS, and inflammation in the superficial cervical LNs.
5. Examine the effect of hVM1 clone 32 transplantation on mechanisms of repair associated with angiogenesis and neurogenesis.

MATERIALS & METHODS

Ethics statement

All animal work and use of SCs were approved by the Research Ethics Committees of the Universidad Autónoma de Madrid and the Comunidad de Madrid (PROEX149/15). Animal work was done in the Animal Facility of the CBMSO (Registration Number ES280790000180) following the 3Rs (Reduce, Reuse, Recycle) principle, as well as national and European legislation regarding the use of laboratory animals.

Cell culture

The cells used in this study were hVM1 clone 32, with details previously described (Ramos-Moreno et al., 2012, Villa et al., 2009). Briefly, it is a clone isolated based on increased TH generation from the stable, *v-myc*-immortalized hVM1 cell line. The hVM1 cells were generated from dissociated VM tissue of a 10 week-old aborted human fetus. Cells were routinely cultured between passages 15 and 30, on plastic plates treated with 10 µg/ml polylysine (PLL) (Sigma-Aldrich P1274) at a density of 20,000 cells/cm² in proliferation medium. The proliferation medium composition was as follows: The base was Dulbecco's modified Eagle's medium/F-12, GlutaMAX supplement medium (Gibco 31331028), 1% AlbuMAX (Gibco 11020021), 50 mM HEPES (Gibco 15630106), and 0.6% D-glucose (Merck 104074). To this, 1X N2 supplement (Gibco 17502048), 1X homemade non-essential amino acids (composed of L-alanine, L-asparagine, L-aspartic acid, L-glutamic acid, and L-proline), 100 U/ml penicillin, 0.1 mg/ml streptomycin, 20 ng/ml human recombinant FGF-2 (R&D systems 233-FB) and 20 ng/ml human recombinant EGF (R&D systems 236-EG) were added. Cells were grown at 37°C, in a 95% humidity, 5% CO₂, and 5% O₂ atmosphere. For differentiation experiments, multiwell plates were treated with 30 µg/ml PLL overnight, and then incubated with 5 µg/ml laminin (Sigma-Aldrich L2020) for 5 h, before seeding cells into wells. Cells were seeded at 20,000 cells/cm², in proliferation medium. Twenty-four hours later, this medium was replaced with differentiation medium, which is the same one used for proliferation experiments, but the growth factors are replaced with 2 ng/ml human recombinant GDNF (Peprotech 450-10) and 1 mM dibutyryl cAMP (Sigma-Aldrich D0627) (Lotharius et al., 2002). After this, 2/3 of the differentiation medium was changed every two days. Differentiated cell samples were collected after seven days of differentiation. Equivalent multiwell plates with proliferation medium were seeded in parallel and these samples were collected at three days post-seeding.

Immunocytochemistry (ICC)

For ICC studies, cells were seeded on cover glasses in multiwell plates. Cells were fixed with cold 4% paraformaldehyde (PFA) for 15 min and stored in cryoprotectant solution (30% glycerol and 30%

ethylene glycol in 1X phosphate-buffered saline (PBS)). Samples were washed in 1X tris-buffered saline (TBS), blocked in 10% serum in 1X TBS/0.5% TritonX-100, and incubated overnight at 4°C with primary antibodies in 2% serum in 1X TBS/0.5% TritonX-100. The samples were then washed and incubated with appropriate secondary antibodies in 2% serum in 1X TBS/0.5% TritonX-100, at RT for 2 h. For MAP2, SYN1, TH, and β -III tubulin, ICCs, samples were subsequently washed and incubated with streptavidin (Invitrogen SA1010) in 1X TBS/0.5% TritonX-100 at RT for 45 min. Nuclei were stained with 4',6-Diamidino-2-phenylindole dihydrochloride (DAPI) (1:1000; Santa Cruz sc-3598). All samples were then washed with 1X TBS, air-dried, and mounted with homemade Mowiol mounting medium, composed of 10% MOWIOL 4-88 Reagent (Merck 475904), 2.5% 1,4-diazabicyclo[2.2.2]octane (Sigma-Aldrich 27802), and 33% glycerol, in dH₂O and 0.2 M Tris (pH 8.5). Primary and secondary antibodies used are listed in the following table (Table 3).

Antibody	Dilution	Supplier	Reference
β -III tubulin	1:250	Sigma-Aldrich	T2200
GABA	1:1000	Sigma-Aldrich	A2052
GFAP	1:500	DAKO	Z0334
Ki-67	1:200	ThermoFisher Scientific	RM-9106-S1
MAP2	1:250	Sigma-Aldrich	M4403
SYN1	1:250	Merck	AB1543
TH	1:250	Sigma-Aldrich	T1299
VIM	1:500	Santa Cruz	sc-6260
Biotinylated Horse Anti-Mouse IgG Antibody, rat adsorbed	1:500	Vector Laboratories	BA-2001
Goat anti-Mouse IgG (H+L) Highly Cross-Adsorbed Secondary Antibody, Alexa Fluor 546	1:500	Invitrogen	A-11030
Donkey anti-Mouse IgG (H+L) Highly Cross-Adsorbed Secondary Antibody, Alexa Fluor 647	1:500	Invitrogen	A-31571
Goat anti-Rabbit IgG (H+L) Highly Cross-Adsorbed Secondary Antibody, Alexa Fluor 546	1:500	Invitrogen	A-11035
Goat anti-Rabbit IgG (H+L) Highly Cross-Adsorbed Secondary Antibody, Alexa Fluor 647	1:500	Invitrogen	A-21245

Table 3: Primary and secondary antibodies used in ICC experiments.

Next-generation sequencing (NGS)

An exploratory NGS study was performed using two samples of both proliferating and differentiated hVM1 clone 32 cells. Cell culture media was removed and cells were rinsed with 1X PBS. In order to isolate RNA from the samples, TRIzol Reagent (Invitrogen 15596026) was added to the cells and RNA extraction was done using the Direct-zol RNA Miniprep Plus kit (Zymo Research R2071). Whole-transcriptome analysis was done on RNA samples with Illumina total RNA-Seq technology using the ScriptSeq Complete kit (Illumina RS-122-2201), which entailed rRNA removal, cDNA synthesis, 3' terminal tagging, and PCR purification, followed by sequencing using the NextSeq 550 Sequencing kit and system (Illumina). Reads were generated from raw total RNA-Seq data and mapped to the human genome, and the htseq-count tool was used to count the number of reads mapping each gene. Differential expression analysis was then performed on raw total RNA-Seq data using the DESeq 2 package, with differences in gene expression between dividing and differentiating cells being expressed as fold change. Negative fold change indicates that the gene is more highly expressed in proliferating cells, and positive fold change indicates that the gene is more highly expressed in differentiated cells.

Luminex assay

Proliferation and differentiation conditioned media (CM) were collected from their respective plates and centrifuged for 10 min at 2500 rpm. Supernatant was collected and stored at -80°C for further analysis. A minimum of three samples of proliferation and differentiation CM were analyzed with the Bio-technie R&D Systems Luminex Human Magnetic Assay custom-made plate (Code LXSAHM-12) for the following analytes: BDNF, Eotaxin, FKN, GDNF, IL-6, IL-10, LIF, MCP-1, RANTES, SCF, VEGF-A, and VEGF-C. Observed concentration (pg/ml) of two replicates of each sample were measured using the Bio-Rad Bio-Plex 100 system.

Animal experimentation

Male C57BL/6JRccHsd mice (Envigo, Netherlands) were used in this study. Animals referred to as "adult" were five months old at the beginning of the experiment, while animals referred to as "middle-aged" were 12 months old. All mice were housed in a temperature- and humidity-controlled room on a 12-hour light/dark cycle, and fed *ad libitum* with standard food and water. Animals were randomly separated into one of three experimental groups. Control mice were injected with 0.9% saline i.p. once every two hours, with a total of three injections, at 10 µl/g. Using the same injection protocol, PD was induced in other mice by injecting MPTP (Sigma-Aldrich M0896) i.p. at 15 mg/kg (acute MPTP protocol). Mice injected with MPTP underwent stereotaxic surgery to receive an intracerebral

injection in the left Str (Coordinates: Anteroposterior 0.25 mm, Mediolateral 2.75 mm, Dorsoventral 3 mm; Figure 3) of either 1.5 μ l transplantation medium or 100,000 mycoplasma-free hVM1 clone 32 cells in passage 26 in 1.5 μ l transplantation medium. The transplantation medium was composed of the following: 49% Leibovitz's L-15 Medium (ThermoFisher Scientific 11415064), 49% filtered 0.6% Glucose (Merck 104074) in 1X PBS, and 2% B-27 Serum-Free Supplement (Gibco 17504044).

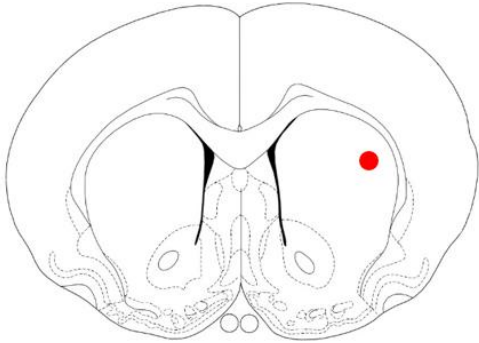


Figure 3: Location of transplant indicated by red dot.

For surgery, animals were anesthetized with a mixture of ketamine at 80 mg/kg (Merial) and xylazine at 10 mg/kg (Calier) i.p. When animals were confirmed to be asleep via toe pinching, surgery began. After positioning the animal's head in the frame of the stereotaxic apparatus, its head was shaved. After the animal's skull was revealed, a 23 gauge needle with 0.635 mm outer diameter was used to make a hole in the skull. Through this hole, a 22 gauge needle (Hamilton Company; 22 gauge, Small Hub RN NDL, length 0.75 in, point style 4 cut at an angle of 10-12°) held in the attached syringe (Hamilton Company; 10 μ l, Model 701 RN, 26s gauge, 51 mm, point style 2), was lowered into the brain to inject either the transplantation medium or hNSCs in the left Str. The speed of injection was 1 μ l/min, and the needle was left in for 2 min after injecting cells before its slow removal, and subsequent suturing of the mice's head (Silkam C0762121). The antibiotic oxytetracycline (0.135-0.25 mg/ml depending on weight; Terramycin®, Zoetis) was delivered *ad libitum* in drinking water of MPTP-treated animals starting the day of surgery for a total period of one week as a preventative measure. In order to avoid graft rejection, two days prior to transplant and for the remainder of the experiment, all animals were treated with daily weekday injections of cyclosporine A (CSA; Novartis) i.p. at 10 mg/kg. Twice a week, CSA was included in the drinking water, prepared with the following components: 0.25 g/L CSA (Novartis), 0.24% sodium cyclamate (Carrefour), and 0.024% sodium saccharin (Carrefour). Two adult mice and five middle-age mice died following MPTP injections. All animals survived both buffer and SC transplant surgeries, and showed no symptoms of distress, infection, or pain. Four months post-transplant, all animals were sacrificed. A timeline of animal experimentation is shown in Figure 4.

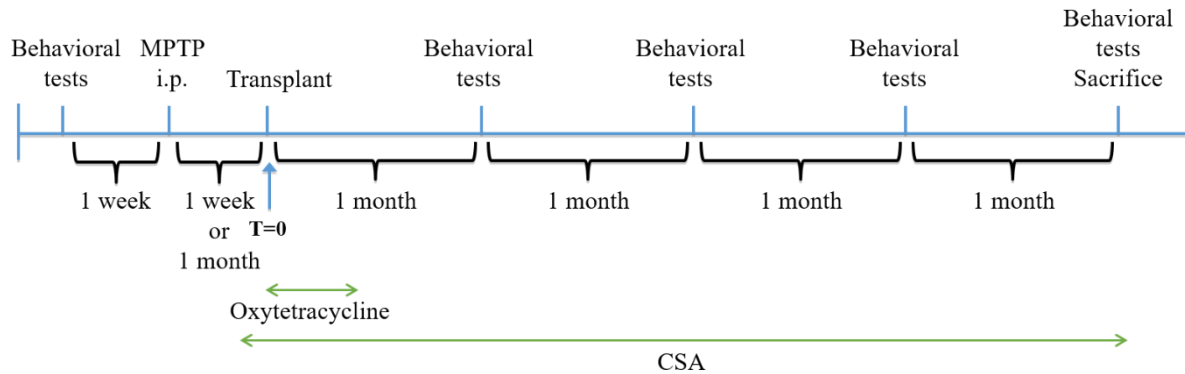


Figure 4: Chronological timeline of animal experiments.

Behavioral tests

Animals received three training sessions prior to taking basal measurements for all behavioral tests, namely OFT and PPT. The former was used to measure locomotion and anxiety, and the latter was used to measure changes in gait. Behavioral tests were performed prior to saline and MPTP injections, and one month, two months, three months, and four months post-transplant. All OFTs were performed in the same room, with the same lighting, and at the same time.

OFT

Animals were placed in a 40 cm x 40 cm x 30 cm (L x W x H) four-walled cubic box and their movements were filmed for 10 min. Distance moved, average speed, time spent in the center (20 cm x 20 cm central area), time spent rearing (mouse stands on hind legs), time spent grooming (mouse licks or scratches itself while being stationary), urination (number of puddles or streaks of urine), and defecation (number of fecal boli), were counted using the ANY-maze behavioral tracking software.

PPT

The animals' paws were painted (forelimbs in green and hindlimbs in orange) and the mice then walked on a 40 cm x 12 cm white piece of paper. Contralateral (CL) and ipsilateral (IL) stride length (the distance between two same-sided forelimbs or two same-sided hindlimbs) (Figure 5A&B), CL-IL and IL-CL stride width (the distance between two opposite-sided forelimbs or two opposite-sided hindlimbs) (Figure 5C&D), and CL and IL paw overlap (the distance between a same-sided forelimb and hindlimb) (Figure 5E&F), were measured.

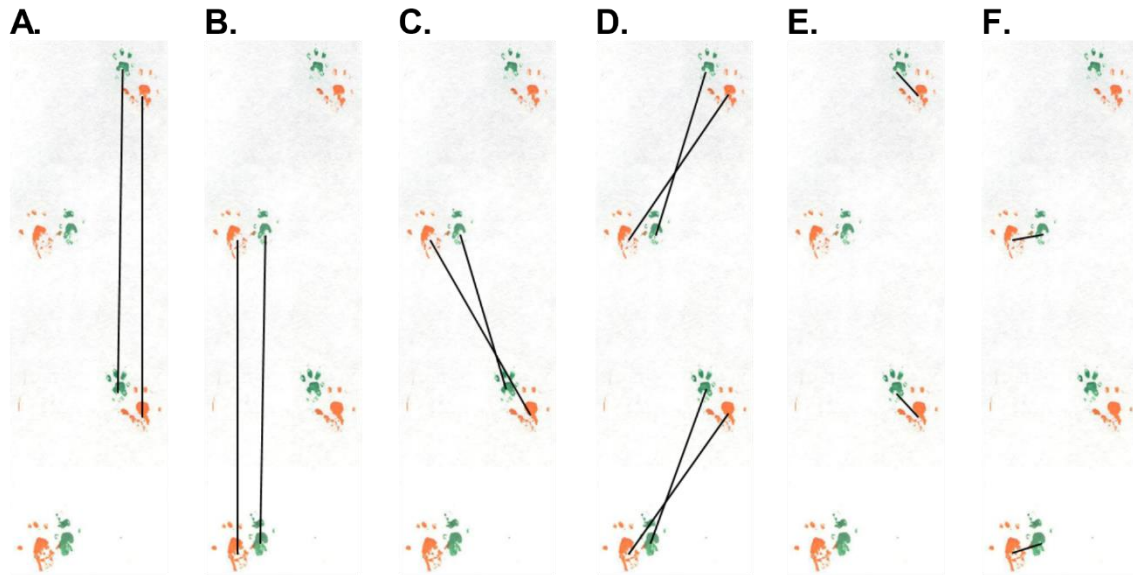


Figure 5: Measurements used in the PPT. Contralateral stride length (A), IL stride length (B), CL-IL stride width (C), IL-CL stride width (D), CL paw overlap (E), and IL paw overlap (F).

Immunohistochemistry (IHC)

Animals were sacrificed via transcardial perfusion and fixation using cold 4% PFA. After 12-hour post-fixing with 4% PFA, the tissue was dehydrated in 30% sucrose until tissue sunk. Ten μm -thick sections of superficial cervical LNs were sliced onto glass slides (Menzel-Gläser) using a cryostat, while free-floating 15 μm -thick coronal sections of the brain were sliced using a freezing microtome.

Brain sections were washed and then blocked in 3-5% serum in 1X PBS/0.3% TritonX-100 and incubated overnight at 4°C with primary antibodies in 1% serum in 1X PBS/0.3% TritonX-100. The next day, fluorescent IHC samples were washed and incubated with adequate secondary antibodies and DAPI (1:1000; Santa Cruz sc-3598), in 1% serum in 1X PBS/0.3% TritonX-100 at RT for 2 h. Primary and secondary antibodies used are listed in the following table (Table 4).

Antibody	Dilution	Supplier	Reference
beta-dystroglycan (β -DAG)	1:100	Leica	NCL-b-DG
DCX	1:300	Santa Cruz	sc-8066
GFAP	1:1000	DAKO	Z0334
Ionized calcium-binding adapter molecule 1 (Iba1)	1:1000	Wako	019-19741
Ki-67	1:100	ThermoFisher Scientific	RM-9106-S1
NES	1:300	Novus Biologicals	NB100-1604
STEM121	1:500	Takara Bio	Y40410
TH	1:400	Pel-Freez	P40101-150
Alexa Fluor 488 AffiniPure Donkey Anti-Chicken IgY (IgG) (H+L)	1:500	Jackson ImmunoResearch	703-545-155
Biotinylated Goat Anti-Rabbit IgG Antibody	1:500	Vector Laboratories	BA-1000
Biotinylated Horse Anti-Goat IgG Antibody	1:200	Vector Laboratories	BA-9500
Goat anti-Mouse IgG (H+L) Highly Cross-Adsorbed Secondary Antibody, Alexa Fluor 488	1:1000	Invitrogen	A-11029
Goat anti-Mouse IgG (H+L) Highly Cross-Adsorbed Secondary Antibody, Alexa Fluor 546	1:1000	Invitrogen	A-11030
Goat anti-Rabbit IgG (H+L) Highly Cross-Adsorbed Secondary Antibody, Alexa Fluor 488	1:1000	Invitrogen	A-11034
Goat anti-Rabbit IgG (H+L) Highly Cross-Adsorbed Secondary Antibody, Alexa Fluor 546	1:500 or 1:1000	Invitrogen	A-11035

Table 4: Primary and secondary antibodies used in IHC experiments.

Sections in β -DAG IHC used 1X TBS and not 1X PBS as a buffer throughout the protocol, sections were blocked with a mix of 10% serum and 5% BSA, and antibodies were prepared in 1X TBS/0.3% TritonX-100, 1% serum, and 1% BSA. All fluorescent IHC samples were washed, mounted onto glass slides (Menzel-Gläser), air-dried, and coverslipped with Mowiol mounting medium.

Sections in TH and DCX IHCs were incubated with a mix of 1% of 30% hydrogen peroxide, 3% methanol, and 6% 1X PBS for 15 min, before blocking, and DCX sections were incubated with 1% SDS in 1X PBS for 5 min prior to the latter step. After incubation with biotinylated secondary antibodies, sections were washed and incubated in ABC solution (VECTASTAIN Elite ABC HRP Kit, Vector Laboratories PK-6100), washed, and developed with the Vector VIP Peroxidase (HRP) Substrate kit (Vector Laboratories SK-4600). Peroxidase samples were mounted onto slides,

air-dried, dehydrated with xylene, and coverslipped with distyrene, plasticiser, and xylene (DPX) mounting medium.

Western blot (WB)

All protein extractions from fresh superficial cervical LN tissue were done using RIPA buffer and sonicating the sample. A Bradford assay was performed to determine sample concentrations and 5x SDS-PAGE Sample Loading Buffer (NZYTech MB11701) was added to the samples. Samples were then denatured at 95°C for 5 min. Amount of proteins loaded were: 2 µg Str and 50 µg LN. Samples were run on 8-12.5% polyacrylamide gels with semi-dry transfer onto nitrocellulose membrane. Membranes were blocked at RT in 5% non-fat milk in 1X TBS. After a quick rinse with 1X TBS, membranes were incubated overnight at 4°C with primary antibody in TBS/T (1X TBS and 0.05% Tween20). The next day, membranes were washed and incubated with adequate peroxidase-conjugated secondary antibodies in TBS/T at RT. After washing, membranes were developed with ECL Prime Western Blotting Detection Reagent (Amersham RPN2232). Primary and secondary antibodies used are listed in the following table (Table 5).

Antibody	Dilution	Supplier	Reference
β-III tubulin	1:500	Sigma-Aldrich	T2200
Neurofilament light (NFL)	1:1000	Chemicon	MAB1615
PSD-95	1:2000	Neuromab	75-028
SYP	1:500	Zymed	180130
TH	1:1000	Pel-Freez	P40101-150
HRP Horse Anti-Mouse IgG Antibody (Peroxidase)	1:500 or 1:1000	Vector Laboratories	PI-2000
Goat Anti-Rabbit IgG (H+L)-HRP Conjugate	1:1000	Bio-Rad	172-1019

Table 5: Primary and secondary antibodies used in WB experiments.

Toluidine histology

Free-floating brain sections were mounted onto glass slides (Menzel-Gläser) prior to staining. Slides containing brain and LN samples were stained with acidic toluidine blue working solution. Toluidine blue is used in histology to detect MCs (Lindsberg, Strbian & Karjalainen-Lindsberg, 2010). The working solution was prepared as follows: 5 ml of toluidine blue stock solution (1% toluidine blue O (Sigma-Aldrich T3260) in 70% ethanol), and 45 ml 1% NaCl (Merck Millipore 7647-14-5) in dH₂O (pH 2.27). After, slides were dehydrated with ethanol, cleared in xylene, and coverslipped with DPX.

Microscopy

Images of DCX and TH IHCs as well as histological staining of LNs, were obtained with an Axioskop 2 Plus microscope (Zeiss) using the 2.5X-10X objectives. Images of STEM121/GFAP and NES IHCs were obtained with a DM IRB microscope (Leica) using the 20X-40X objectives. If necessary, images of the aforementioned stainings were then automatically merged using Adobe Photoshop CS5 Extended. Images of β -DAG, GFAP, and Iba1, IHCs, were obtained with the Tile Scan of an Axiovert 200 microscope (Zeiss) using the 20X objective. Representative brightfield images were obtained with an Axioskop 2 plus microscope (Zeiss). Except for Figure 9 images which were obtained with a DM IRB microscope (Leica), all representative fluorescent images were obtained with a LSM800 confocal microscope (Zeiss).

Histological quantifications

For all β -DAG, DCX (SGZ), GFAP, Iba1, and TH IHCs, region of interest was drawn, threshold was set to be the same for all animals for each IHC, and area fraction, or integrated density in the case of β -DAG, was measured. For TH IHCs, the area fraction in the Str is made up of fibers and that of the SNpc is made up of cells and their prolongations. For DCX and NES quantifications in the SVZ, after setting threshold, immunopositive area was measured. Number of Ki-67+ cells in the SVZ was counted at the with a DM IRB microscope (Leica) using the 20X objective by an unbiased observer. After taking photos of LNs, area was measured and number of MCs was counted manually. ImageJ was used to do all quantifications except that of Ki-67. Two-five sections, including both IL and CL sides, of a minimum of three animals per experimental group were quantified for every experiment, and all six experimental groups were tested at once in order to allow for comparison.

Statistical analysis

Two replicas of the adult mouse experiments and one of the middle-aged mouse experiments were performed. All statistical analyses were done and figures were made using GraphPad Prism 7.0. Error bars on figures indicate standard error of the mean. For NGS differential expression analysis, p-values and q-values were calculated; the latter is a p-value adjusted for the false discovery rate used in the case of multiple testing. For comparisons between two groups, as in the case of the Luminex assays, two-tailed unpaired t-tests were performed. For comparisons between more than two groups, one-way analysis of variance followed by Tukey's post-hoc test were performed. Linear correlation was calculated using Pearson correlation coefficient (r). A p-value or q-value of less than 0.05 was considered significant.

Significance legend: *, # = $p < 0.05$, **, ## = $p < 0.01$, ***, ### = $p < 0.001$, ****, #### = $p < 0.0001$.

RESULTS

In vitro characterization of hVM1 clone 32 cell line

In concordance with Ramos-Moreno et al., 2012, which originally described the hVM1 clone 32 cells, after seven days of differentiation, the cells expressed DAN marker TH and immature neuronal marker β -III tubulin. At this stage of differentiation, the hNSCs still express NSC/NPC markers Ki-67 and VIM, and begin to express mature neuronal markers like MAP2 and SYN1. Although the differentiated hVM1 clone 32 cells tend to generate DAN because of their tissue of origin, the VM, in addition to their purposeful direction of differentiation toward DAN based on the factors in the differentiation media, namely GDNF and dibutyryl cAMP, the culture is not entirely homogeneous; markers for astrocytes (GFAP) and GABAergic neurons (GABA), were found in the culture after seven days of differentiation (Figure 6).

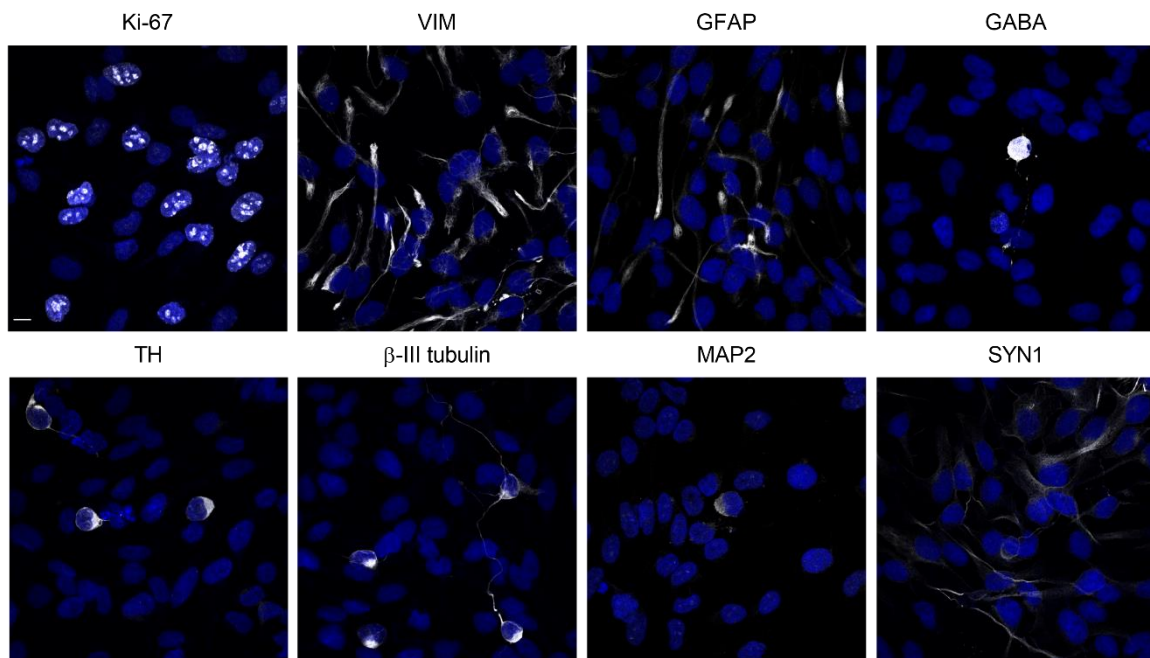


Figure 6: Photos of the proteins expressed by hVM1 clone 32 cells after seven days of differentiation. Top row images show, from left to right, Ki-67, VIM, GFAP, and GABA. Bottom row images show, from left to right, TH, β -III tubulin, MAP2, and SYN1. Scale bar = 10 μ m.

To further characterize the hVM1 clone 32 cells, an exploratory NGS study was performed on RNA extracted from the cells under proliferation and differentiation conditions. This was done in order to identify genes expressed in both settings and to perform a differential expression analysis of which genes were more highly expressed under each condition. Around 34,000 genes were matched to the human genome in proliferating cells and more than 37,000 genes in differentiated cells were mapped to this genome. A total of 15,212 statistically significant differentially expressed genes were identified (Supplementary Figure 1).

The genes of higher interest for the purpose of this thesis were genes related to NSCs and NPCs, general neuronal markers, and DAN. The majority of NSC/NPC-associated genes were upregulated in dividing cells and downregulated in differentiated cells, while the majority of general neuronal markers and DAN-associated genes were upregulated in differentiated cells and downregulated in proliferating cells (Figure 7).

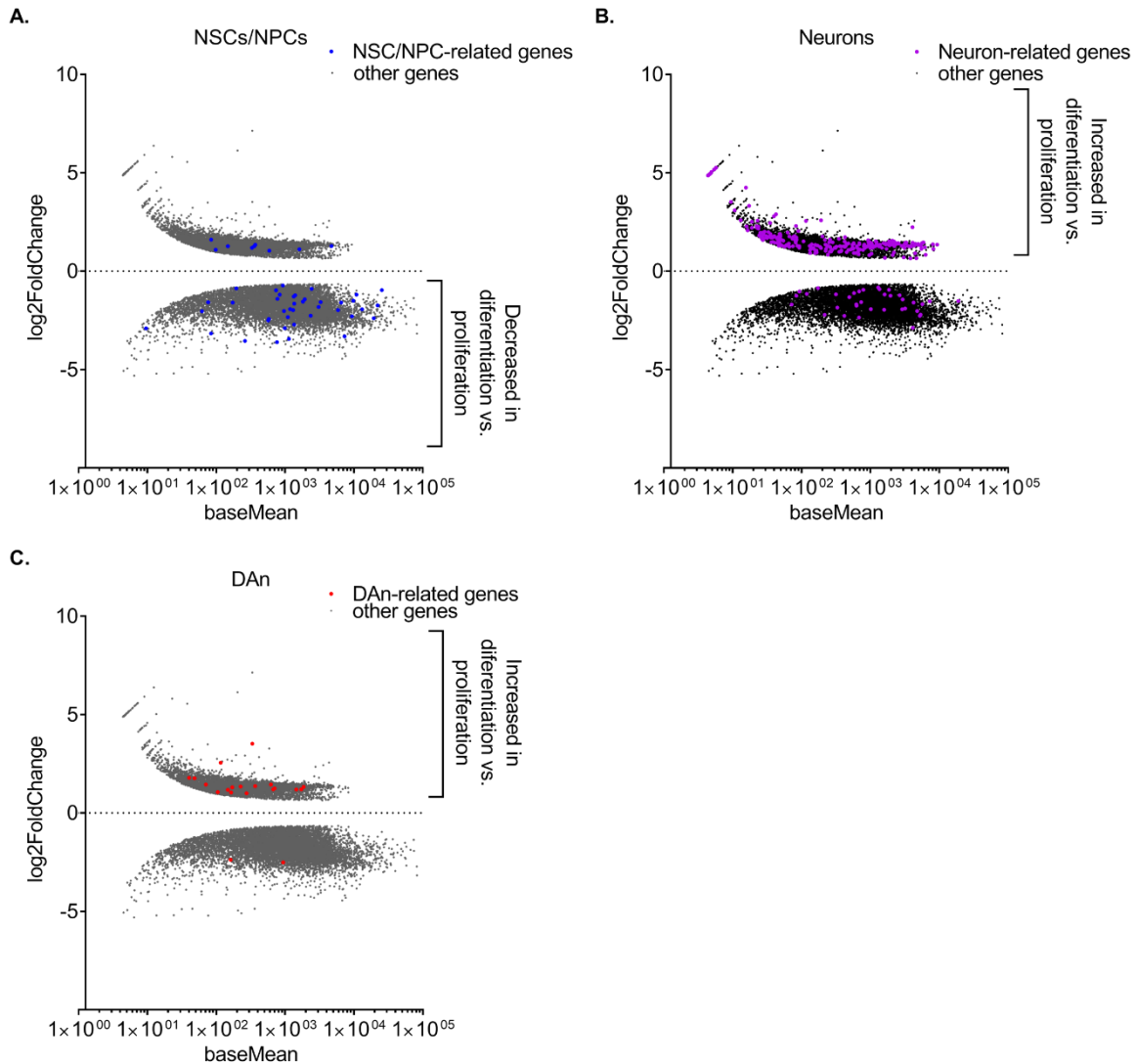


Figure 7: Dotblots representing NSC/NPC- (A), neuron- (B), and DAN- (C) related gene expression fold change of hVM1 clone 32 cells in proliferation and differentiation conditions.

Hallmark NSC/NPC markers *NES* and *VIM* were upregulated in proliferation conditions compared to differentiation, while surprisingly *SOX2* was not detected in the whole-transcriptome analysis. Other NSC/NPC-associated genes with higher expression levels in proliferation compared to differentiation, were *BLBP*, *MKI67* (which codes for Ki-67), *NOTCH1*, *NOG*, and *NUMB* (Table 6). Some NSC/NPC markers were found to be expressed higher in differentiation conditions than proliferation conditions,

including *ROR2*, *OCN*, and *PAX6* (Supplementary Table 1). Although one would expect all of the NSC/NPC genes to be downregulated upon differentiation, this is still an early stage of differentiation at seven days so it is not out of the ordinary that there would still be some NSC/NPC genes still highly expressed.

Immature neuron marker *STMN1* had higher expression in division while *DCX* had higher expression in differentiation. Many genes important in the maintenance of mature neurons were upregulated in differentiated cells, most notably *CALB2*, neural cell adhesion molecule 2 (*NCAM2*), *NEUN*, neuregulins, neurexins, synapsins, synaptotagmins, synaptopodins, synaptoporins, and microtubule-associated protein Tau (Table 6, Supplementary Table 1).

Because of the tissue of origin of the hVM1 clone 32 cells, the VM, and with the goal of generating DAN for CRT for PD, it was important to analyze which genes involved in DAN generation and maintenance were expressed in the differentiated hNSCs. All genes listed in Table 1 of the Introduction section were expressed by hVM1 clone 32 cells after seven days of differentiation, including *DAT*, *GIRK2*, *LMX1A*, *LMX1B*, *NURR1*, *PITX3*, and *TH*. Signaling by SHH, WNT 1/2/3a/5, and BMP 2/5/7, has been shown to be important in DAN differentiation, and all of these genes were also expressed by differentiated hVM1 clone 32 cells. Furthermore, expression of *EGF*, *FGF-1*, *FGF-2*, *FGF-8*, *FGF-9*, and *FGF-20*, all of which play a role in the survival, differentiation, and protection of DAN (Kriks et al., 2011, Tome et al., 2017, Xia et al., 2016), were present in the differentiated hNSCs' transcriptome.

The hVM1 clone 32 cells expressed astrocyte-related genes such as *HES1*, *S100B*, and *GFAP*, at high levels under both proliferation and differentiation states (Table 6). This is not surprising as these genes are markers for both undifferentiated radial glia and differentiated astrocytes. Moreover, oligodendrocyte-associated genes *MBP*, *MOBP*, and *OPALIN*, were expressed higher under differentiation conditions compared to proliferation conditions (Table 6).

Astrocyte-secreted NTFs *MANF* and *CNTF* were more highly expressed in proliferating cultures. Several NTF receptors were upregulated in differentiated cultures, namely genes coding for GFR α 1 (*GFRA1*), GFR α 2 (*GFRA2*), TrkA (*NTRK1*), TrkB (*NTRK2*), and TrkC (*NTRK3*). To reiterate, GFR α 1 and GFR α 2 bind GDNF, ARTN, and NRTN, while TrkA binds NGF and NT-3, TrkB binds BDNF, NT-3, and NT-4, and TrkC binds NT-3 (Allen et al., 2013, Sampaio et al., 2017, Tome et al., 2017). Several VEGF family members and their receptors were expressed in both proliferating and

differentiated hVM1 clone 32 cells including *VEGFA*, *VEGFB*, *VEGFC*, *VEGFR1*, *VEGFR2*, *NRP1*, and *NRP2* (Table 6).

The *MCP1* gene was upregulated in proliferating cells, while its receptor *CCR2* was expressed higher under differentiation conditions. Fractalkine and its receptor *CX3CR1*, and *SCF* and its receptor *KIT*, were all expressed in differentiated cultures. Genes encoding pro-inflammatory cytokines IL-1 β (*IL1B*) and IL-6 (*IL6*), were upregulated in differentiated cells. Other genes of interest found to be expressed higher in differentiated cultures than proliferation cells were *SNCA* and *LRRK2*, two genes involved in familial PD (Table 6, Supplementary Table 1).

Like the ICCs in Figure 6 show, DAn are not the only neuronal type found in the differentiated hNSC cell culture. Serotonergic neuron-related genes *SLC6A4* and *TPH2*, GABAergic neuron-related genes *GABBR1*, *GABBR2*, and *SLC6A*, glutamatergic neuron-associated genes *GRIN2B* and *SLC17A6*, and cholinergic neuron-associated gene *CHAT*, all had increased expression in differentiated cultures compared to dividing cultures, confirming the heterogeneity of the differentiated culture (Table 6).

Category	Gene symbol	Gene ID	Fold change	q-value
NSCs/NPCs	<i>MKI67</i>	ENSG00000148773	-3.31	4.73E-24
	<i>NOTCH1</i>	ENSG00000148400	-2.89	1.23E-16
	<i>NES</i>	ENSG00000132688	-2.29	1.08E-10
	<i>NOG</i>	ENSG00000183691	-2.03	0.000214
	<i>BLBP</i>	ENSG00000164434	-1.82	1.13E-05
	<i>VIM</i>	ENSG00000026025	-1.74	1.10E-06
	<i>NUMB</i>	ENSG00000133961	-0.72	0.0322
Immature neurons	<i>STMN1</i>	ENSG00000117632	-2.35	2.77E-10
	<i>DCX</i>	ENSG00000077279	1.07	0.00581
Mature neurons	<i>CALB2</i>	ENSG00000172137	1.00	0.0448
	<i>NEUN</i>	ENSG00000167281	1.17	0.00124
	<i>SYN1</i>	ENSG00000008056	1.29	0.0158
Factors and their receptors	<i>VEGFR2</i>	ENSG00000128052	-2.26	2.98E-11
	<i>MANF</i>	ENSG00000145050	-2.25	1.02E-09
	<i>CNTF</i>	ENSG00000242689	-1.90	0.0138
	<i>VEGFB</i>	ENSG00000173511	-1.90	7.80E-08
	<i>NRP2</i>	ENSG00000118257	-1.90	5.57E-09
	<i>VEGFA</i>	ENSG00000112715	-1.42	1.17E-05
	<i>SCF</i>	ENSG00000049130	-1.25	0.000233
	<i>NRP1</i>	ENSG00000150630	-0.83	0.0158
	<i>EGF</i>	ENSG00000138798	0.75	0.0356
	<i>NTRK3</i>	ENSG00000140538	0.82	0.0150
	<i>NTRK1</i>	ENSG00000198400	0.96	0.0345
	<i>VEGFC</i>	ENSG00000150630	1.33	0.00194
	<i>GFRA2</i>	ENSG00000168546	1.34	0.00248
	<i>VEGFR1</i>	ENSG00000102755	1.38	0.000631
	<i>KIT</i>	ENSG00000157404	1.49	0.000148

Category	Gene symbol	Gene ID	Fold change	q-value
	<i>GFRA1</i>	ENSG00000151892	1.53	8.19E-05
	<i>NTRK2</i>	ENSG00000148053	1.55	5.42E-06
Astrocytes/Radial glia	<i>HES1</i>	ENSG00000114315	-2.43	1.20E-09
	<i>S100B</i>	ENSG00000160307	-1.97	3.95E-07
	<i>SLC1A3</i>	ENSG00000079215	-1.65	5.29E-06
	<i>ALDH1L1</i>	ENSG00000144908	0.86	0.0326
	<i>GFAP</i>	ENSG00000131095	2.65	3.89E-09
Oligodendrocytes	<i>MOBP</i>	ENSG00000168314	1.15	0.0118
	<i>MBP</i>	ENSG00000197971	1.20	0.00505
	<i>OPALIN</i>	ENSG00000197430	2.18	0.00116
DAn	<i>DRD2</i>	ENSG00000149295	1.00	0.0102
	<i>WNT3A</i>	ENSG00000154342	1.04	0.0180
	<i>WNT2</i>	ENSG00000105989	1.06	0.0297
	<i>DAT</i>	ENSG00000142319	1.18	0.0223
	<i>GIRK2</i>	ENSG00000157542	1.19	0.00152
	<i>ALDH1A2</i>	ENSG00000128918	1.20	0.000892
	<i>ALDH1A1</i>	ENSG00000165092	1.20	0.00281
	<i>PAX5</i>	ENSG00000196092	1.25	0.00111
	<i>SLC6A2</i>	ENSG00000103546	1.31	0.00310
	<i>DRD3</i>	ENSG00000151577	1.32	0.000901
	<i>MYT1L</i>	ENSG00000186487	1.33	0.000204
	<i>LMX1B</i>	ENSG00000136944	1.34	0.00103
	<i>BMP5</i>	ENSG00000112175	1.36	0.00182
	<i>LMX1A</i>	ENSG00000162761	1.44	0.000189
	<i>PITX2</i>	ENSG00000164093	1.45	0.0105
	<i>BMP2</i>	ENSG00000125845	1.76	0.00622
	<i>PITX3</i>	ENSG00000107859	1.78	0.0121
	<i>TH</i>	ENSG00000180176	2.55	2.41E-07
Cytokines and their receptors	<i>MCP1</i>	ENSG00000108691	-1.70	5.48E-05
	<i>CCR2</i>	ENSG00000121807	1.82	0.0151
	<i>IL1B</i>	ENSG00000125538	2.53	0.00480
	<i>IL16</i>	ENSG00000136244	2.92	0.0382
Serotonergic neurons	<i>SLC6A4</i>	ENSG00000108576	1.07	0.0186
	<i>TPH2</i>	ENSG00000139287	1.27	0.00269
GABAergic neurons	<i>SLC6A1</i>	ENSG00000157103	1.07	0.0203
	<i>GABBR1</i>	ENSG00000204681	1.09	0.00480
	<i>GABBR2</i>	ENSG00000136928	1.32	0.000261
Glutamatergic neurons	<i>SLC17A6</i>	ENSG00000091664	0.92	0.0405
	<i>GRIN2B</i>	ENSG00000273079	1.43	0.000233
Cholinergic neurons	<i>CHAT</i>	ENSG00000070748	1.11	0.00847

Table 6: Gene expression of dividing and differentiated hVM1 clone 32 cells. In blue are genes upregulated in proliferation, and in red are genes upregulated in differentiation.

With ICC and NGS data indicating that these cells had the potential to differentiate into DAn, the CM of the hVM1 cells in proliferation and differentiation conditions were analyzed to see if the cells were secreting any factors that may be beneficial to Parkinsonian mice upon transplantation. The proliferation and differentiation media were composed of 1% AlbuMAX (Gibco 11020021), which is BSA. Thus, before performing a proteomic study by mass spectrometry to identify all of the proteins being released by the cells, a preliminary experiment was performed to see if the high amount

of albumin in the CM would interfere in the identification of other proteins. This did in fact occur, and even an attempt at albumin depletion did not manage to reduce the amount of albumin enough to be able to perform the proteomic study.

Therefore, a magnetic-based assay was done to study the levels of pre-determined proteins in the CM. The analytes were chosen based on PD pathogenesis and treatment literature, as well as NGS results. Eotaxin-1, IL-10, LIF, and RANTES levels were practically undetectable in all CM. Their genes were not identified in the NGS either. The chemokine MCP-1 was increased in differentiation CM compared to proliferation, but this did not reach statistical significance. However, *MCP1* had upregulated gene expression in dividing cells in the whole-transcriptome study. Concentrations of BDNF, VEGF-A, VEGF-C, SCF, FKN, and IL-6, were all significantly increased in differentiation compared to proliferation CM. However, their concentration in differentiation CM varied greatly, with IL-6 barely being present (approximately 0.3 pg/ml) and the concentrations of the other analytes ranged from around 3 pg/ml (BDNF) to over 10,000 pg/ml (MCP-1) (Figure 8). This coincided with NGS data because the genes encoding BDNF receptor TrkB, FKN receptor CX3CR1, SCF receptor KIT, and VEGF-C, were expressed in differentiated hVM1 clone 32 cell cultures. Although *VEGFA* gene expression was upregulated in proliferating cells, its protein concentration was significantly increased in differentiation CM. Furthermore, in the whole-transcriptome study, *IL6* expression was more elevated in differentiated cells. At the moment, GDNF is the NTF which shows the most promise in PD NTF replacement and gene therapy treatments. It was not detected in either basal proliferation medium (20/20+) nor proliferation CM. The NTF GDNF is a difficult analyte to study under differentiation conditions because although basal levels of differentiation media (Lotharius) components are subtracted from CM levels, GDNF is added to the media during the medium change several times throughout the hNSC differentiation protocol. As seen in Figure 8, there was a non-significant increase in GDNF concentration in differentiated CM compared to proliferation CM, while NGS results showed a significantly higher expression of GDNF receptors *GFRA1* and *GFRA2* in differentiation conditions.

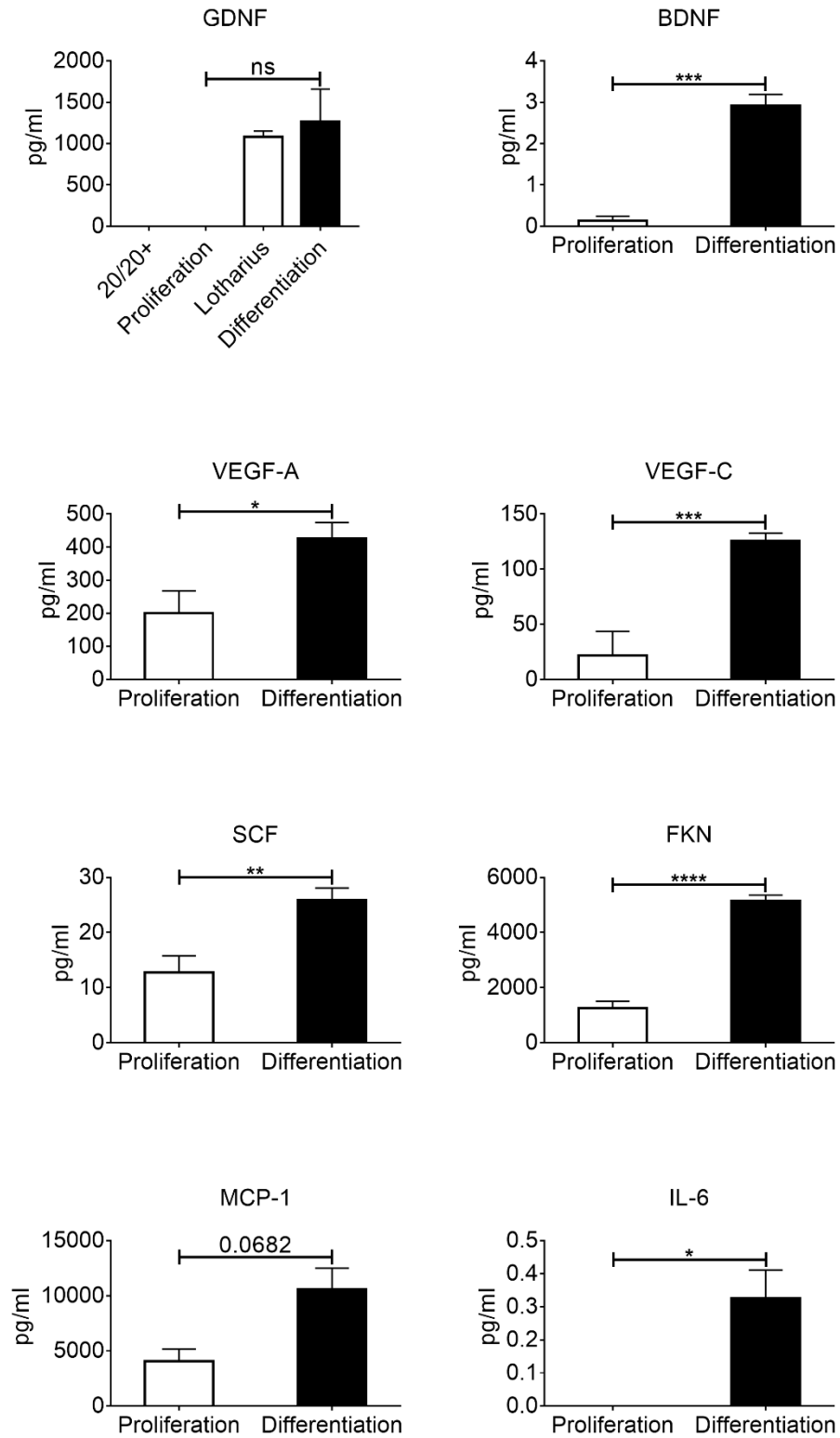


Figure 8: Concentration (pg/ml) of GDNF, BDNF, VEGF-A, VEGF-C, SCF, FKN, MCP-1, and IL-6, released by hVM1 clone 32 cells in proliferation and differentiation conditions. 20/20+ = basal proliferation medium, which does not contain GDNF. Lotharius = basal differentiation medium, which contains GDNF. ns = not significant.

Therefore, it can be stated that *in vitro* characterization via ICC, NGS, and Luminex assay, revealed that hVM1 clone 32 cells are true hNSCs that have the capability of generating genuine A9 DAN that release factors beneficial to DAN.

Survival, differentiation, and maturation, of engrafted hVM1 clone 32 cells

A few surviving hVM1 clone 32 NSCs were detected in the Str of some, but not all, animals, four months post-grafting (Figure 9). Some cells were found at the transplantation site (Figure 9A-B) whereas others were located in other parts of the Str (Figure 9C-D). No hNSCs were detected in the SNpc or Hip of transplanted animals. Therefore, this indicates that there was little to no graft survival. Although transplanted cells did not label for GFAP, they were in close contact with the host's astrocytes (Figure 9E-G).

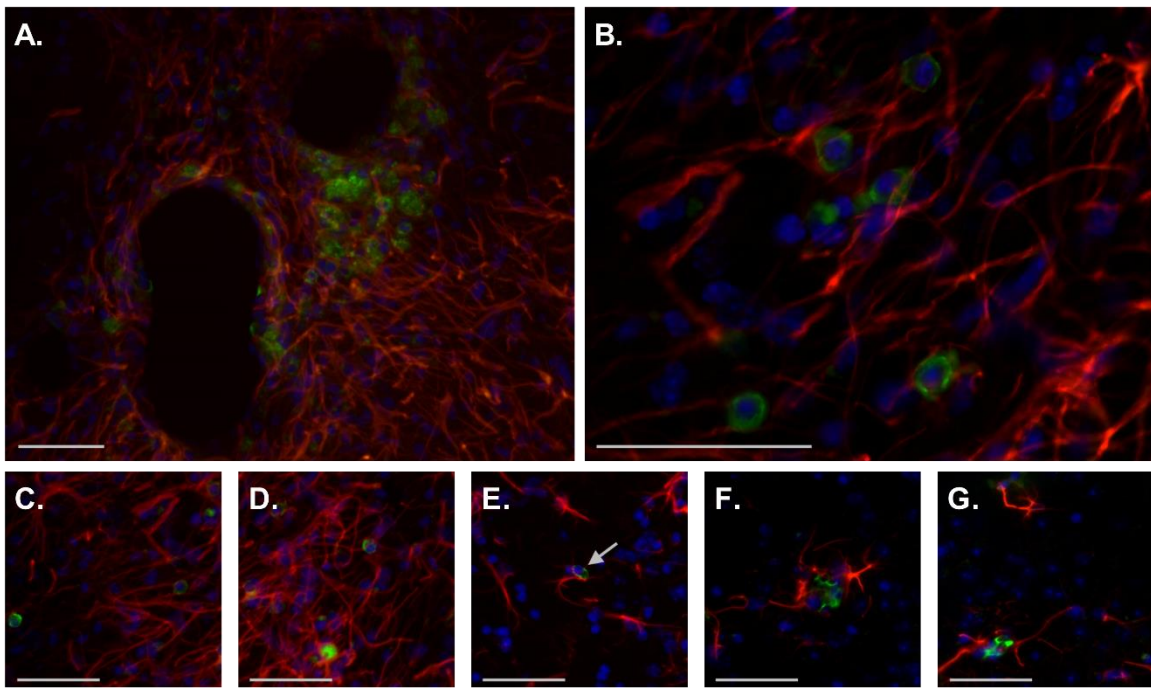


Figure 9: Surviving transplanted hVM1 clone 32 cells (green) and astrocytes (red) at the transplantation site (A). Image zoom of A (B). Transplanted hNSCs and astrocytes in other parts of the Str (C, D). Close-up images of transplanted cells (E-G). Scale bar in A, C-G = 50 μm and scale bar in B = 100 μm.

Therefore, although the grafted cells did not survive four months post-transplant, it was demonstrated, via protein secretion studies *in vitro*, that these cells could have exerted beneficial effects while they were still alive, by secreting NTFs GDNF, BDNF, VEGF-A, and VEGF-C, as well as SCF, FKN, and MCP-1.

Transplantation of hVM1 clone 32 cells in adult mice

Adult MPTP-treated mice were transplanted one week after MPTP injections because it has been reported that the loss of DAN in the SNpc is stable by this time (Jackson-Lewis, Przedborski, 2007).

The effect of hVM1 clone 32 cell transplantation on nigrostriatal pathway degeneration

Four months post-transplant, mouse brains were analyzed for TH immunoreactivity in the Str and in the SNpc, the two main regions affected in PD. Analysis of TH+ fibers was done at two different levels of the Str, namely the rostral Str, closer to the site of transplant, and the caudal Str, further from the site of transplant.

In the rostral Str, there was a significant decrease in TH+ fiber density on the side IL to the transplant in buffer-transplanted mice compared to control animals of around 61% ($p < 0.0001$). This decrease, although still significant, was less, at around 57%, when TH immunostaining of the rostral Str CL to the transplant in buffer-treated mice was compared to controls ($p < 0.001$). Mice lesioned with MPTP transplanted with hNSCs had a significant increase in TH+ fibers in the rostral Str of both hemispheres compared to buffer-transplanted animals, with an increase of approximately 37% ($p < 0.01$) (Figure 10).

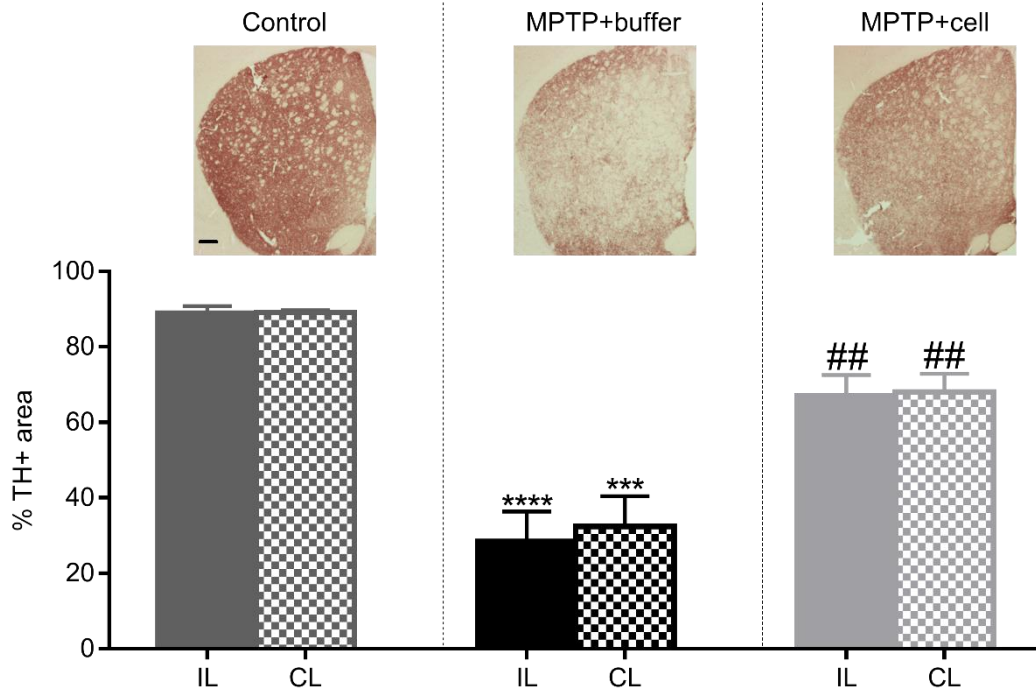


Figure 10: Rostral striatal TH expression, with quantification (bottom) and representative images (top). * compared to same brain hemisphere of control, # compared to same brain hemisphere of MPTP+buffer. Scale bar = 200 μ m.

In the caudal Str, there was a significant decrease in TH+ fiber density of approximately 40% on both sides of the brain in buffer-treated mice compared to controls ($p < 0.001$). Mice transplanted with hVM1 clone 32 cells had a significant increase, ranging from 31-35%, in TH immunoreactive area compared to buffer-treated animals ($p < 0.001$) (Figure 11).

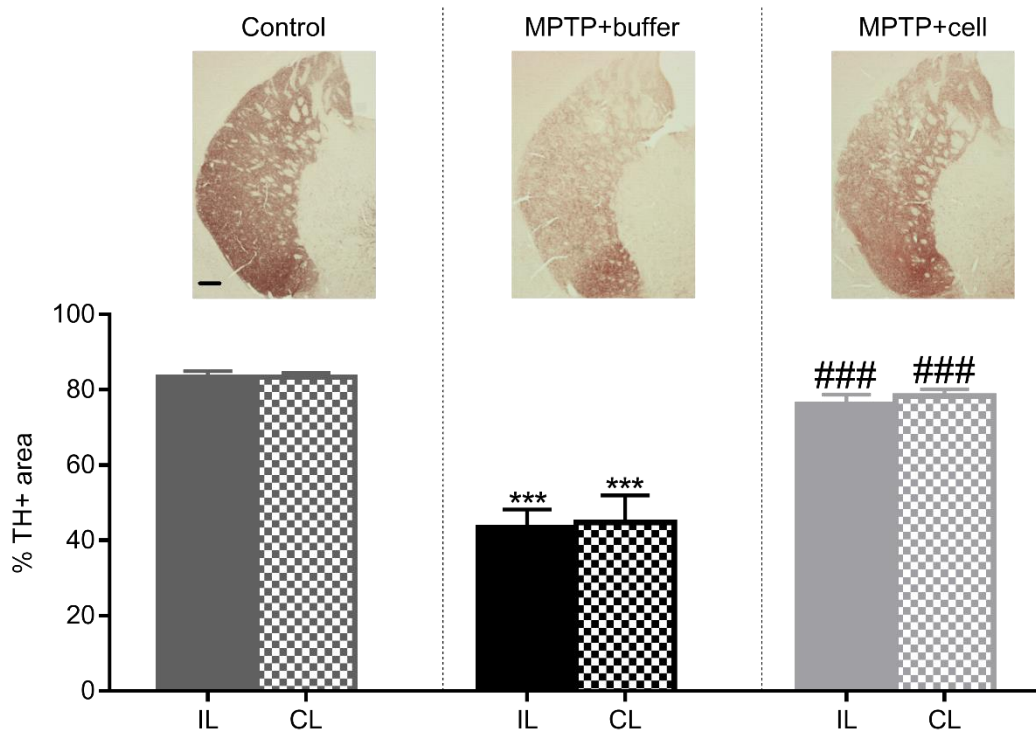


Figure 11: Caudal striatal TH expression, with quantification (bottom) and representative images (top). * compared to same brain hemisphere of control, # compared to same brain hemisphere of MPTP+buffer. Scale bar = 200 μ m.

In the rostral and caudal Str, there were no statistical differences between IL and CL sides in any of the groups, and there were no statistical differences between control and SC-treated animals. Although not statistically significant, TH+ fiber population in the caudal Str of SC-transplanted mice was more similar to controls, with a difference of around 6%, compared to rostral Str TH+ area of the same two experimental groups, which had a difference of approximately 22%. Overall, at both levels of the Str studied, the loss of TH+ fibers upon treatment with MPTP was alleviated by hNSC transplant to the level of that of controls.

In the SNpc, there was a significant decrease in the TH+ area in buffer-treated mice compared to control animals, with a difference of approximately 6.5% ($p < 0.001$). Mice transplanted with hVM1 clone 32 cells showed a significant recuperation in TH+ area in the SNpc compared to buffer-treated mice, around 3%, and this improvement was strongest when comparing the IL SNpc of buffer-treated

mice and CL SNpc of SC-transplanted animals ($p < 0.01$). There were no statistical differences between IL and CL sides in any of the treatment groups. When comparing control and SC-transplanted mice, there was a significant difference between the TH immunostained area in the SNpc, with control animals have from 3-4% more TH+ area than cell-treated mice ($p < 0.01$). Therefore, buffer-treated mice show a loss of DAN which is improved by hNSC transplant, but not to the level of controls (Figure 12).

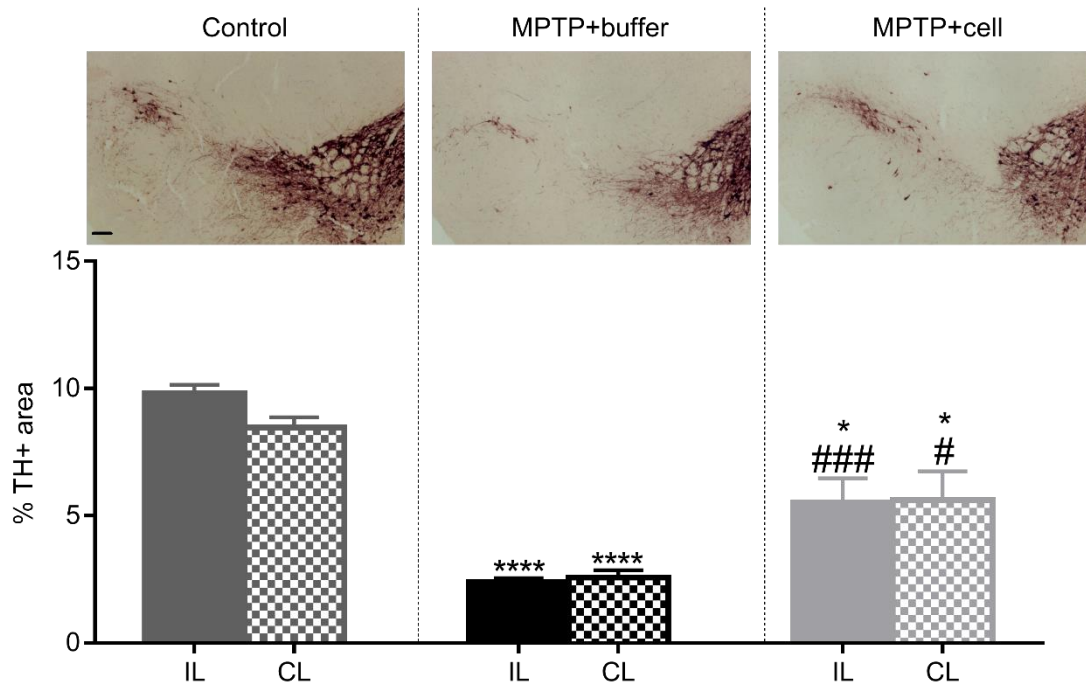


Figure 12: Nigral TH expression, with quantification (bottom) and representative images (top).
 * compared to same brain hemisphere of control, # compared to same brain hemisphere of MPTP+buffer.
 Scale bar = 100 μ m.

Thus, it can be stated that the transplant of hVM1 clone 32 cells significantly prevented the damage to the nigrostriatal pathway in MPTP-treated adult mice.

The effect of hVM1 clone 32 cell transplantation on behavior

Using the OFT, the following factors were evaluated: distance traveled, time spent in the center, grooming, and rearing. Distance traveled allows for the determination of motor impairment and is also related to exploratory activity, anxiety, and depressive-like behavior that can be further detected by patterns in time spent in the center of the box, grooming, and rearing. For all of these aspects of behavior studied, there were no significant differences between the three groups at the beginning of the experiment.

Control mice and buffer-treated displayed no trends nor significant changes in total distance traveled over the course of the study, and at four months post-transplant, there were no significant differences between all three groups. At one month post-transplant, SC-transplanted mice showed a non-significant increase in distance traveled which decreased at month two. However, at month two and three post-grafting, mice transplanted with hVM1 clone 32 cells traveled a significantly larger distance in the OFT compared to control mice ($p < 0.05$). This did not continue past month three, and at the final timepoint, four months post-transplant, control mice traveled around 10 m and MPTP-lesioned animals traveled approximately 18 m (Figure 13).

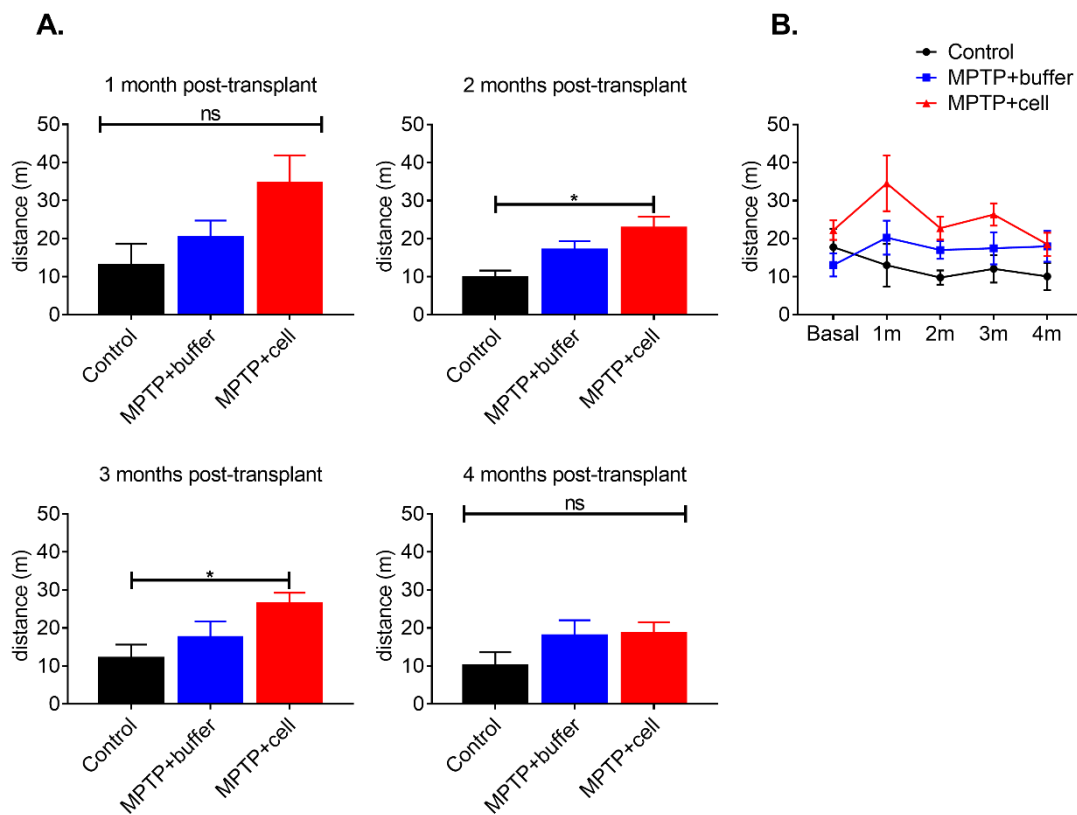


Figure 13: Total distance traveled one-four months post-transplant (A), and graph showing evolution from experiment initiation to completion (B). In B, each colored line represents an experimental group. Black = control, blue = MPTP+buffer, red = MPTP+cell. 1m = one month post-transplant, 2m = two months post-transplant, 3m = three months post-transplant, 4m = four months post-transplant. ns = not significant.

For time spent in the center of the box in the OFT, control mice showed habituation as starting at one month post-transplant and as the months went on, control animals spent basically no time in the center. Experimental groups treated with MPTP spent a non-significant higher amount of time in the center compared to controls at one and three months post-transplant, but two months post-transplant, buffer-treated animals spent a similar amount of time in the center as control mice. At the final timepoint, four months post-transplant, there was a significant difference in the amount of time spent

in the center between control mice and buffer-treated mice ($p < 0.05$). Although not statistically significant, this increased time spent in the center had a tendency to decrease in hNSC-treated mice at four months post-transplant (Figure 14).

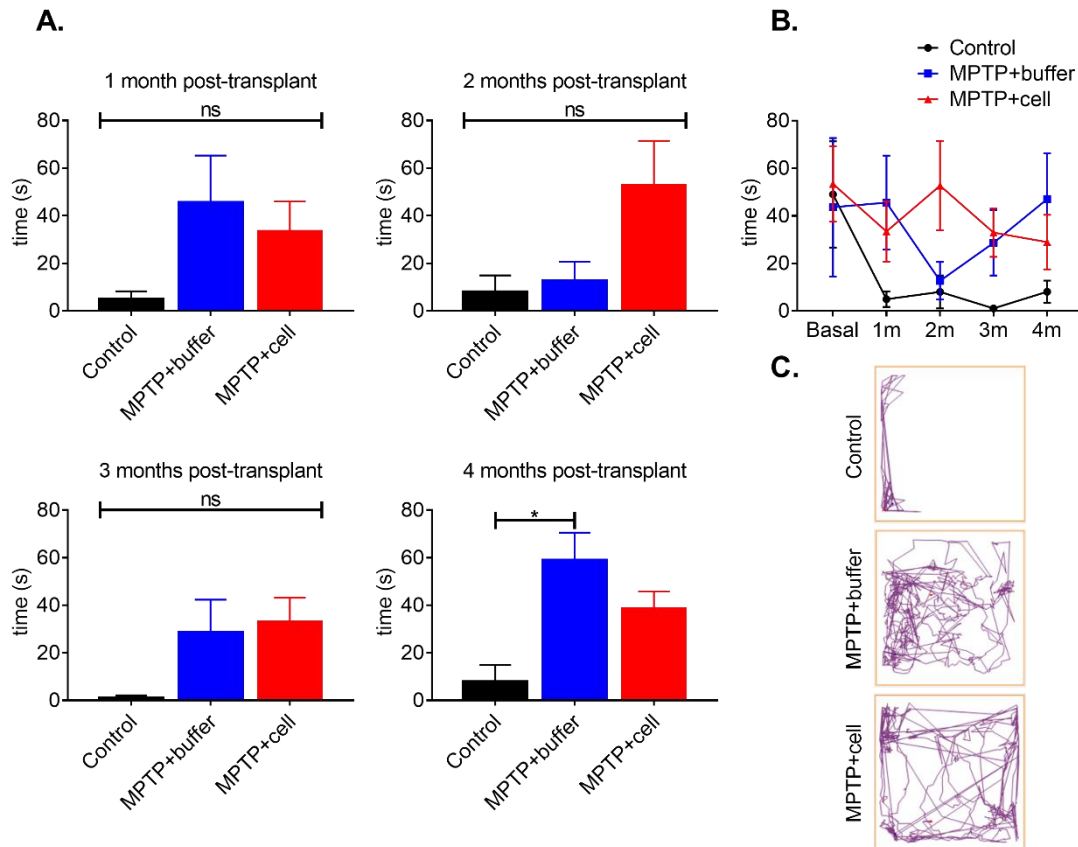


Figure 14: Time spent in center one-four months post-transplant (A), and graph showing evolution from experiment initiation to completion (B). In B, each colored line represents an experimental group. Black = control, blue = MPTP+buffer, red = MPTP+cell. 1m = one month post-transplant, 2m = two months post-transplant, 3m = three months post-transplant, 4m = four months post-transplant. Representative images of movement in OFT box at four months post-transplant (C). ns = not significant.

For time spent grooming, an anxiety-like behavior, from basal conditions to four months post-transplant, there were no significant differences between all three groups as they all spent a statistically similar amount of time grooming (Figure 15).

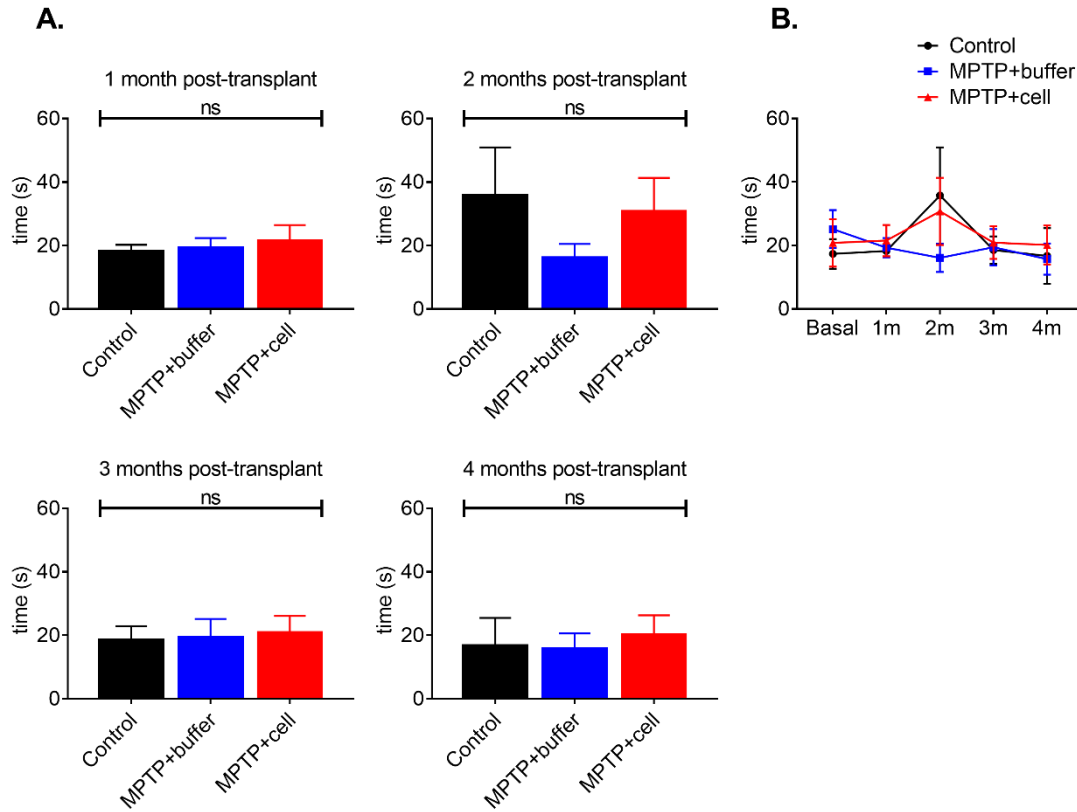


Figure 15: Time spent grooming one-four months post-transplant (A), and graph showing evolution from experiment initiation to completion (B). In B, each colored line represents an experimental group. Black = control, blue = MPTP+buffer, red = MPTP+cell. 1m = one month post-transplant, 2m = two months post-transplant, 3m = three months post-transplant, 4m = four months post-transplant. ns = not significant.

For time spent rearing, all three groups of mice had similar basal conditions. Stem cell-transplanted mice demonstrated a pattern of increased time spent rearing compared to control and buffer-treated animals; this pattern was statistically significant at two months post-transplant ($p < 0.05$). At the last timepoint, four months post-transplant, there were no differences in time spent rearing between the three groups (Figure 16).

Therefore, at the completion of this study, there were no differences between the three groups in terms of locomotor activity or anxiety-like behaviors of rearing and grooming. However, buffer-treated mice spent significantly more time in the center in the OFT compared to controls, which was non-significantly decreased by hSNC transplantation. Furthermore, urination and defecation were similar across all three groups (not shown).

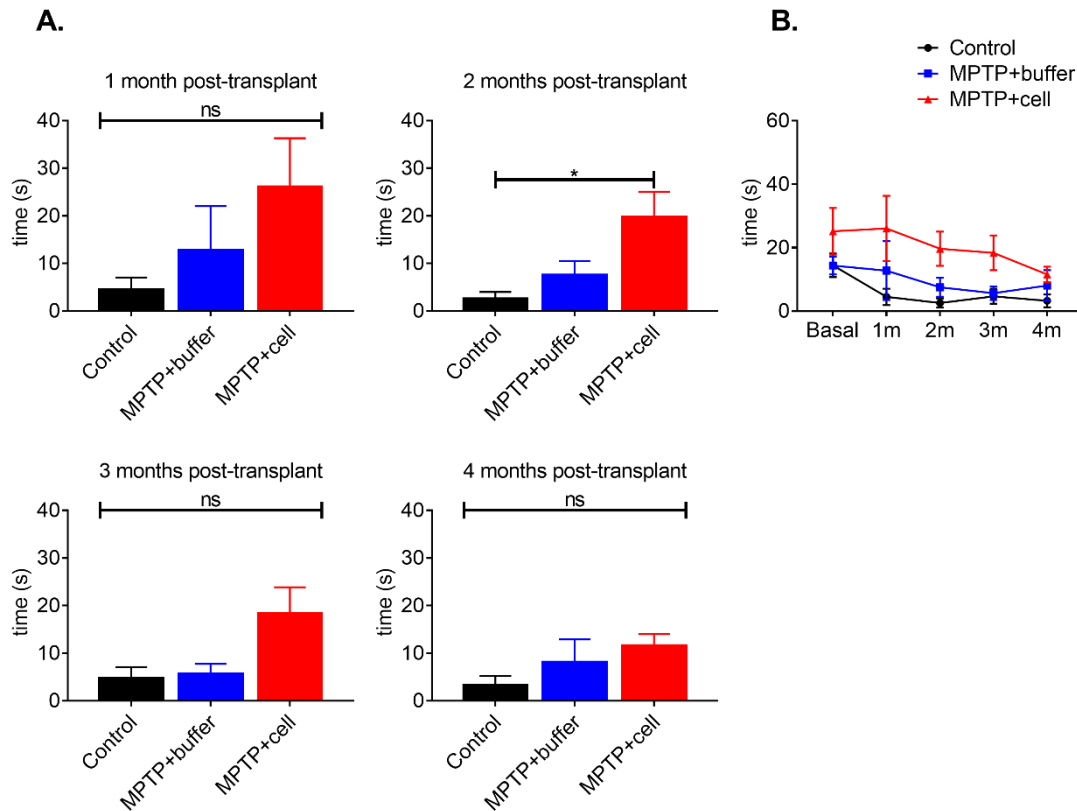


Figure 16: Time spent rearing one-four months post-transplant (A), and graph showing evolution from experiment initiation to completion (B). In B, each colored line represents an experimental group. Black = control, blue = MPTP+buffer, red = MPTP+cell. 1m = one month post-transplant, 2m = two months post-transplant, 3m = three months post-transplant, 4m = four months post-transplant. ns = not significant.

The PPT was employed to study differences in gait between the three groups of animals. Forelimb stride lengths, both CL and IL to the side of transplant, were measured and compared between the three groups. Upon treatment with MPTP, there was a decrease in forelimb stride length. At month one and two post-transplant, there was a tendency for both CL and IL forelimb stride lengths to decrease in MPTP-treated groups compared to controls, which was statistically significant at month three (Control vs. MPTP + buffer $p < 0.05$, Control vs. MPTP + cell $p < 0.01$). At four months post-transplant, there was a significant decrease in CL and IL forelimb stride lengths between control and hNSC-transplanted mice ($p < 0.05$) (Figure 17).

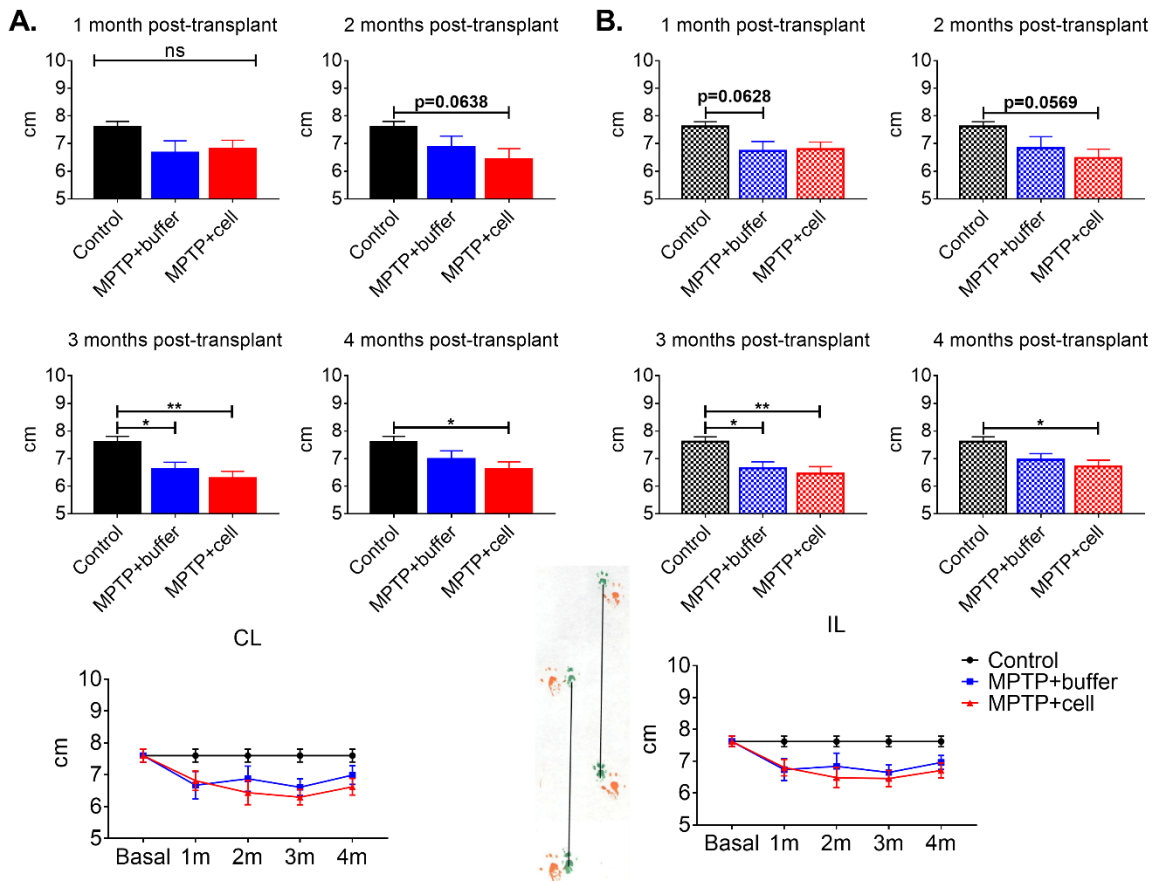


Figure 17: Forelimb stride length one-four months post-transplant, and graphs showing evolution from experiment initiation to completion (A = CL, B = IL). In summary graphs, each colored line represents an experimental group. Black = control, blue = MPTP+buffer, red = MPTP+cell. 1m = one month post-transplant, 2m = two months post-transplant, 3m = three months post-transplant, 4m = four months post-transplant. ns = not significant.

Hindlimb stride length, both CL and IL to the side of transplant, were also measured and compared between control mice and the two MPTP-treated groups. There a trend of decrease in hindlimb stride length in all MPTP-treated animals at one month post-transplant compared to basal measurements. At the one and two month timepoints, there were no differences in CL or IL hindlimb stride lengths among the three experimental groups. At three months post-transplant, buffer-treated animals had a shorter IL hindlimb stride length compared to control mice ($p < 0.05$). Additionally, CL and IL hindlimb stride lengths were significantly decreased in SC-treated mice compared to controls three months post-transplant ($p < 0.05$). This trend continued in a non-significant manner until experiment completion (Figure 18).

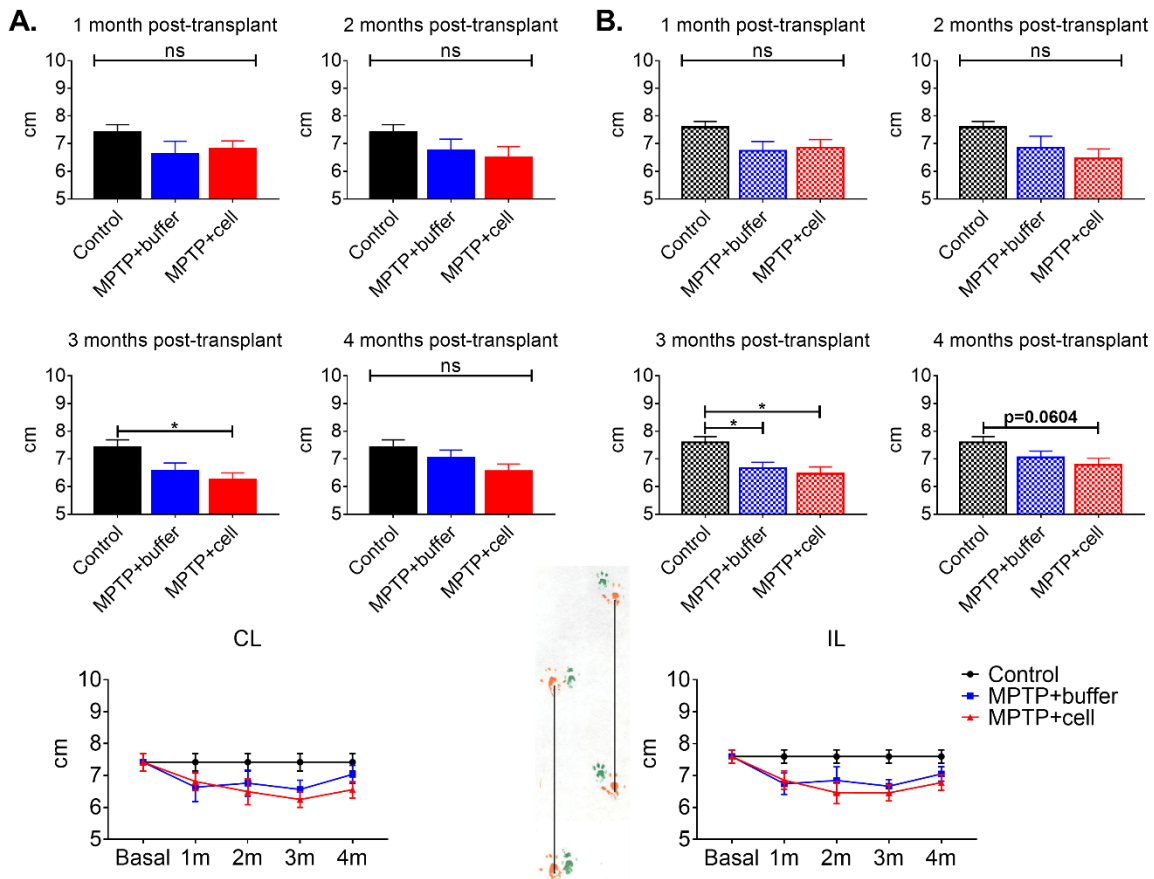


Figure 18: Hindlimb stride length one-four months post-transplant, and graphs showing evolution from experiment initiation to completion (A = CL, B = IL). In summary graphs, each colored line represents an experimental group. Black = control, blue = MPTP+buffer, red = MPTP+cell. 1m = one month post-transplant, 2m = two months post-transplant, 3m = three months post-transplant, 4m = four months post-transplant. ns = not significant.

Forelimb stride width was analyzed by measuring the distance from one right forelimb to the subsequent left forelimb (CL-IL) and from one left forelimb to the following right forelimb (IL-CL). Starting at one month post-transplant, there was a tendency for the forelimb stride width to be decreased in all MPTP-treated mice compared to controls. This tendency was found to be significant in the IL-CL forelimb stride width at three and four months post-transplant ($p < 0.05$ and $p < 0.01$, respectively). The CL-IL forelimb stride width was significantly different at two and three months post-transplant between control and SC-transplanted mice ($p < 0.05$) (Figure 19).

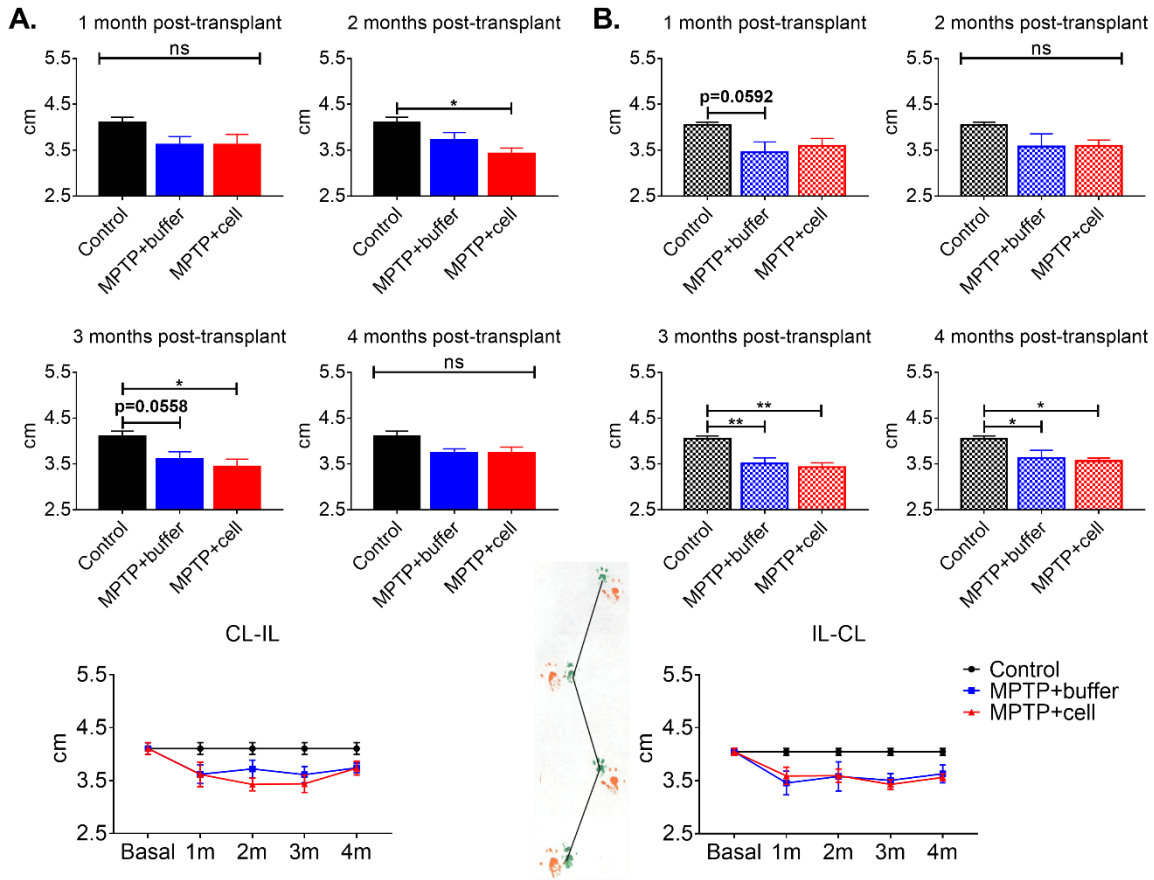


Figure 19: Forelimb stride width one-four months post-transplant, and graphs showing evolution from experiment initiation to completion (A = CL-IL, B = IL-CL). In summary graphs, each colored line represents an experimental group. Black = control, blue = MPTP+buffer, red = MPTP+cell. 1m = one month post-transplant, 2m = two months post-transplant, 3m = three months post-transplant, 4m = four months post-transplant. ns = not significant.

Hindlimb stride width measurements were significantly similar among all three experimental groups throughout the experiment, besides one exception. At one month post-transplant the IL-CL hindlimb stride width of buffer-treated mice was significantly decreased compared to controls ($p < 0.01$). This tended to be alleviated by transplant ($p = 0.0549$) (Figure 20).

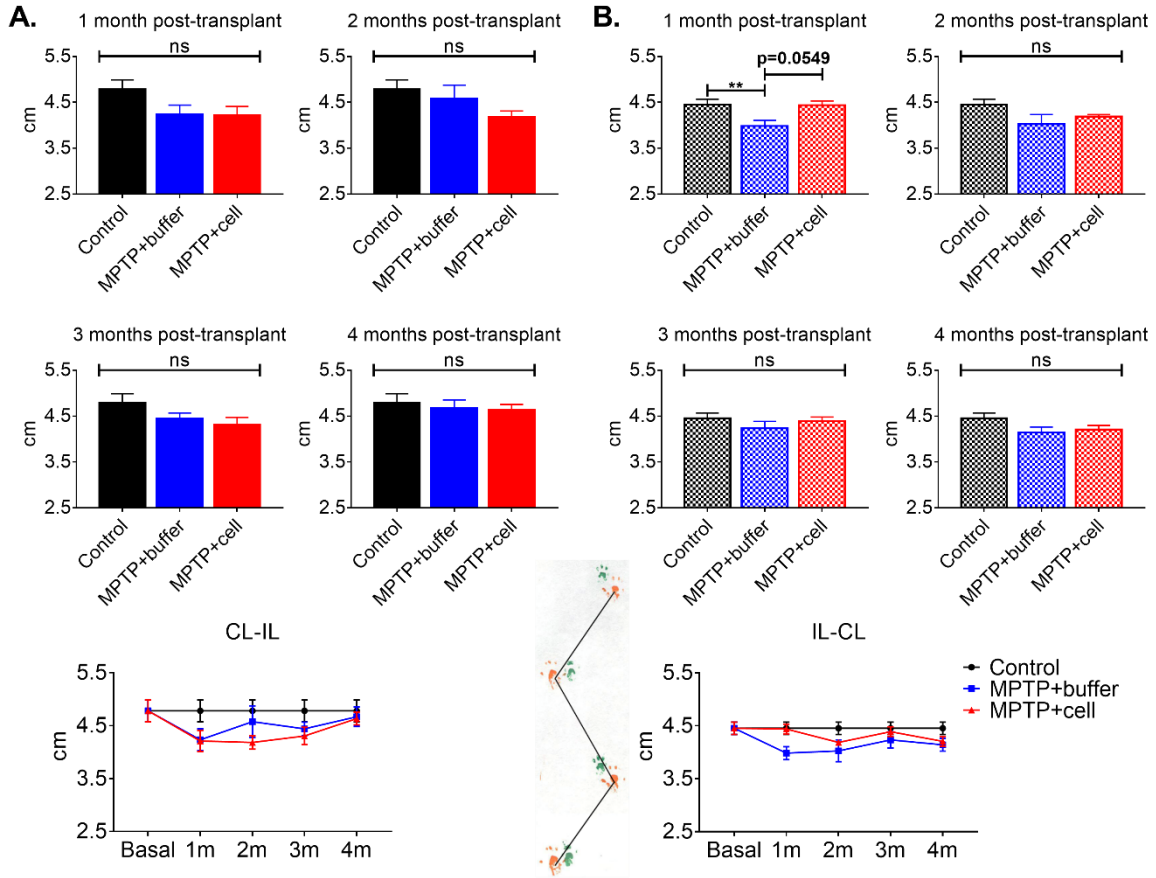


Figure 20: Hindlimb stride width one-four months post-transplant, and graphs showing evolution from experiment initiation to completion (A = CL-IL, B = IL-CL). In summary graphs, each colored line represents an experimental group. Black = control, blue = MPTP+buffer, red = MPTP+cell. 1m = one month post-transplant, 2m = two months post-transplant, 3m = three months post-transplant, 4m = four months post-transplant. ns = not significant.

All paw overlap measurements showed no statistically significant differences between any group at any of the timepoints studied, and starting and endpoint values were statistically similar. (Figure 21).

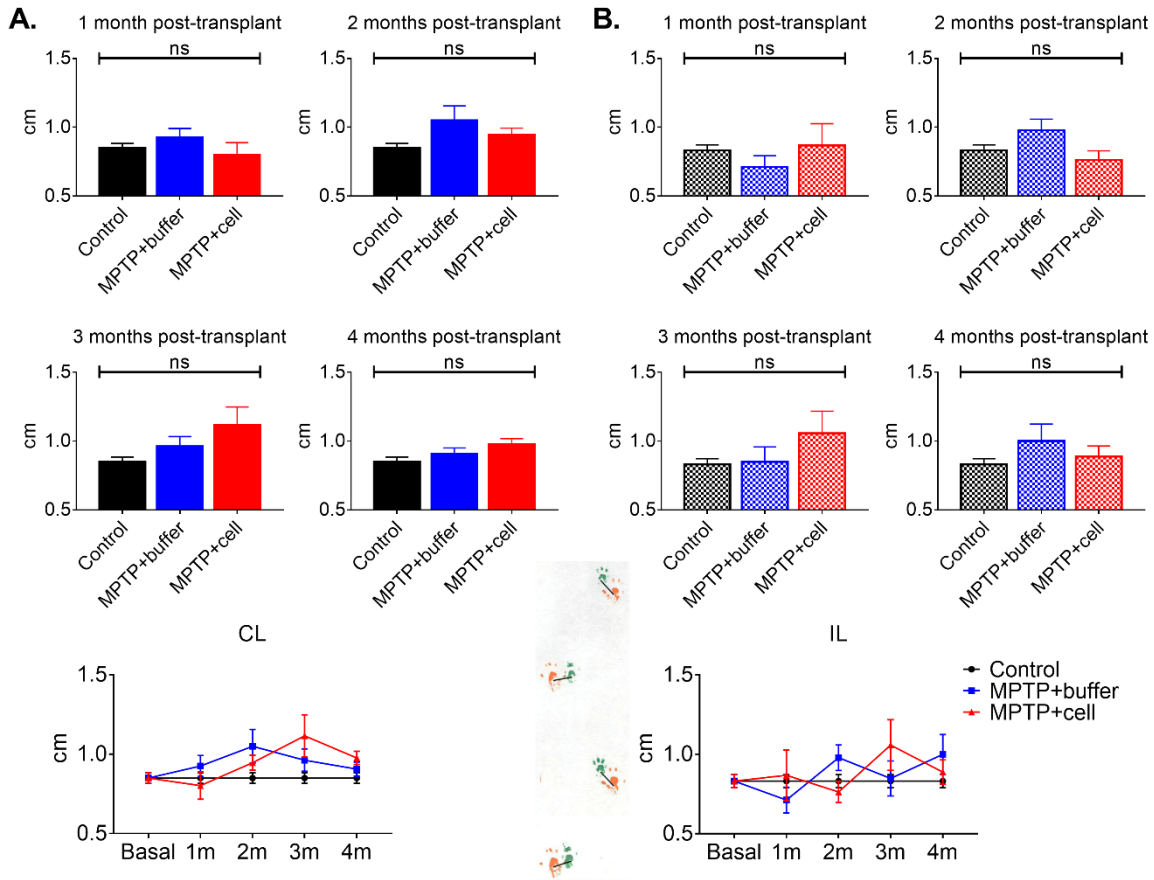


Figure 21: Paw overlap one-four months post-transplant, and graphs showing evolution from experiment initiation to completion (A = CL, B = IL). In summary graphs, each colored line represents an experimental group. Black = control, blue = MPTP+buffer, red = MPTP+cell. 1m = one month post-transplant, 2m = two months post-transplant, 3m = three months post-transplant, 4m = four months post-transplant. ns = not significant.

Therefore, from PPT measurements, there were strong tendencies and sometimes statistically significant differences between stride length and stride width of MPTP-treated animals compared to controls. Four months post-transplant, CL and IL forelimb stride lengths were shorter in hNSC-treated animals compared to controls, and IL-CL forelimb stride width was significantly shorter in all MPTP-treated mice compared to control animals. As well, paw overlap was not a good indicator of gait problems.

The effect of hVM1 clone 32 transplantation on inflammation

Next, the inflammatory reaction in the brain at the two regions of interest, namely the Str and SNpc, were studied in order to see if there were differences in glial populations between control, and buffer- and SC-transplanted animals. In the rostral Str, closer to the transplantation site, astrocytes were quantified via GFAP immunostaining.

In the rostral Str, control and buffer-treated animals had a similar amount of astrocytes. The rostral Str IL to the side of the transplant in animals grafted with hVM1 clone 32 cells had significantly higher GFAP+ area compared to all other groups, including the rostral Str CL to the side of transplant of hNSC-treated animals, having almost twice as much astroglial immunoreactivity ($p < 0.01$). Compared to the other groups, the rostral Str IL to the side of the transplant of hNSC-treated mice had up to 0.7% more GFAP+ area. Moreover, the rostral Str CL to the side of the transplant of SC-treated mice tended to have from two-four times more GFAP immunostaining than control and buffer-transplanted animals, which reached statistical significance when compared to the CL rostral Str of these two experimental groups ($p < 0.05$) (Figure 22).

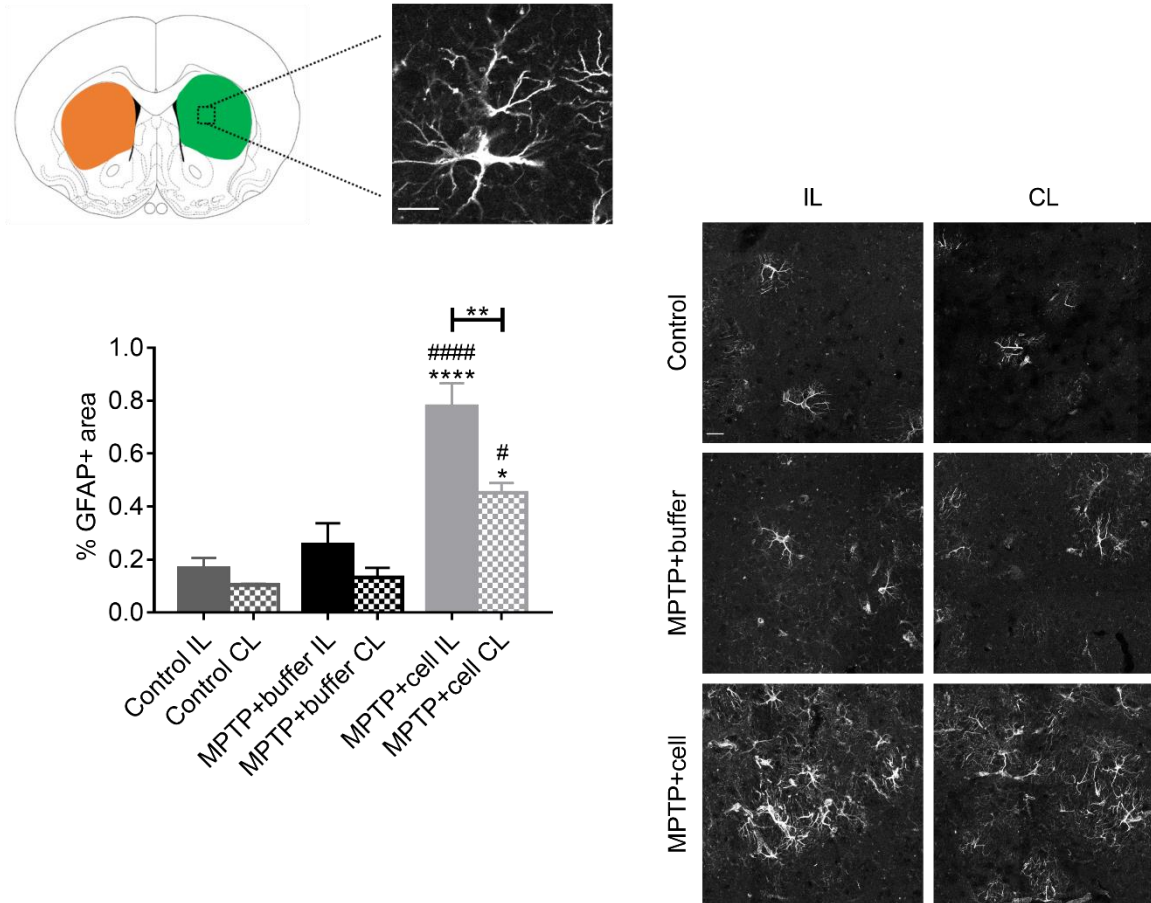


Figure 22: Rostral striatal GFAP expression, with quantification (left) and representative images (right).
 * compared to same brain hemisphere of control, # compared to same brain hemisphere of MPTP+buffer.
 Top scale bar = 10 μ m and scale bar in control IL panel = 25 μ m.

In the SNpc, the levels of GFAP immunoreactivity of the three experimental groups were statistically equivalent, with a slight tendency for hNSC-treated mice to have a larger GFAP+ area compared to control animals (Figure 23A). Microglia expression was studied using Iba1 immunostaining. In the SNpc, there was a clear trend in that all MPTP-treated mice showed approximately 2.5% more Iba1 immunoreactivity compared to control groups. This tendency was statistically significant when comparing the IL SNpc Iba1+ area of control mice to the IL and CL SNpc Iba1+ area of buffer-treated and SC-transplanted animals, respectively ($p < 0.05$). As well, Iba1 expression was significantly increased in the CL SNpc of hNSC-transplanted mice compared to the equivalent region of controls ($p < 0.05$) (Figure 23 B).

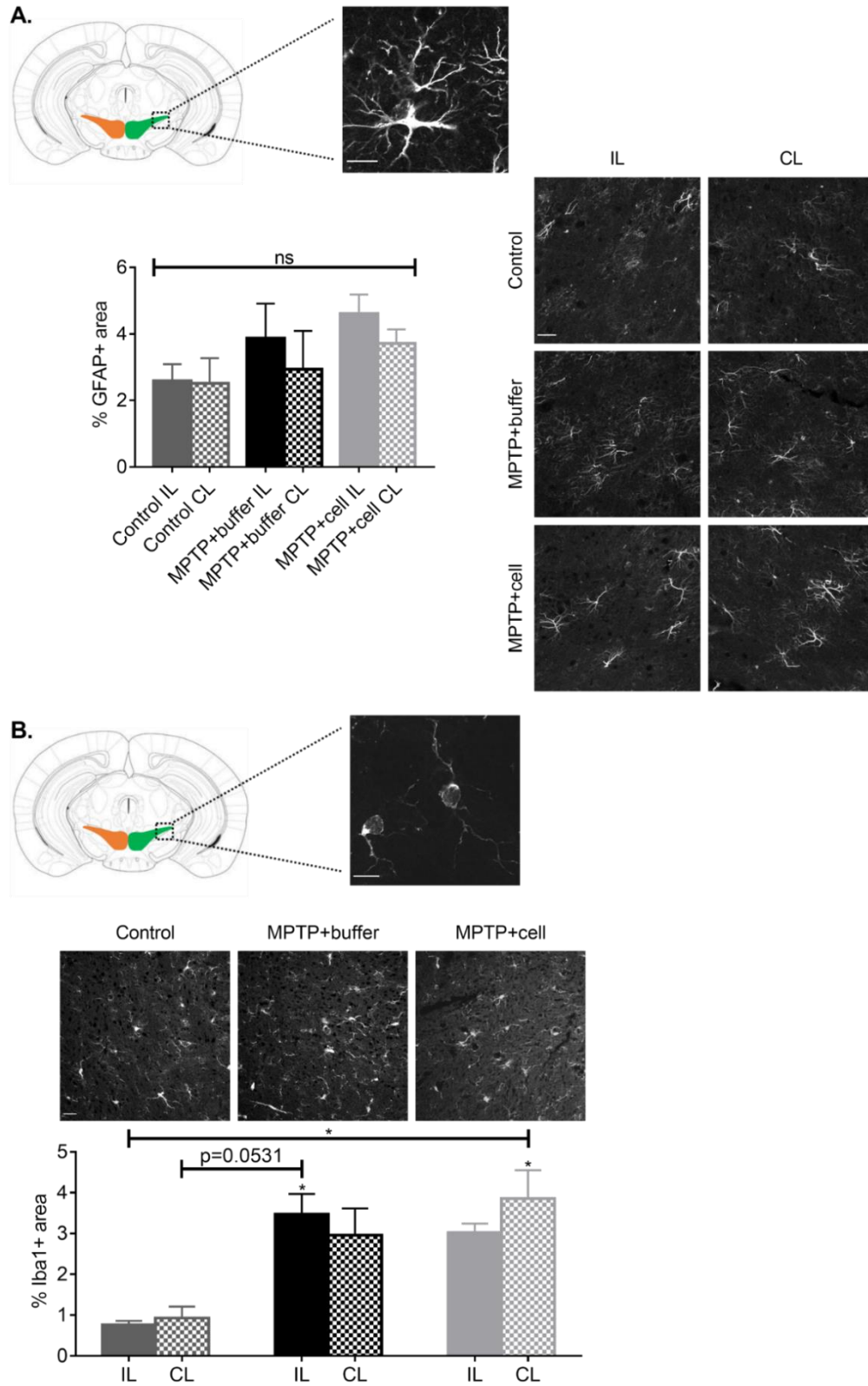


Figure 23: Nigral GFAP expression, with quantification (left) and representative images (right) (A), and nigral Iba1 expression with quantification (bottom) and representative images (top) (B). * compared to same brain hemisphere of control. ns = not significant. Top scale bar = 10 μ m and scale bar in control IL panel = 25 μ m.

From these data, it can be said that hNSC grafting led to increased astrocytic population in the IL Str, the site of the transplant. In the SNpc, astrocytes and microglia showed distinct reactions to MPTP lesions; while astroglial populations did not increase significantly, microglial cells did, indicating a more vital role for microglia in the SNpc in PD. As well, microglial cells are already more populous in SNpc than astrocytes under normal conditions. Although there is evidence that inflammation can be detrimental to the nigrostriatal pathway and CNS in general, in this case the elevated levels of inflammation, especially those in SC-treated mice in the Str and SNpc, did not negatively affect the TH+ fiber and cell number in the Str and SNpc, respectively. Also, it is not unexpected that the mouse brain would have this reaction to a foreign substance of human origin, and because the CSA treatment silences the adaptive immune response, perhaps this is the reason there was a bigger response from glial cells.

Data on inflammation in the CNS show that there is a distinct pattern of astroglial and microglial activation in hNSC-treated mice. In addition to this, immunosuppression with CSA inhibits the adaptive immune response, thus allowing to see what happens to the innate immune system. Therefore, it was decided that the focus would be MCs, innate immune cells located in the CNS and CNS-connected LNs, which play a role in inflammation, transplant tolerance, immunosuppression, and possibly PD pathology.

First, confirmation of neuronal markers present in the superficial cervical LNs was done via WB, using the rostral Str of control adult mice. It was found that control LNs expressed β -III tubulin, NFL, PSD-95, and SYP. In addition, these LNs expressed DAN marker TH (Figure 24).

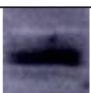




Protein	Str	LN	
β -III tubulin	✓	✓	
NFL	✓	✓	
PSD-95	✓	✓	
SYP	✓	✓	
TH	✓	✓	

Figure 24: Summary of neuronal and DAN proteins expressed in LNs.

Analysis of the superficial cervical LNs showed a trend in that all MPTP-treated mice had larger LNs compared to control animals; however, this increase was not statistically significant ($p = 0.0561$) (Figure 25A). Mast cell density quantification revealed that SC-transplanted mice displayed a tendency of increased MC density compared to both buffer-treated control animals, which reached statistical significance when comparing controls and hNSC-transplanted mice ($p < 0.05$) (Figure 25B).

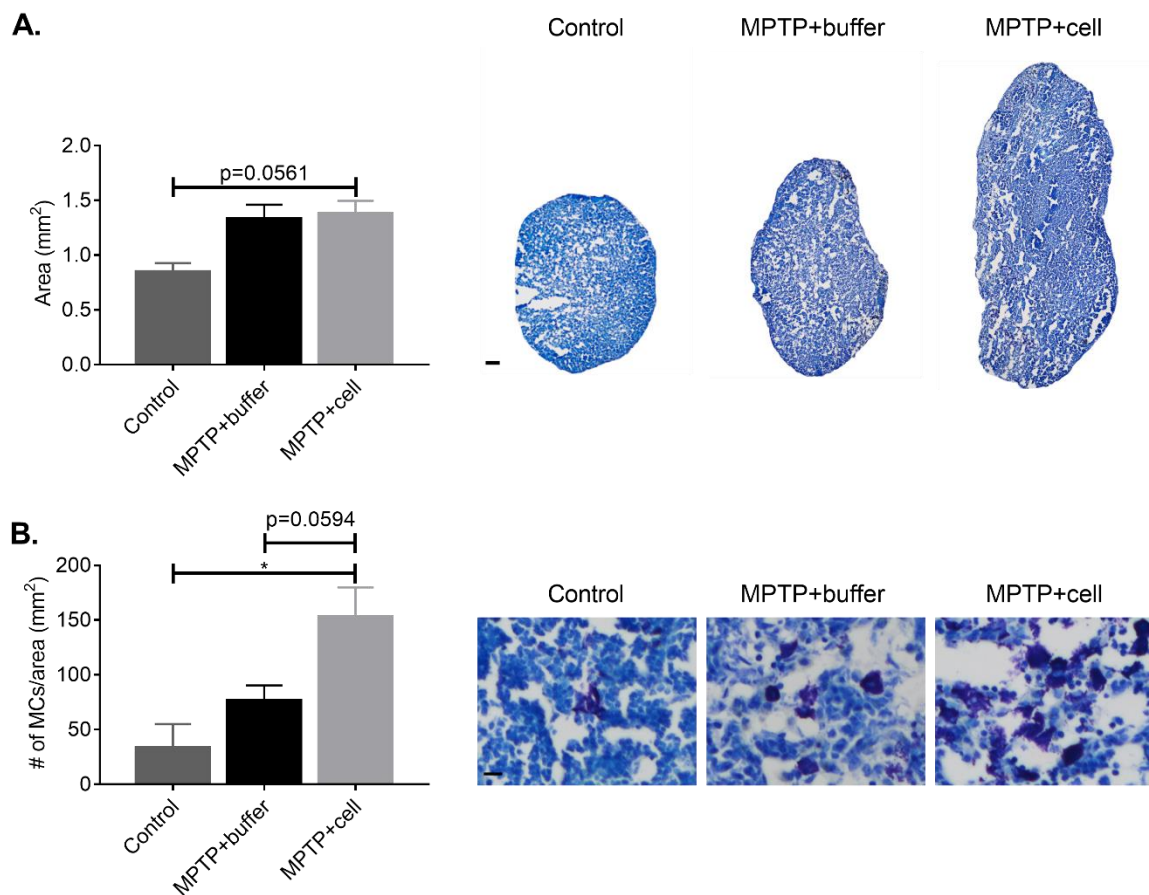


Figure 25: Lymph node size (A) and MC density in the LNs (B), with quantification (left) and representative images (right). Scale bar A = 100 μ m and scale bar B = 25 μ m.

This demonstrates that the transplant had an influence on non-CNS structures and processes, re-emphasizing the connection between the CNS and LNs. As well, it shows that MCs are affected by hNSC transplantation.

With this increase in MC density, it was speculated that MC populations within the CNS could be playing a role, specifically in the nigrostriatal pathway. However, there was no quantifiable amount of MCs in either the rostral Str or SNpc (not shown). Therefore, within the CNS, MCs do not appear

to be contributing to the increased inflammation observed nor are they aiding in transplant tolerance as seen by their absence and lack of grafted cell survival. Moreover, MC quantities are rare in the mouse CNS under normal conditions, and they tend to be most abundant in the Hip and thalamus (Silver, Curley, 2013).

The effect of hVM1 clone 32 transplantation on mechanisms of repair

Mechanisms of repair associated with angiogenesis and neurogenesis were subsequently analyzed. Although there were practically no MCs, which release pro-angiogenic factors, in either the rostral Str or SNpc, angiogenesis was analyzed in these two regions in order to see if the transplant, and more specifically the increased astrocyte population, as well as VEGF-A and VEGF-C potentially released by the hNSCs *in vivo*, was able to stimulate the growth of new blood vessels. To do this, an immunostaining of β -DAG was performed.

In the rostral Str, there was a non-significant decrease in the number in blood vessels in all MPTP-treated mice (Figure 26A). By contrast, in the SNpc, there were no significant differences nor trends between any of the groups (Figure 26B). Therefore, there was no angiogenesis found in the nigrostriatal pathway of hNSC-treated animals.

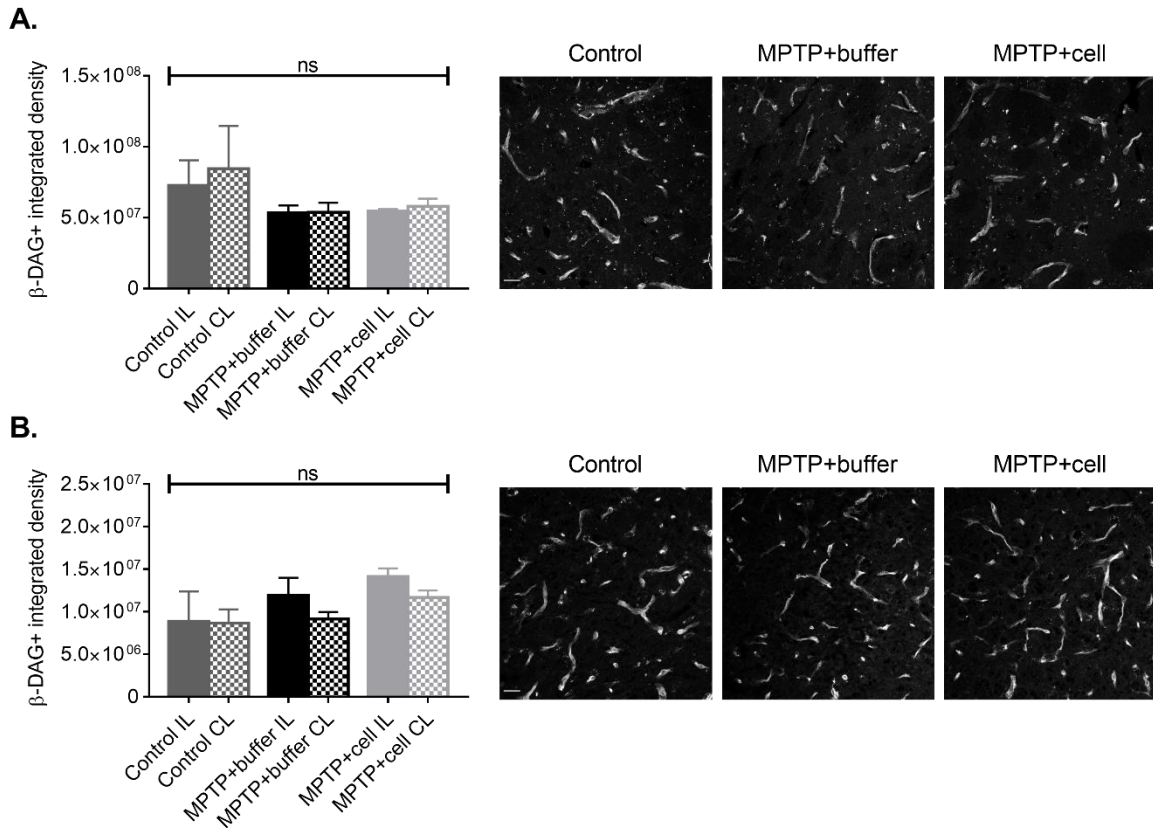


Figure 26: Blood vessels in the rostral Str (A) and SNpc (B), with quantification (left) and representative images (right). ns = not significant. Scale bar = 25 μ m.

Neurogenesis was studied in the SVZ and SGZ, and in order to get a general idea of how the transplant affected each stage of neurogenesis, immunostaining was done for NES and Ki-67, NSC/NPC markers, and DCX, a marker for immature neurons.

In the SVZ of adult mice, there were no significant differences in amount of NES immunostaining nor the number of Ki-67+ cells when comparing the three treatment groups. By contrast, there was a strong tendency for all MPTP-treated mice to have less DCX expression compared to control animals, with the decrease ranging from 22-44%. This decrease was statistically significant when comparing the CL SVZ of controls to the equivalent region in buffer-treated mice and to the IL SVZ of hNSC-transplanted animals ($p < 0.05$) (Figure 27).

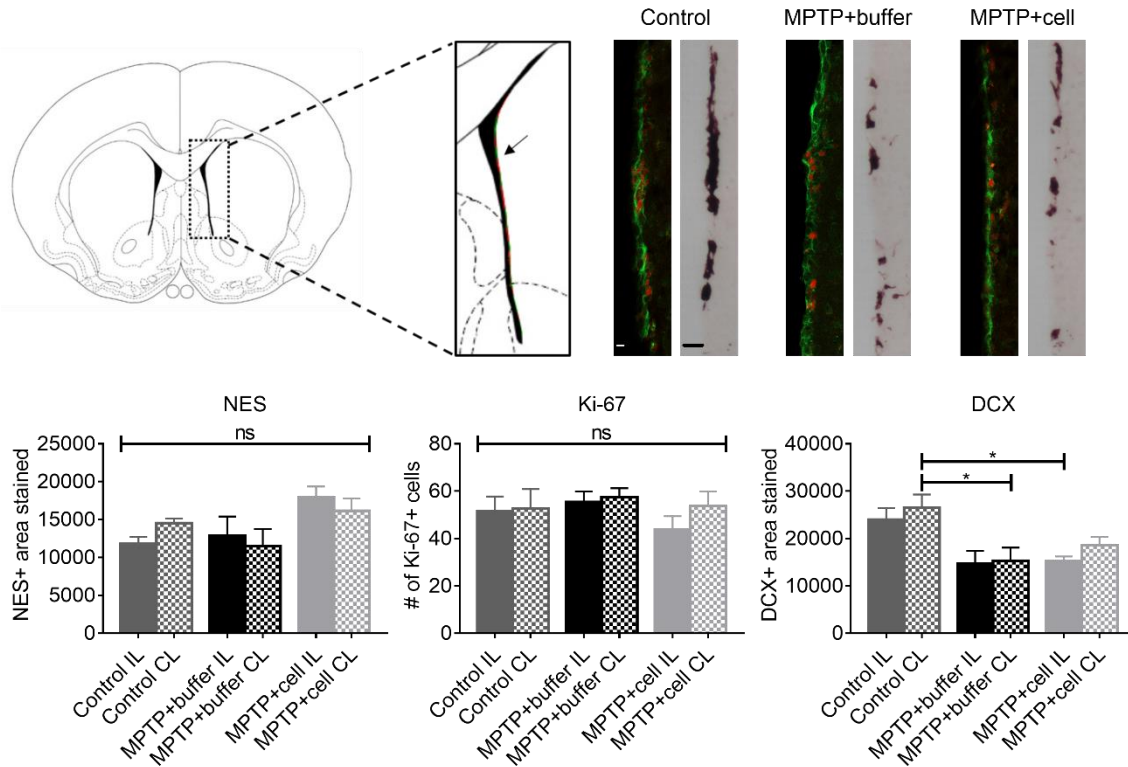


Figure 27: Neurogenesis in the SVZ. Quantification of NES (bottom left), Ki-67 (bottom middle), and DCX (bottom right), expression, in the SVZ with representative NES/Ki-67 (top left; NES in green and Ki-67 in red) and DCX images (top right). ns = not significant. Left scale bar = 10 μ m and right scale bar = 25 μ m.

In the SGZ of adult mice, there was either no expression or no quantifiable amount of immunostaining of either NES or Ki-67. This is not surprising as at the time of sacrifice, these animals were nine months old, an age where proliferating cells have shown to be practically null in rodent SGZ. In contrast to the lack NSC/NPC populations in the SGZ, the neuroblasts showed a completely different pattern. Control animals showed variation in DCX expression in the SGZ, and there was a tendency for DCX immunostaining to decline in buffer-treated animals (Control IL vs. MPTP+buffer IL $p=0.0628$ and Control IL vs. MPTP+buffer CL $p < 0.05$). Transplantation with hVM1 clone 32 cells alleviated this decline as SC-transplanted mice showed increased DCX+ area compared to the CL SGZ of buffer-treated animals ($p < 0.05$). Moreover, there were no statistically significant differences in DCX expression between the control and SC-grafted groups (Figure 28A). Additionally, there was a non-significant decrease in microglia in the SGZ of hNSC-transplanted animals compared to control and buffer-treated mice (Figure 28B).

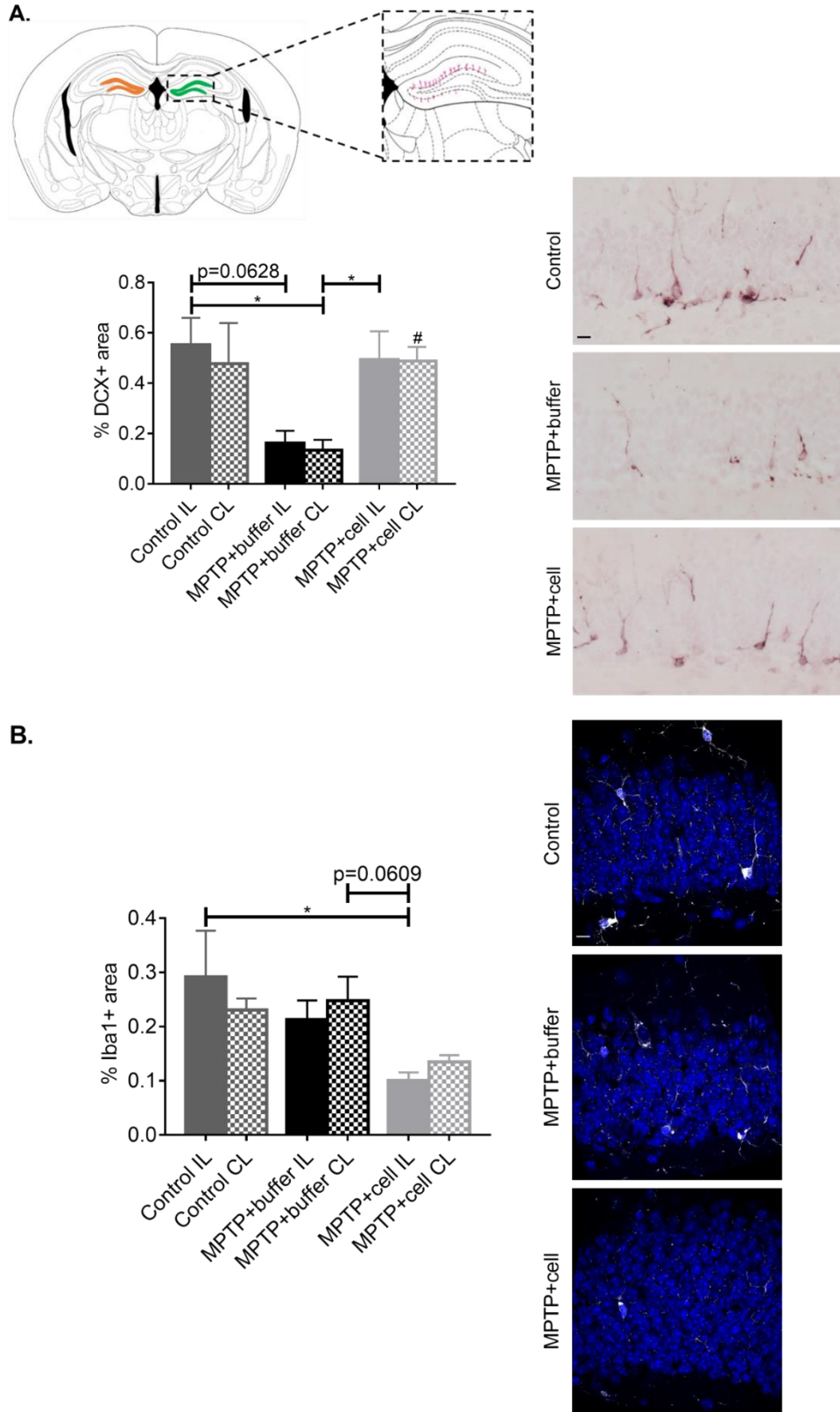


Figure 28: Neurogenesis and neuroinflammation in the SGZ, as shown via DCX (A) and Iba1 (B; white with cell nuclei in blue) expression, respectively, with quantification (left) and representative images (right). # compared to same brain hemisphere of MPTP+buffer. Scale bar A = 25 μ m and scale bar B = 10 μ m.

These results indicate that NSCs/NPCs in the SVZ were not affected by MPTP treatment nor by hNSC transplantation, however immature neurons were affected by MPTP treatment as demonstrated by decreased DCX expression. In the SGZ, there were no NSC/NPC populations, but immature neurons remained. This neuroblast population declined upon administration with MPTP, and hVM1 clone 32 grafting restored this loss. The increase in neuroblast neurogenesis coincided with a decrease in microglial inflammation in the SGZ.

It is interesting to note that in adult mice, the most significant improvements upon transplantation were in the rescue of TH+ fibers and cells in the Str and SNpc, respectively, and the rescue of immature neurons in the SGZ. Therefore, the correlation coefficient (r) of these groups was calculated. The r value correlating TH+ area percentage in the rostral and caudal Str, with DCX+ area percentage in the SGZ was 0.9350 ($p < 0.0001$), and the correlation coefficient correlating TH+ area percentage in SNpc with DCX+ area percentage in the SGZ was 0.8734 ($p < 0.05$) (Figure 29). Although the correlation was stronger between DCX expression in the SGZ to TH expression in the Str rather than the SNpc, both coefficients were very high and emphasize the important relationship between the nigrostriatal pathway and hippocampal neurogenesis.

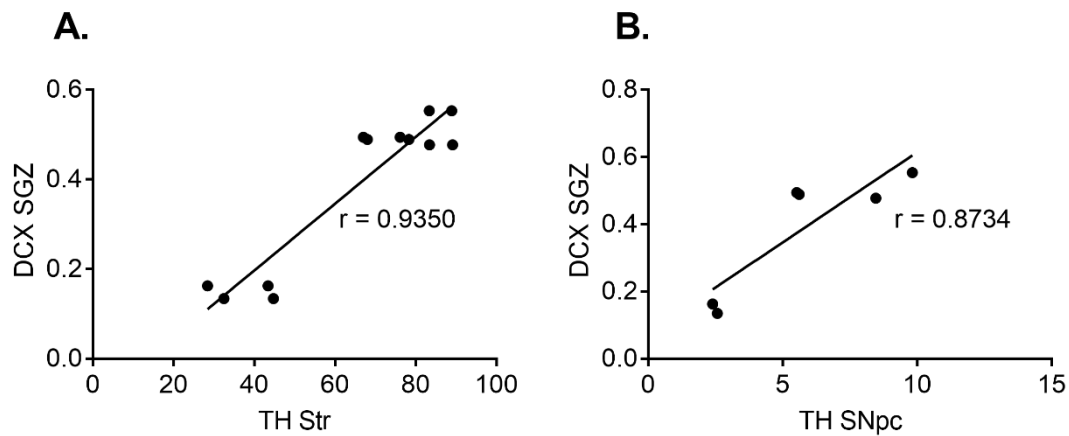


Figure 29: Linear correlation between DCX expression in the SGZ and TH expression in the Str (A) and SNpc (B).

Transplantation of hVM1 clone 32 cells in middle-aged mice

Because PD motor symptom onset as well as diagnosis tends to occur after the age of 60 and the fact that most *in vivo* studies and clinical trials are done in younger animals and patients, respectively, the hVM1 clone 32 cells were tested in a more translational model using middle-aged mice and doing the stem cell transplantation one month after MPTP injections. The purpose of this was to see if hVM1 clone 32 cells were able to induce improvement or if they would also fail like other cells in *in vivo* studies and clinical trials do on older animals and patients, respectively. Regardless of outcome, the purpose was to explore the same key features of PD and the effect of hNSC transplant as was done in adult PD mice, by analyzing TH fiber and cell recuperation, inflammation, angiogenesis, and neurogenesis, in middle-aged mice, and see if there were differences compared to adult mice.

The effect of hVM1 clone 32 cell transplantation on nigrostriatal pathway degeneration

Looking at TH immunostaining in the rostral Str, the means of the groups were statistically different ($p < 0.05$). However, there were no statistically significant differences when comparing all of the groups, but there was a trend that MPTP-lesioned mice had approximately 22% less TH expression in the rostral Str compared to control animals (Figure 30).

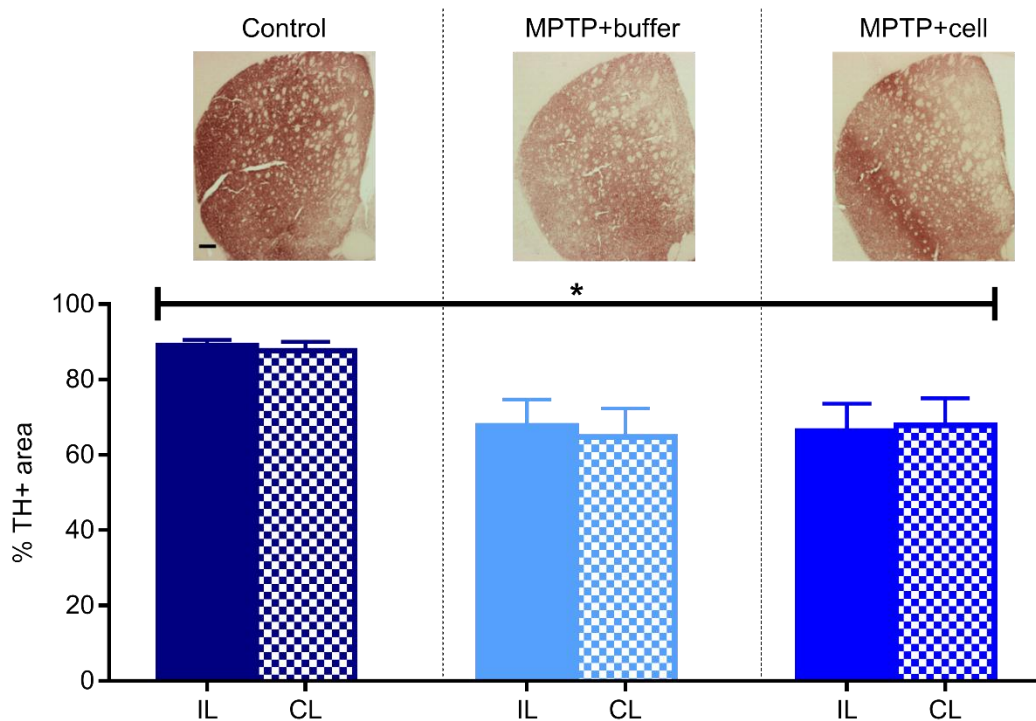


Figure 30: Rostral striatal TH expression, with quantification (bottom) and representative images (top). Scale bar = 200 μ m.

Expression of TH followed a similar pattern in the caudal Str, with a tendency for TH immunoreactivity to decrease by approximately 14-20% upon administration of MPTP (Control IL vs. MPTP+cell IL $p = 0.0530$, Control CL vs. MPTP+buffer CL $p = 0.0569$) (Figure 31).

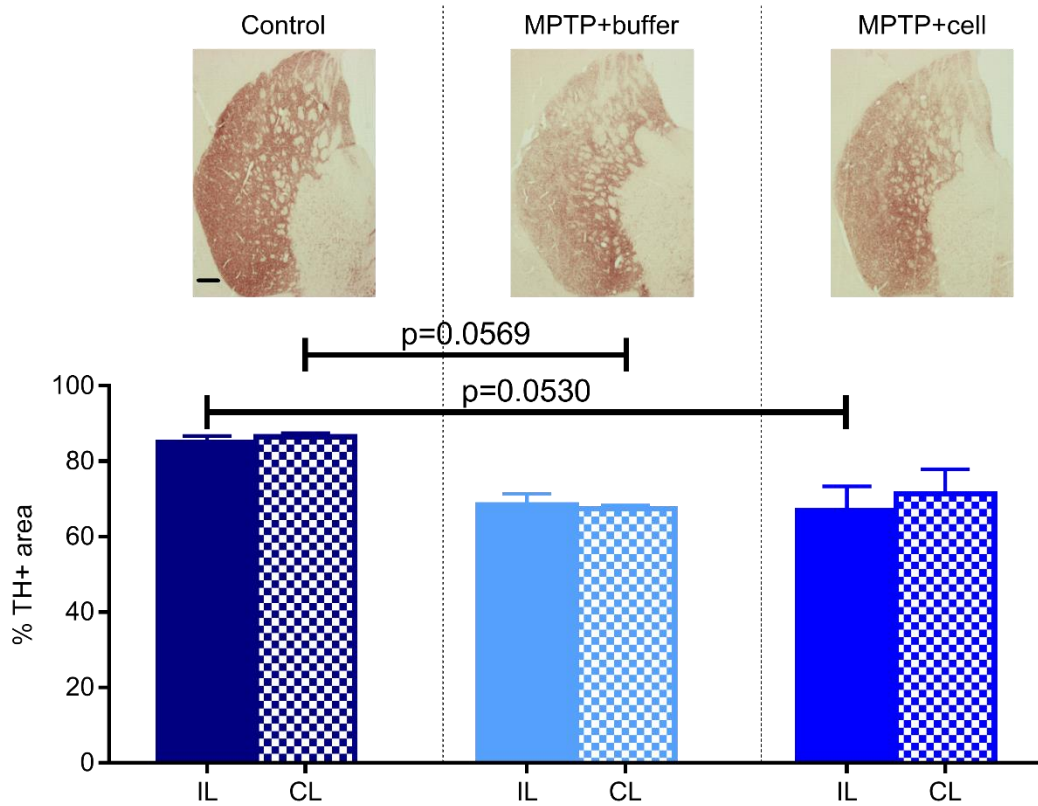


Figure 31: Caudal striatal TH expression, with quantification (bottom) and representative images (top). Scale bar = 200 μm .

In the SNpc, there was a significant decrease in TH expression in buffer-treated animals ($p < 0.05$), while SC-treated animals showed no statistically significant decreases compared to either control or buffer-transplanted groups. Although in general TH expression followed the same pattern as that in the Str with a decrease in TH immunostaining upon MPTP lesion, TH expression in the SNpc of hNSC-treated mice decreased by around 3% compared to controls, while that of buffer-treated animals dropped a bit more, by approximately 5% (Figure 32).

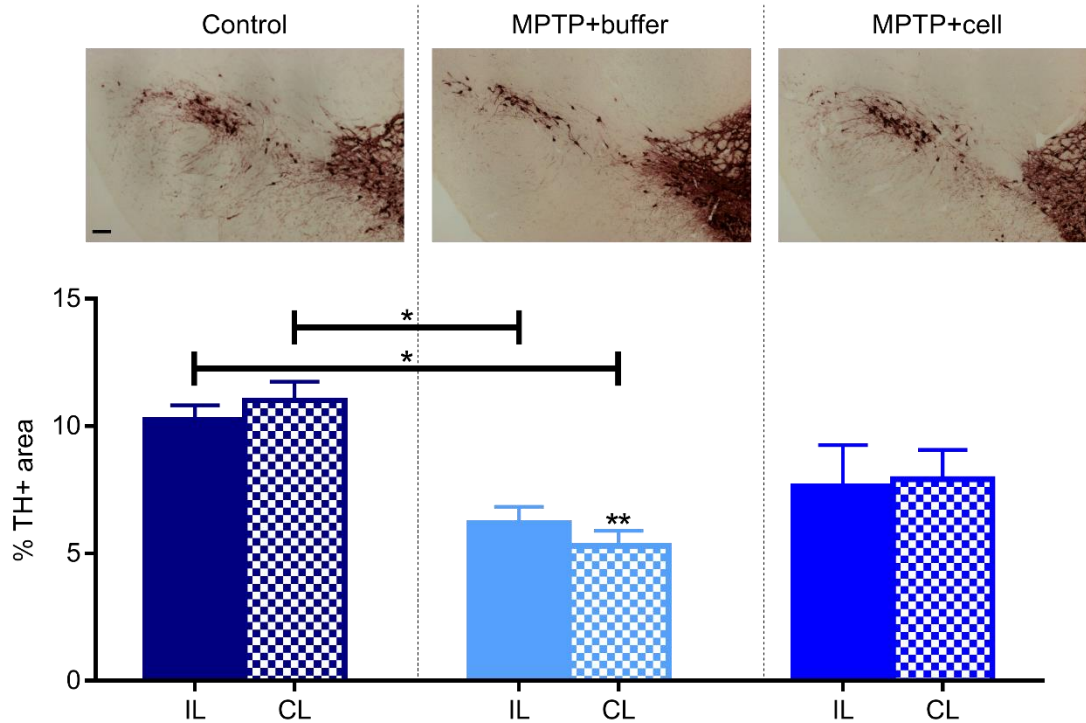


Figure 32: Nigral TH expression, with quantification (bottom) and representative images (top). * compared to same brain hemisphere of control. Scale bar = 100 μ m.

Therefore, it can be stated that upon administration of MPTP in middle-aged mice, there is a tendency for TH+ fibers in the Str and TH+ cells in the SNpc to decrease, and this diminution is not alleviated by transplant of hVM1 clone 32 cells.

Adult and middle-aged control mice had the same percentages of TH immunostaining in the rostral and caudal Str, and the SNpc. It is interesting to note that while TH+ fiber density decreased by approximately 60% in the rostral Str of adult mice, in middle-aged mice, it decreased by only around 22%, and in the caudal Str, TH expression dropped by approximately 40% in adult mice and in middle-aged mice this diminution was only around 16%. However, in the SNpc, the decrease in TH expression in adult and middle-aged mice was more similar, being between around 6.5% in adults and 5% in middle-aged animals. Lastly, in adult mice, the diminution of TH expression in the nigrostriatal pathway was alleviated by transplant with hVM1 clone 32 cells, while in middle-aged mice it was not.

The effect of hVM1 clone 32 cell transplantation on behavior

Behavioral changes were studied using OFT and PPT. In the OFT, locomotor activity was monitored by measuring the total distance traveled by the mice in the box. To this regard, there were no significant differences between any of the groups at any of the timepoints analyzed, including at four months post-transplant. The only noticeable trend was that SC-treated mice tended to travel shorter distances throughout the entire experiment. At the final timepoint, four months post-transplant, control and buffer-treated mice traveled around 22 m and SC-transplanted animals traveled approximately 12 m (Figure 33). As with middle-aged mice, adult mice demonstrated the same lack of changes in total distance traveled when comparing all treatment groups.

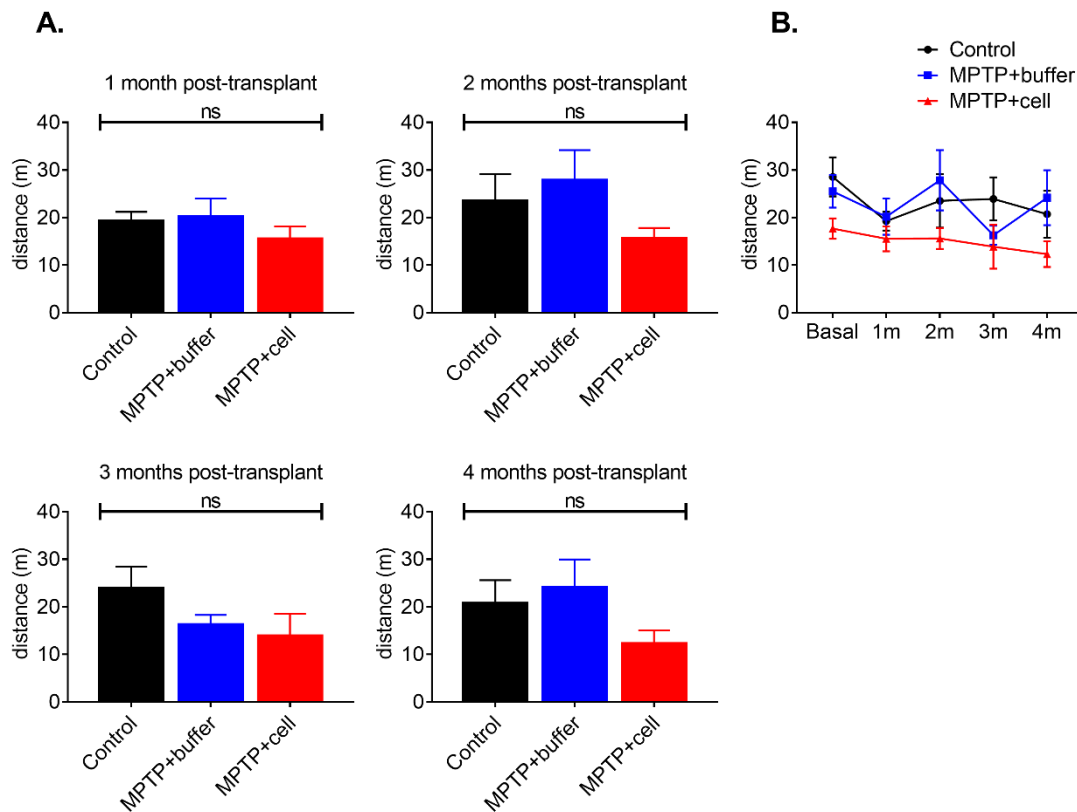


Figure 33: Total distance traveled one-four months post-transplant (A), and graph showing evolution from experiment initiation to completion (B). In B, each colored line represents an experimental group. Black = control, blue = MPTP+buffer, red = MPTP+cell. 1m = one month post-transplant, 2m = two months post-transplant, 3m = three months post-transplant, 4m = four months post-transplant. ns = not significant.

In terms of time spent in the center, from basal measurements to completion of the experiment, hNSC-transplanted mice maintained a very low amount of time in this area. Control mice showed this same pattern starting at one month post-transplant, probably due to habituation. One month post-transplant, buffer-treated mice spent more time in the center of the box compared to control animals ($p < 0.05$).

This was alleviated by hNSC transplant as SC-treated mice spent significantly less time in the center ($p < 0.05$). This trend also appeared at four months post-grafting, but was only significant when comparing the amount of time spent in the center by buffer- and cell-treated mice ($p < 0.05$) (Figure 34). Adult and middle-aged control mice exhibited the same patterns of time spent in the center, however hNSC-transplanted mice of both age groups differed in the amount of time, with adult SC-treated mice spending up to 24 times more total amount of minutes in the center compared to middle-aged equivalents. For both age groups, the buffer-treated group seemed to be the determinant of differences among groups as at month two and three, they spent less time in the center than at month one and four. Four months post-transplant, both adult and middle-aged mice treated with hVM1 clone 32 cells tended to spend less time in the center of the OFT box compared to buffer-treated animals.

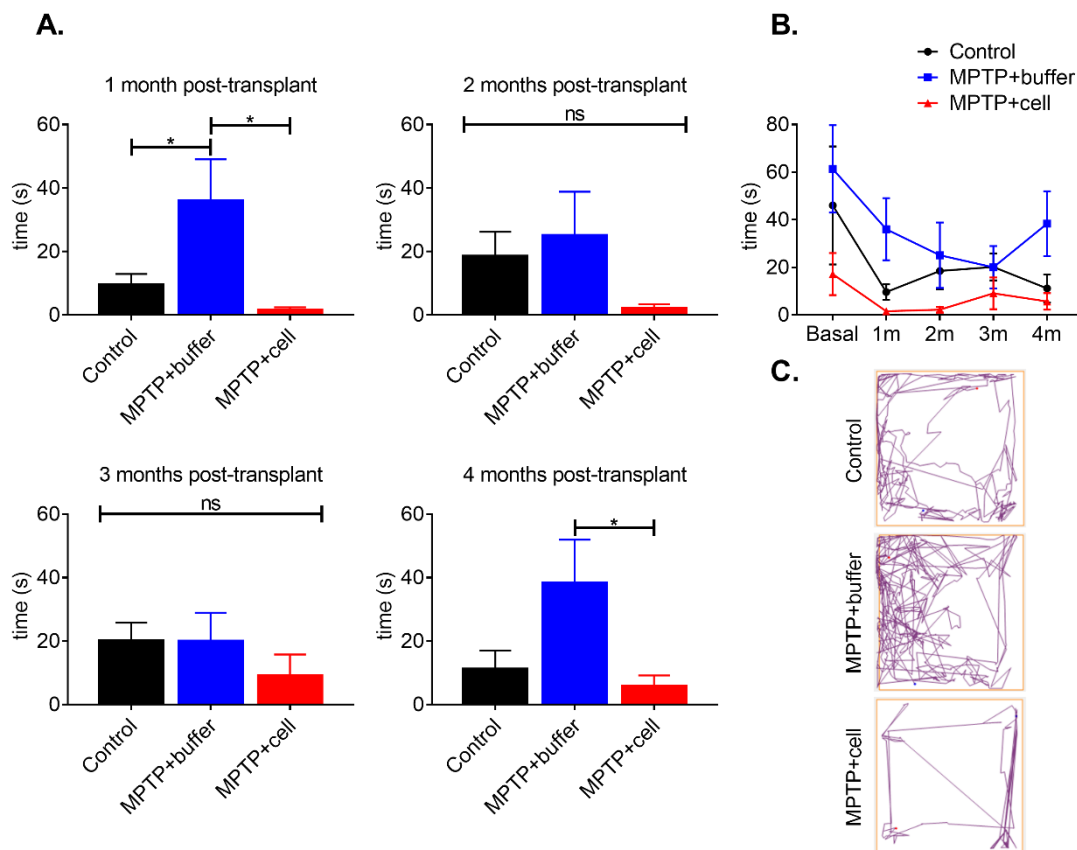


Figure 34: Time spent in center one-four months post-transplant (A), and graph showing evolution from experiment initiation to completion (B). In B, each colored line represents an experimental group. Black = control, blue = MPTP+buffer, red = MPTP+cell. 1m = one month post-transplant, 2m = two months post-transplant, 3m = three months post-transplant, 4m = four months post-transplant. Representative images of movement in OFT box (C). ns = not significant.

For all of the timepoints studied post-transplant, there were no significant differences between any of the three groups in terms of time spent grooming (Figure 35). This same trend occurred in all adult mice treatment groups.

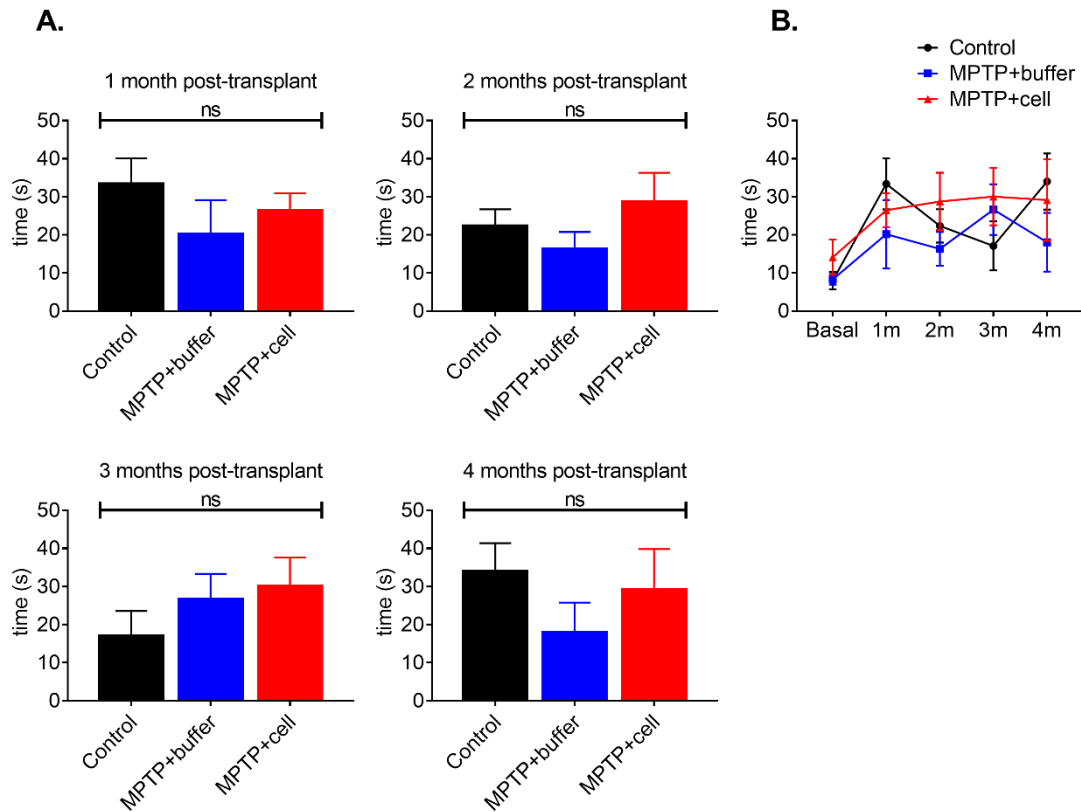


Figure 35: Time spent grooming one-four months post-transplant (A), and graph showing evolution from experiment initiation to completion (B). In B, each colored line represents an experimental group. Black = control, blue = MPTP+buffer, red = MPTP+cell. 1m = one month post-transplant, 2m = two months post-transplant, 3m = three months post-transplant, 4m = four months post-transplant. ns = not significant.

There were no significant differences nor trends observed for time spent rearing when comparing the three groups. Similar to distance traveled and time spent in center, SC-treated mice maintained a low amount of time rearing throughout the experiment (Figure 36). The lack of trend in time spent rearing appeared in adult mice too, but SC-treated adult mice tended to spend more time rearing compared to middle-aged cell-treated animals.

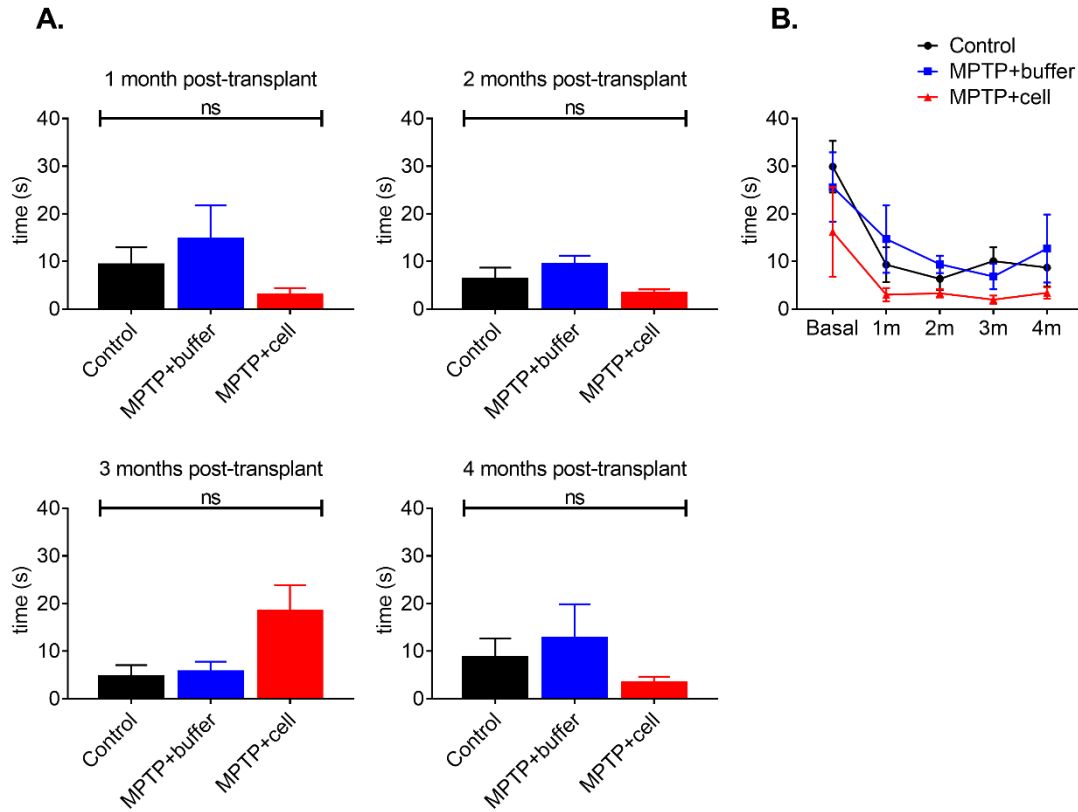


Figure 36: Time spent rearing one-four months post-transplant (A), and graph showing evolution from experiment initiation to completion (B). In B, each colored line represents an experimental group. Black = control, blue = MPTP+buffer, red = MPTP+cell. 1m = one month post-transplant, 2m = two months post-transplant, 3m = three months post-transplant, 4m = four months post-transplant. ns = not significant.

Therefore, middle-aged mice showed no clear patterns or differences among groups in total distance traveled, and time spent grooming and rearing. This was true of adult mice too. In addition, similar to adult mice, buffer-treated middle-aged mice showed a trend of spending more time in the center in the OFT compared to controls four months post-transplant, which was reduced in SC-treated mice of all ages, but only significantly in middle-aged mice. Like adult mice, urination and defecation tendencies were similar across all three experimental groups in middle-aged mice (not shown).

In the PPT, changes in gait were analyzed by measuring stride length, stride width, and paw overlap. There was a decrease in CL and IL forelimb stride lengths upon administration with MPTP. Compared to controls, buffer-treated mice had significantly decreased CL forelimb stride length at all timepoints tested and cell-transplanted animals had significantly decreased CL forelimb stride length at two and three months post-transplant. At experiment endpoint, four months post-transplant, this decreased CL forelimb stride length was alleviated by transplant ($p < 0.01$). This same pattern occurred for IL forelimb stride length, but the improvement at four months post-transplant was less significant than

the CL equivalent ($p < 0.05$) (Figure 37). In both middle-aged and adult mice, upon administration of MPTP, there was a decrease in forelimb stride length, but this decrease was more minute in adult mice, thus there was really nothing for the hNSCs to improve. In middle-aged mice, this more severe decrease in stride length was alleviated by SC transplant four months post-transplant.

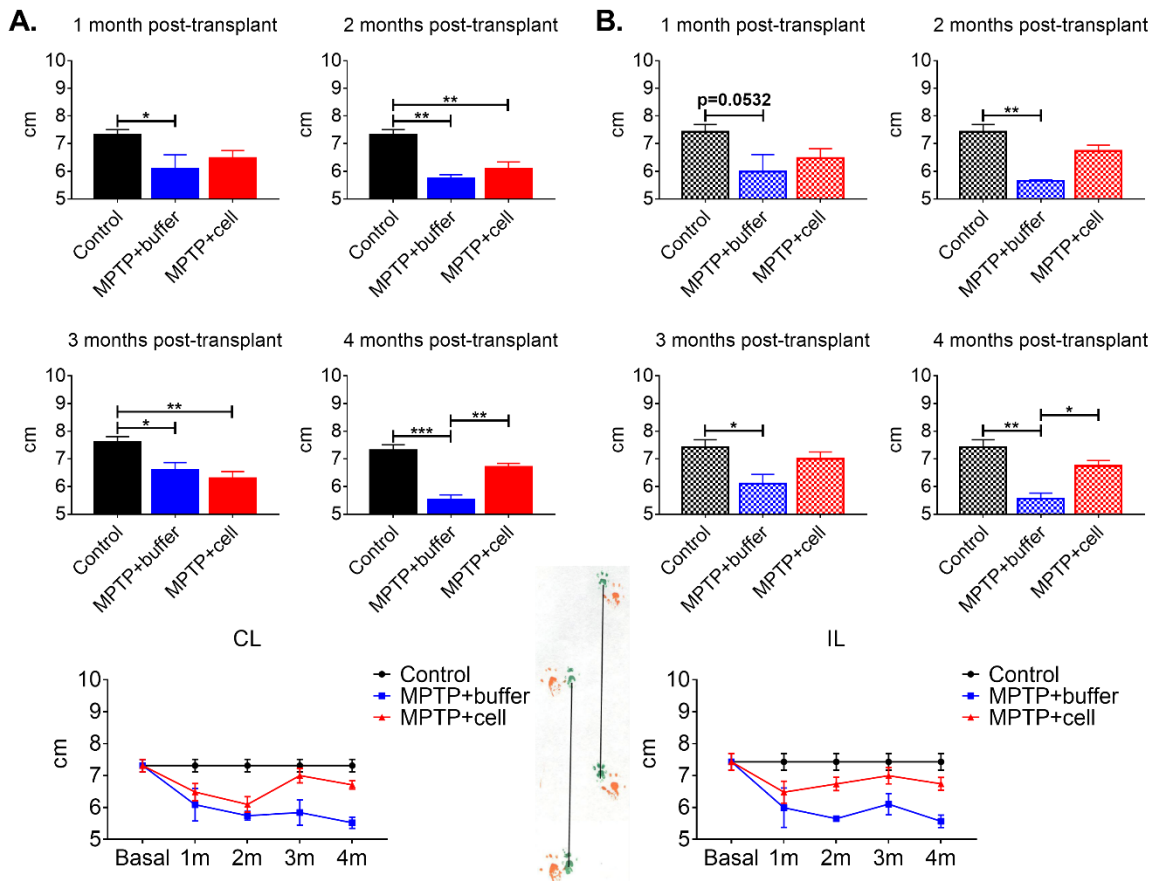


Figure 37: Forelimb stride length one-four months post-transplant, and graphs showing evolution from experiment initiation to completion (A = CL, B = IL). In summary graphs, each colored line represents an experimental group. Black = control, blue = MPTP+buffer, red = MPTP+cell. 1m = one month post-transplant, 2m = two months post-transplant, 3m = three months post-transplant, 4m = four months post-transplant.

Both CL and IL hindlimb stride lengths showed very similar patterns. At every timepoint tested, there was a (near-)significant decrease in hindlimb stride length in buffer-treated mice compared to controls ($p \leq 0.0514$). Two months post-transplant, there was also a decrease in CL hindlimb stride length of hNSC-transplanted animals ($p < 0.01$). At this same timepoint, the decrease in IL hindlimb stride length had a tendency to be alleviated in SC-treated mice ($p = 0.0552$). At experiment endpoint, the decrease in both CL and IL hindlimb stride length was alleviated by transplant ($p < 0.05$) (Figure 38). Similar to forelimb stride length, hindlimb stride length decrease was less severe in adult mice compared to middle-aged animals, and was only alleviated by transplant in middle-aged mice at four months post-transplant.

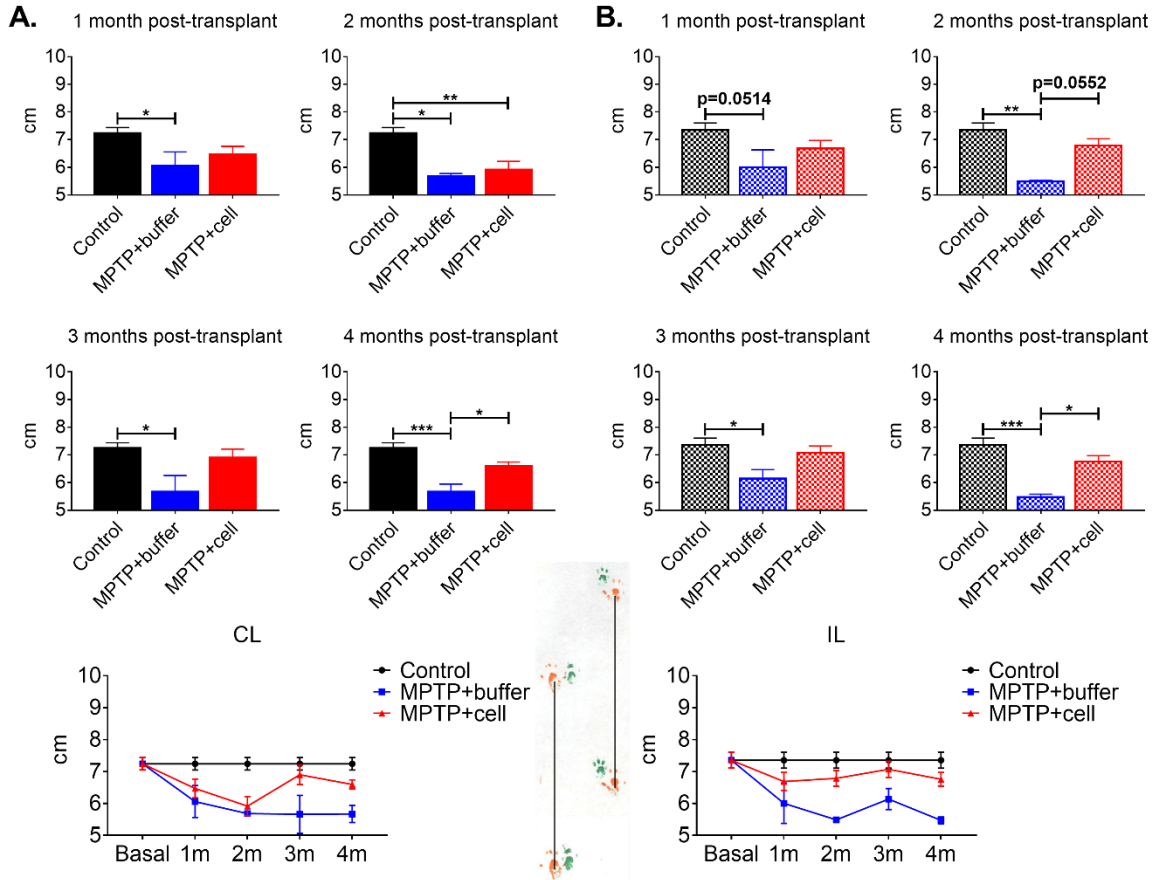


Figure 38: Hindlimb stride length one-four months post-transplant, and graphs showing evolution from experiment initiation to completion (A = CL, B = IL). In summary graphs, each colored line represents an experimental group. Black = control, blue = MPTP+buffer, red = MPTP+cell. 1m = one month post-transplant, 2m = two months post-transplant, 3m = three months post-transplant, 4m = four months post-transplant.

Forelimb CL-IL stride width was decreased in buffer-transplanted mice compared to controls at every timepoint tested, and three and four months post-transplant, this decrease was alleviated by SC transplant ($p < 0.05$). Forelimb IL-CL stride width was unchanged at one and three months post-transplant, and when it was significantly decreased two and four months post-transplant ($p < 0.05$), this was not improved by hNSC transplant (Figure 39). Forelimb CL-IL stride width was more significantly decreased in middle-aged buffer-treated mice compared to adult equivalents, and in the case of middle-aged SC-treated animals, this diminution was significantly rescued at experiment endpoint. Four months post-transplant, forelimb IL-CL stride width trends were similar in both age groups as the decrease seen in buffer-treated mice was not alleviated by hNSC transplant.

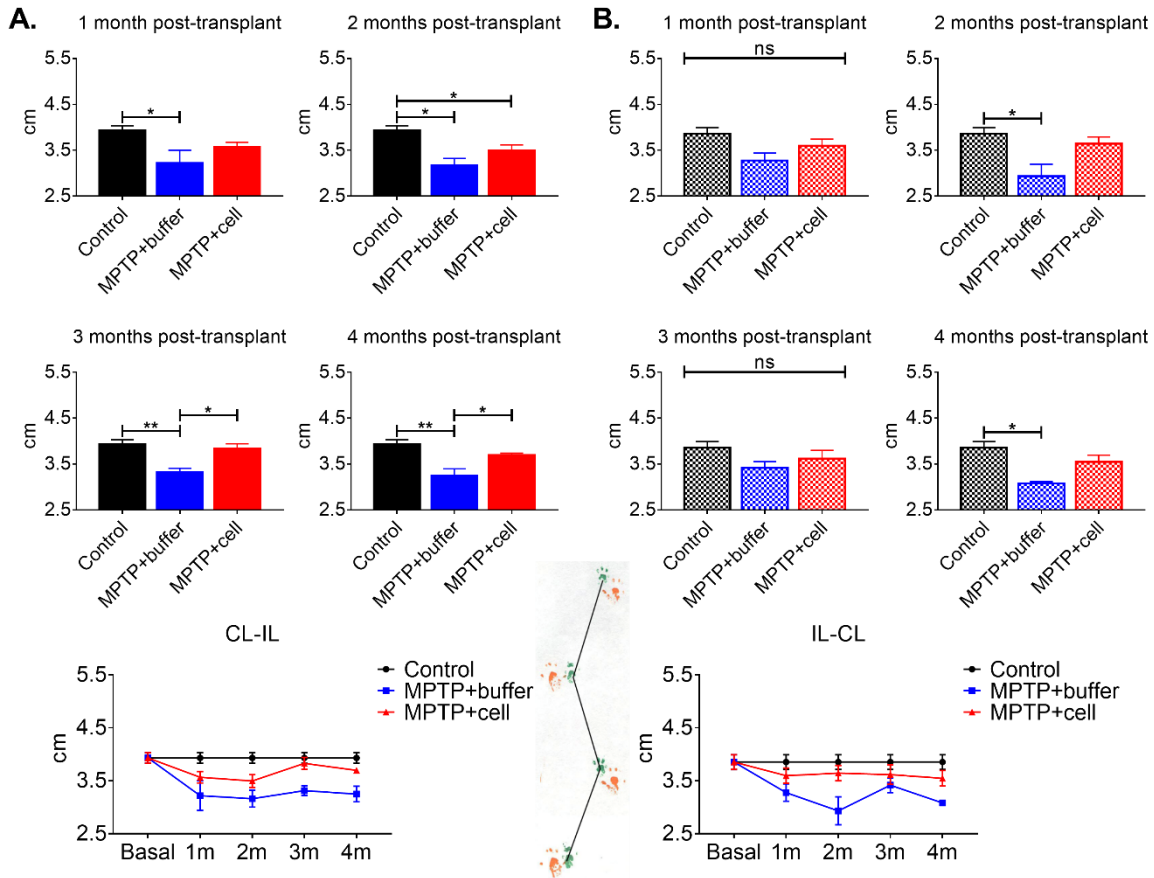


Figure 39: Forelimb stride width one-four months post-transplant, and graphs showing evolution from experiment initiation to completion (A = CL-IL, B = IL-CL). In summary graphs, each colored line represents an experimental group. Black = control, blue = MPTP+buffer, red = MPTP+cell. 1m = one month post-transplant, 2m = two months post-transplant, 3m = three months post-transplant, 4m = four months post-transplant. ns = not significant.

For hindlimb CL-IL stride width, there were no significant differences nor trends between any of the groups. Hindlimb IL-CL stride width followed quite a different pattern. Buffer-treated mice had decreased IL-CL stride width throughout the experiment ($p < 0.01$). Animals given hNSC transplant showed improvement at two months post-transplant, however at one month post-transplant, and more importantly, four months post-transplant, there was a significant decrease in hindlimb IL-CL stride width in SC-treated mice compared to controls ($p < 0.05$) (Figure 40). Middle-aged and adult mice showed a similar trend in hindlimb CL-IL stride width in that there were no clear differences between all groups. By contrast, buffer-treated middle-aged, and not adult, mice showed significant differences in hindlimb IL-CL stride width compared to controls.

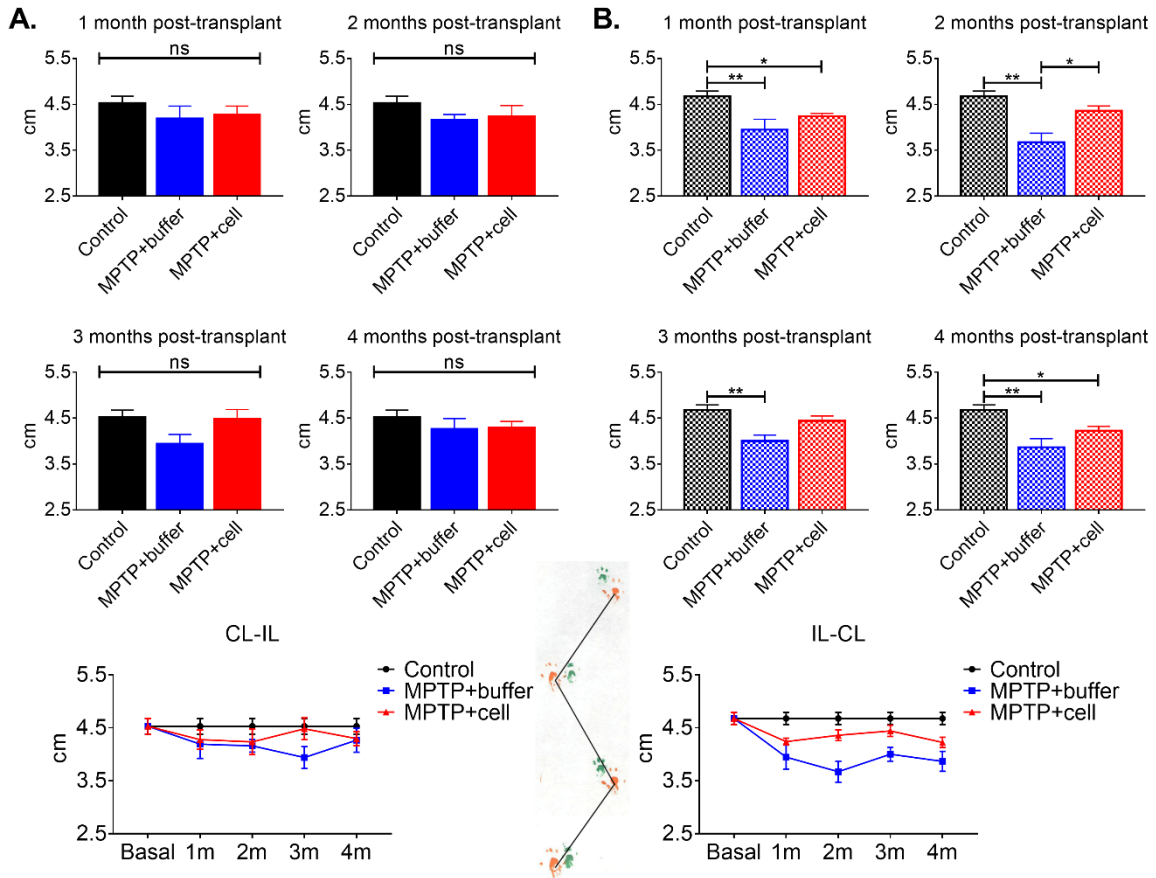


Figure 40: Hindlimb stride width one-four months post-transplant, and graphs showing evolution from experiment initiation to completion (A = CL-IL, B = IL-CL). In summary graphs, each colored line represents an experimental group. Black = control, blue = MPTP+buffer, red = MPTP+cell. 1m = one month post-transplant, 2m = two months post-transplant, 3m = three months post-transplant, 4m = four months post-transplant. ns = not significant.

Three months post-transplant, there was a significant increase in CL paw overlap in SC-treated mice compared to buffer-treated animals. Other than this, there were no differences nor trends between any of the groups in paw overlap measurements (Figure 41). The aforementioned observation occurred in adult mice as well.

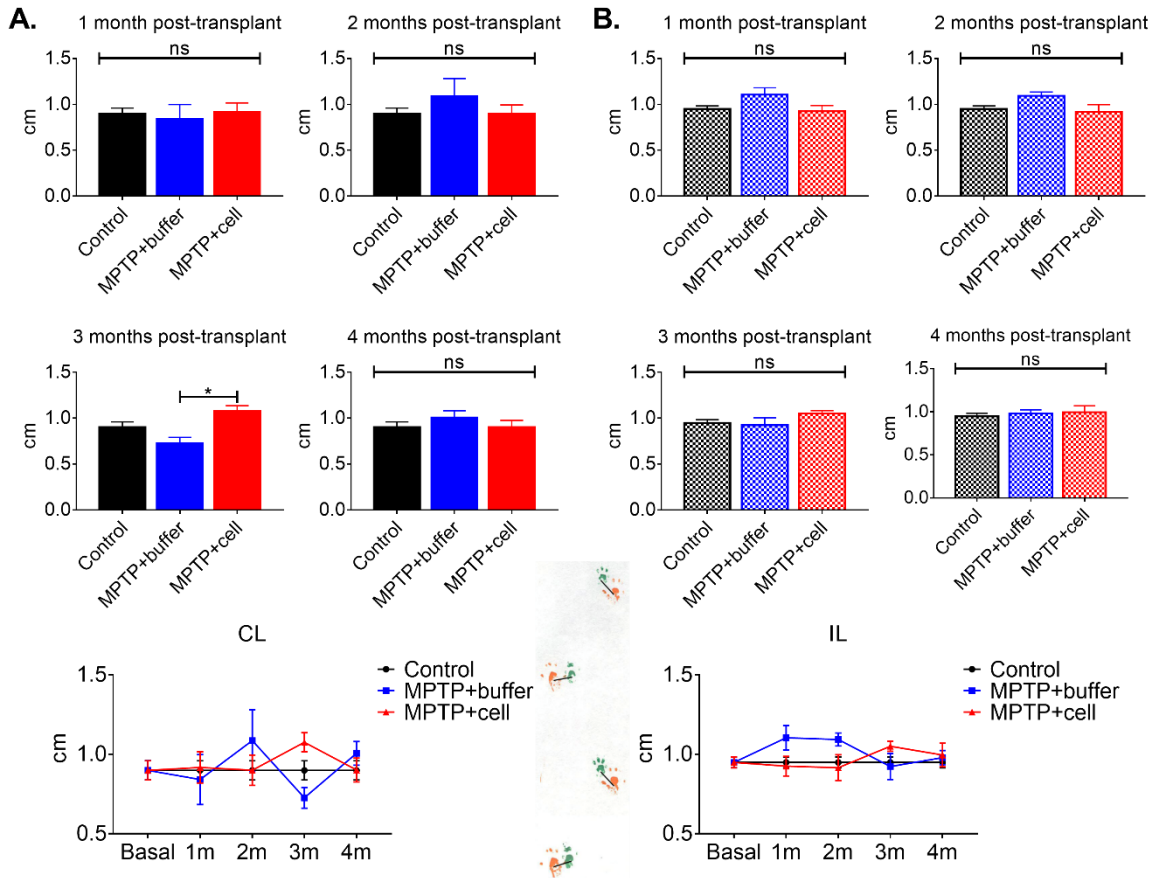


Figure 41: Paw overlap one-four months post-transplant, and graphs showing evolution from experiment initiation to completion (A = CL, B = IL). In summary graphs, each colored line represents an experimental group. Black = control, blue = MPTP+buffer, red = MPTP+cell. 1m = one month post-transplant, 2m = two months post-transplant, 3m = three months post-transplant, 4m = four months post-transplant. ns = not significant.

Therefore, paw overlap analysis was not able to serve as a measure of gait impairment as there were no significant differences between treatment groups in both adult and middle-aged mice. Furthermore, forelimb and hindlimb stride lengths, forelimb stride width, and IL-CL hindlimb width, decreased more significantly in middle-aged mice, and was sometimes alleviated by hNSC transplant.

The effect of hVM1 clone 32 transplantation on inflammation

Neuroinflammation was analyzed in the rostral Str and SNpc of middle-aged mice. In the rostral Str, the astroglial population tended to increase in buffer-treated animals compared to controls (Figure 42).

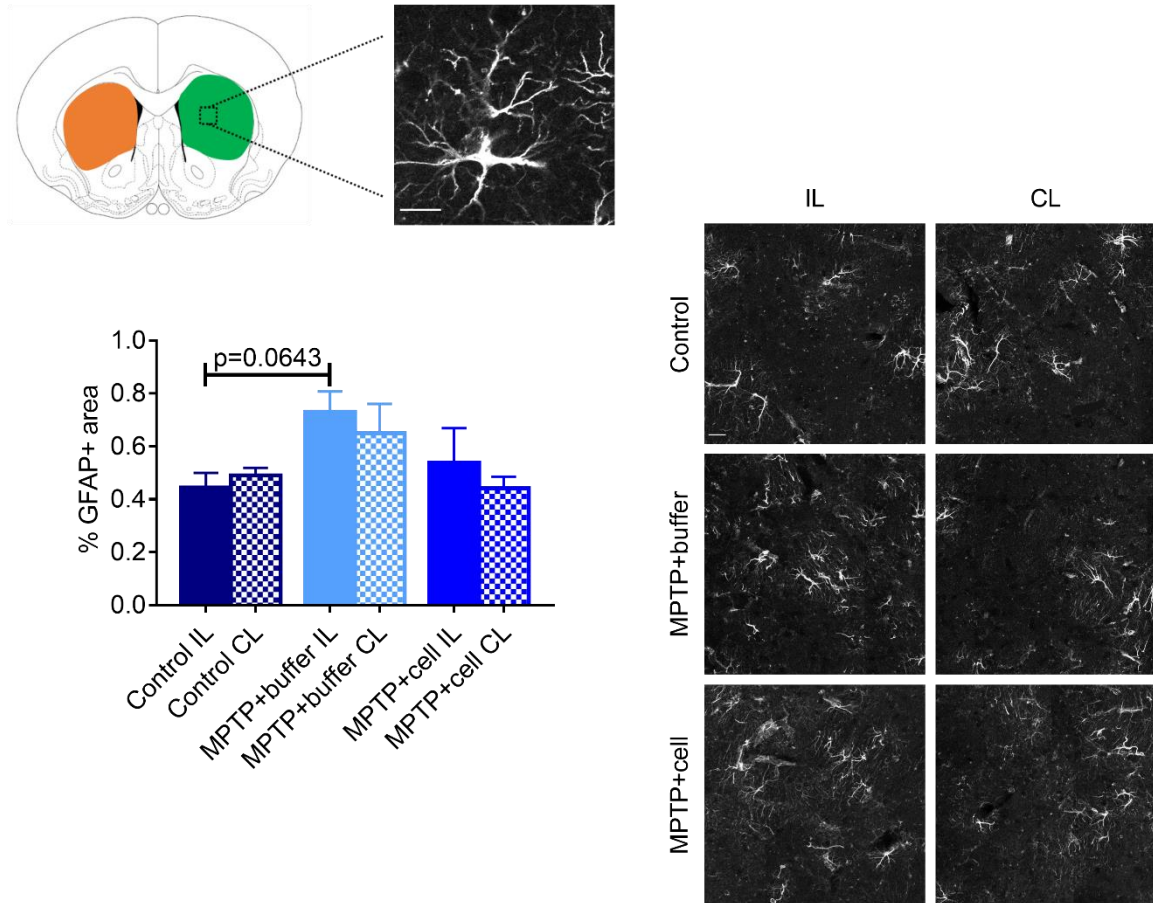


Figure 42: Rostral striatal GFAP expression, with quantification (left) and representative images (right). Top scale bar = 10 μm and scale bar in control IL panel = 25 μm.

In the SNpc, all groups had similar percentages of GFAP immunostaining except for the Str CL to the side of the transplant of hNSC-grafted mice, which had significantly decreased GFAP expression compared to the IL Str of buffer-treated animals (Figure 43A). It is worth noting that the CL rostral Str of SC-treated mice had a tendency to show equal or lower GFAP immunoreactivity compared to every other group (Figure 42). Expression of the microglial marker Iba1 in the SNpc showed no differences nor trends when comparing all groups (Figure 43B).

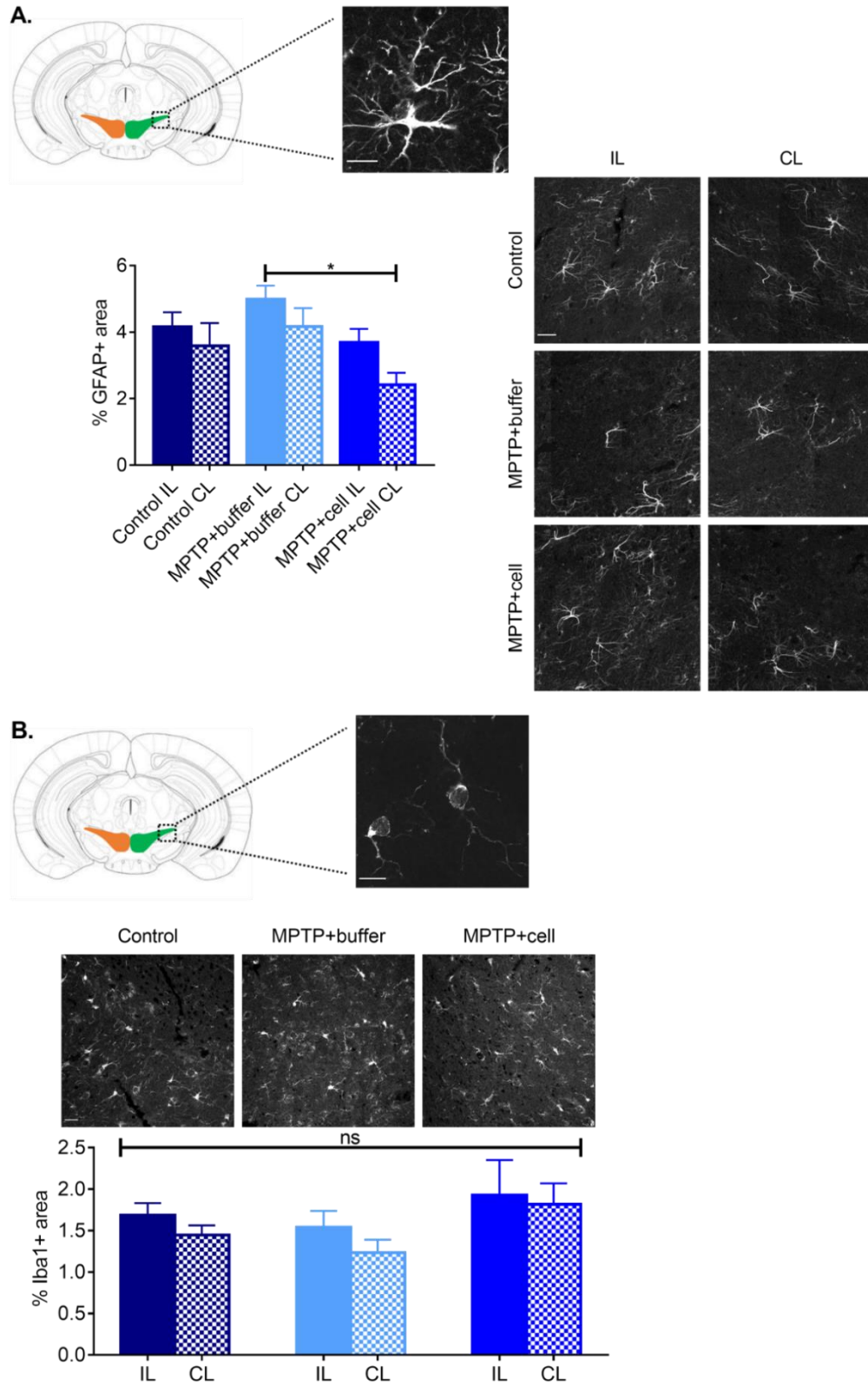


Figure 43: Nigral GFAP expression, with quantification (left) and representative images (right) (A), and nigral Iba1 expression with quantification (bottom) and representative images (top) (B). ns = not significant. Top scale bar = 10 μ m and scale bar in control IL panel = 25 μ m.

When comparing GFAP expression in adult and middle-aged control mice, the latter had around three times more astroglial immunoreactivity than the former. In middle-aged mice, buffer-treated animals had increased GFAP expression compared to controls but this did not occur in adult animals. The rostral Str IL to the side of transplant of adult hNSC-transplanted mice saw an enormous increase in astroglial immunostaining, but this did not occur in the equivalent group of middle-aged mice. Most notably, the CL rostral Str of both adult and middle-aged SC-treated mice had almost equal levels of GFAP expression. In the SNpc, GFAP immunostaining was increased by approximately 1% in middle-aged control mice compared to adult equivalents. Both age groups showed similar patterns in GFAP expression increase except for the decreased GFAP+ area in the CL rostral Str in middle-aged SC-treated mice, which did not occur in equivalent adult mice. Although Iba1 expression levels of both adult and middle-aged control mice were similar, the two age groups showed very contrasting patterns upon administration of MPTP. In adult mice, there was a clear increase in Iba1 immunostaining while in middle-aged mice, there was no change in Iba1 expression.

When analyzing superficial cervical LNs, both buffer-treated and SC-treated mice had decreased LN area compared to control mice ($p < 0.01$) (Figure 44A). This is the opposite pattern that was seen in adult mice, where MPTP-lesioned mice showed a tendency to have smaller LN size compared to controls. Interestingly, adult and middle-aged MPTP-treated animals had similar LN area, but the control mice of both age groups differed greatly, with middle-aged controls having LNs three times larger than adult equivalents.

Next, MC populations in the LNs were studied. Although not statistically significant, hNSC-transplanted mice had a tendency to have increased MC density compared to control animals (Figure 44B). This same pattern occurred in adult mice. While middle-aged control animals had almost double the MC density compared to adult equivalents, MC density in MPTP-treated mice of all ages was similar. In both age groups, there is a clear connection between the CNS and LNs, and an evident reaction of the LNs and their MC population to both MPTP administration and hNSC transplant.

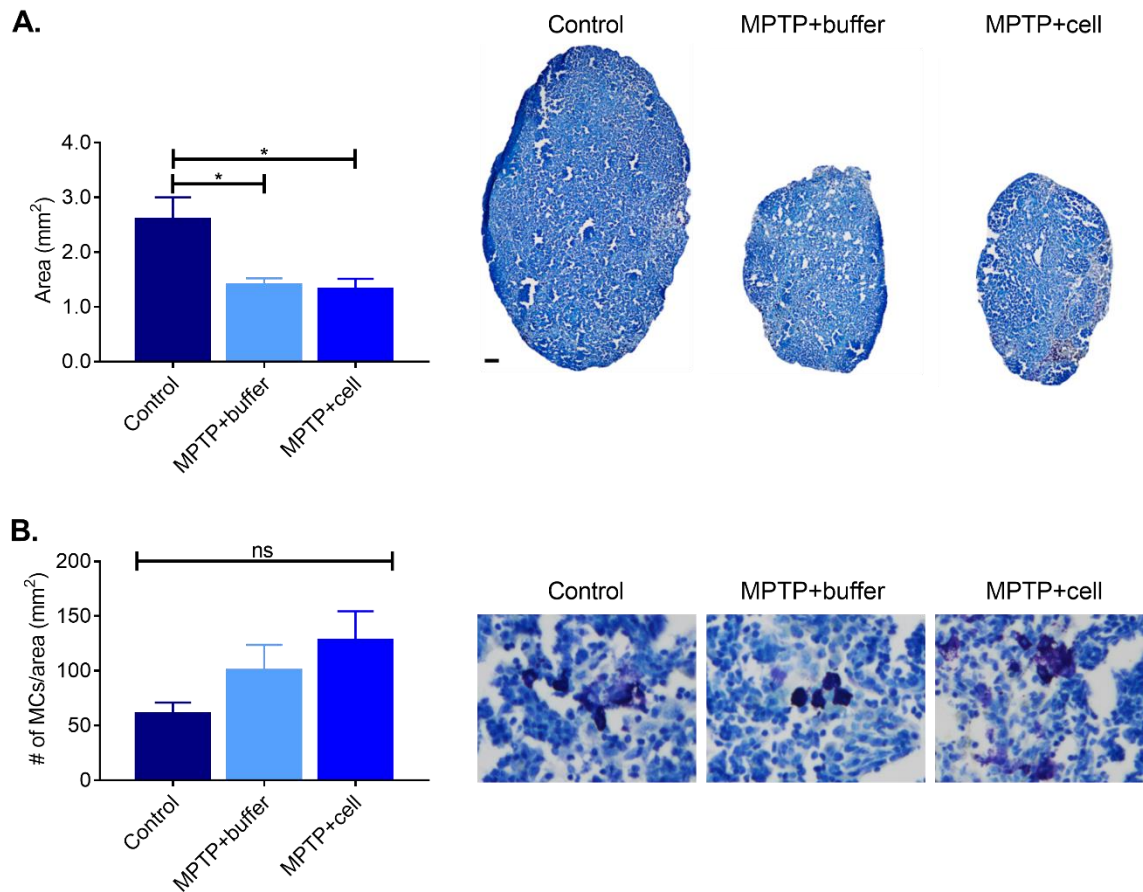


Figure 44: Lymph node size (A) and MC density in the LNs (B), with quantification (left) and representative images (right). ns = not significant. Scale bar A = 100 μ m and scale bar B = 25 μ m.

There was no quantifiable amount of MCs in either the rostral Str or SNpc (not shown), so similar to adult mice, in middle-aged mice, MCs in the CNS do not appear to play an important role in the CNS in this particular experimental PD study.

The effect of hVM1 clone 32 transplantation on mechanisms of repair

Angiogenesis was subsequently studied in the rostral Str and SNpc. In the rostral Str, there were no changes among the groups in blood vessel staining (Figure 45A). In the SNpc, although there were no statistically significant differences between all groups, there was a tendency for all MPTP-treated mice to have increased β -DAG immunostaining in the SNpc (Figure 45B). In general, β -DAG expression was similar in adult and middle-aged mice. Based on observed tendencies, upon treatment with MPTP, adult mice showed a decrease in angiogenesis in the Str while middle-aged mice showed no changes, and in the SNpc, adult mice showed no expression changes while middle-aged animals demonstrated increased angiogenesis.

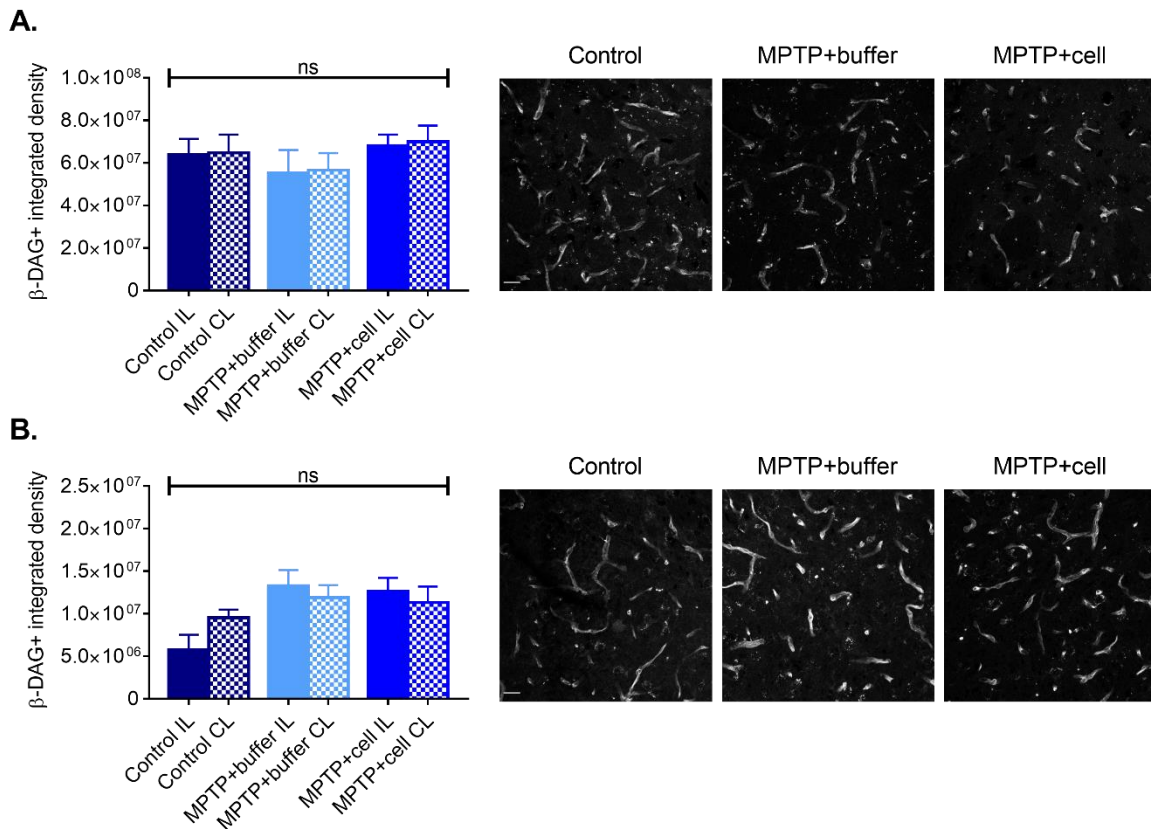


Figure 45: Blood vessels in the rostral Str (A) and SNpc (B), with quantification (left) and representative images (right). ns = not significant. Scale bar = 25 μ m.

In the SVZ, there were no statistically significant differences nor trends observed in NES, Ki-67, and DCX, expression among the three groups. Only Ki-67 expression tended to increase in the SVZ of buffer-treated mice compared to control animals (Figure 46). Adult and middle-aged control mice had similar expression levels of NES in the SVZ, and neither age group showed a change in immunoreactivity upon administration of MPTP. Adult control mice had more Ki-67+ cells compared to middle-aged equivalents (approximately 52 vs. 35 per slice). Both age groups demonstrated parallel

patterns but they differed in that, unlike adult mice, middle-aged buffer-treated mice had a tendency to have increased Ki-67 expression in the SVZ compared to control animals. When comparing DCX expression, upon treatment with MPTP, there was a decrease in DCX immunostaining in adult mice, which did not occur in middle-aged mice. It is important to note that DCX expression levels in all middle-aged mice are similar to those of all adult MPTP-treated mice.

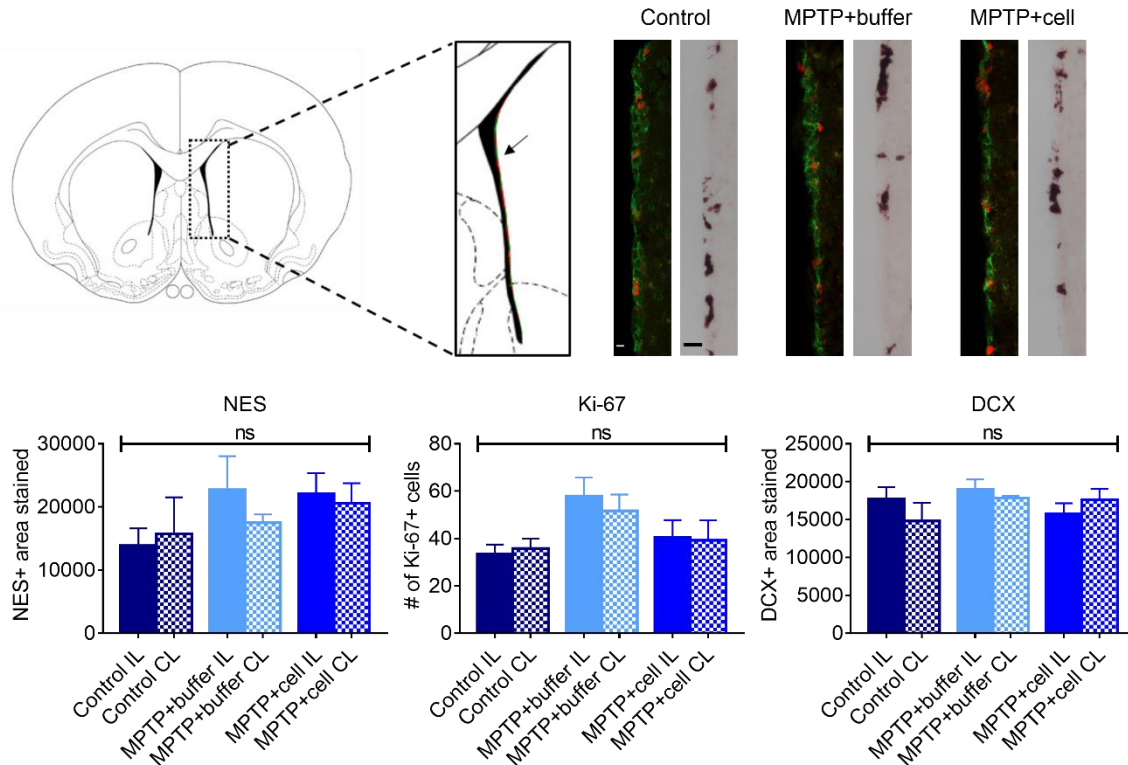


Figure 46: Neurogenesis in the SVZ. Quantification of NES (bottom left), Ki-67 (bottom middle), and DCX (bottom right), expression, in the SVZ with representative NES/Ki-67 (top left; NES in green and Ki-67 in red) and DCX images (top right). ns = not significant. Left scale bar = 10 μ m and right scale bar = 25 μ m.

In middle-aged mice, neurogenesis was only able to be analyzed and quantified in the SVZ because in the SGZ, in agreement with previous publications, there was no quantifiable amount of immunostaining present for NSC/NPC markers NES and Ki-67, or immature neuron marker DCX. At the time of sacrifice, these animals were around 17 months old, almost approaching the aged category for mice. In adult mice, neither NES nor Ki-67 were expressed in the SGZ either, but DCX immunostaining was still present in the SGZ of adult mice.

In the case of middle-aged mice, it was not possible to make a correlation between the nigrostriatal system and hippocampal neurogenesis because there was no hippocampal neuroblast neurogenesis

present and there was no improvement seen in either the Str or SNpc of SC-treated middle-aged mice compared to buffer-treated mice of the same age.

In summary, TH expression, inflammation, and angiogenesis, in the nigrostriatal pathway along with behavior, neurogenesis, and MC populations in the LNs, were analyzed in Parkinsonian mice transplanted with hVM1 clone 32 cells in adult and middle-aged animals. This allowed for an in-depth look at the sometimes shared and sometimes contrasting mechanisms occurring at these two distinct ages, which will be further elaborated in the next section.

DISCUSSION

Parkinson's disease, the second most common neurodegenerative disease in the world, is characterized by the death or impairment of DAN in the SNpc and DA depletion in the Str (Chai, Lim, 2013, De Virgilio et al., 2016, Kalia, Lang, 2015, Lesage, Brice, 2009, Sarkar, Raymick & Imam, 2016, Stoker, Torsney & Barker, 2018, Wirdefeldt et al., 2011). It is a disease affecting the elderly with a prevalence expected to grow exponentially during the next decades (De Virgilio et al., 2016, Kalia, Lang, 2015, Lesage, Brice, 2009). There is currently no cure for PD, but there are several ongoing experimental studies and clinical trials searching for biological or chemical agents able to protect, replace, and/or regenerate the cells lost during PD, among them SCs. (Chai, Lim, 2013, De Virgilio et al., 2016, Kalia, Lang, 2015, Lesage, Brice, 2009, Sarkar, Raymick & Imam, 2016, Stoker, Torsney & Barker, 2018, Wirdefeldt et al., 2011).

To this extent, the purpose of this thesis was to explore if transplanted hNSCs could replace and take over the functions of the impaired or lost DAN in an experimental PD rodent model by integrating in the host environment, consequently rescuing nigrostriatal innervation, improving motor deficits, and exerting neurotrophic effects. Because many experimental PD studies are done in adult animals, which translates poorly into clinical situations as PD patients are older, this experimental CRT study was done in both adult and middle-aged Parkinsonian mice using the hNSC line hVM1 clone 32.

This thesis strived to characterize the hNSCs *in vitro*, study the fate of transplanted cells, and examine the effects of hNSC transplantation on nigrostriatal TH populations, behavior, inflammation, angiogenesis, and neurogenesis.

In vitro characterization revealed that hVM1 clone 32 cells are true NSCs with the capability of generating genuine A9 DAN. They showed an upregulation of NSC/NPC-associated genes in proliferation conditions, and after seven days of differentiation, they displayed a downregulation of the aforementioned genes and an upregulation in DAN-associated genes. In addition, differentiated hVM1 clone 32 cells expressed protein markers related to DAN.

In a prior publication done in 6-OHDA-lesioned rats, not only did the hVM1 clone 32 cells survive two months post-grafting, they also expressed TH and human neuron specific enolase markers at this timepoint (Ramos-Moreno et al., 2012). This is in stark contrast to the present study where the transplanted cell survival rate was negligible four months post-transplant, although there is evidence of transplantation with the needle mark. One of the problems in CRT is cell survival, with only up to 20% of cells surviving *in vivo* and in patients, and cell survival is linked to functional recovery

(Cooke, Vulic & Shoichet, 2010, Emgard et al., 1999, Emgard et al., 2003, Johann et al., 2007, Tam et al., 2014). Around 95% of transplanted cells die in experimental PD animals and PD patients shortly after transplantation (Rafuse et al., 2005). Even in the most successful clinical trials in PD patients to date, there is low graft survival, with some surviving cells expressing TH (Emgard et al., 2003, Stoker, Barker, 2016).

Transplanted cell survival depends on the technique implemented, grafting of single cells or neurospheres, animals used, and the time from injury to transplant, among other factors (Cooke, Vulic & Shoichet, 2010, Johann et al., 2007). In both studies, the same technique and single cells were used, but more cells were transplanted in rats, 300,000, compared to 100,000 in mice. Rat brains are around four times bigger than mouse brains and need more cells transplanted as they have more cells and more neurons in the brain ((Bolon, Graham, 2011, Herculano-Houzel, Mota & Lent, 2006). Although in one case the proportion of surviving cells was found to be the same no matter how many cells were transplanted (Cooke, Vulic & Shoichet, 2010), perhaps 100,000 cells were too few. Also, the experiment endpoint was earlier in the rat experiment, two months versus four months post-transplant. However, it has been shown that transplanted cells that die normally do so within the first seven days after being transplanted via apoptosis and/or necrosis (Cooke, Vulic & Shoichet, 2010, Emgard et al., 1999, Emgard et al., 2003, Pallet et al., 2012).

Another reason why grafted cells die is because the environment in which they are being transplanted is not ideal (Cooke, Vulic & Shoichet, 2010, Emgard et al., 2003, Johann et al., 2007, Tam et al., 2014). However, this inadequate environment is not created by the neurotoxins 6-OHDA or MPTP as there was no difference in transplanted cell survival in Parkinsonian compared to control rats (Emgard et al., 1999), and in this thesis, astrocytes in the Str did not react to the MPTP, they only reacted to the hNSC transplant. Astrocytes in the Str have a clear augmentation in response to the cell transplant in adult mice which could explain cell death, but this is not the case for middle-aged SC-treated animals, where transplanted hNSCs also died. However, the three month-old rats used in Ramos-Moreno et al., 2012, and the 12 month-old mice used in this thesis cannot be compared in terms of environment because in older rodents, there is more neuroinflammation and less neurogenesis. Therefore, comparing the adult rat and mouse studies using hVM1 clone 32 cells, the time of transplantation could be very important as rats were transplanted five weeks after 6-OHDA lesion and mice were transplanted one week after MPTP lesion. This four-week difference could be critical, maybe not in terms of astroglial activation (which was not studied in Ramos-Moreno et al., 2012), but in terms of other things like DAN death, pro-inflammatory cytokine release, mitochondrial

dysfunction, apoptosis, and autophagy processes occurring after neurotoxin injection, which after five weeks are probably more stabilized than after one week.

Since an irrelevant number of surviving transplanted cells were found in the Str, the majority of them must have either migrated or died. However, there were no hVM1 clone 32 cells found in other brain regions such as the SNpc and Hip. Therefore, the more plausible explanation is that the transplanted cells died, but in adult mice, there were still beneficial effects upon transplantation of the hNSCs. One conceivable option for this could be that the cells secreted factors before dying, and as shown, these cells release VEGF-A, VEGF-C, MCP-1, FKN, SCF, GDNF, and BDNF, *in vitro*. Also, all of these factors' receptors were expressed on the hVM1 clone 32 cells *in vitro*, with upregulated gene expression under differentiation conditions, with exception of *VEGFR2*, *NRP1*, and *NRP2*, which bind VEGF-A and VEGF-C, and were upregulated in proliferating cells.

The hVM1 clone 32 cells have the potential to trigger beneficial effects because *in vitro* they secrete the aforementioned factors. Although they were not detected *in vivo*, due to low concentration values and difficulty in distinguishing between human and mouse proteins, it is plausible that the positive outcome of the hNSC transplantation in adult mice could very likely be a response to the secretion of these factors.

The VEGF family promotes angiogenesis, neurogenesis, and glial proliferation, and protects DAN in experimental PD models (Caballero, Sherman & Falk, 2017, Falk, Zhang & Sherman, 2009, Falk, Gonzalez & Sherman, 2010, Falk et al., 2011, Piltonen et al., 2011, Shim, Madsen, 2018, Tian et al., 2007, Troncoso-Escudero et al., 2018, Yasuhara et al., 2004, Yasuhara et al., 2005, Yasuhara, Date, 2007). Neural stem cells secreting VEGF-A were encapsulated and transplanted into the Str either before or after 6-OHDA lesion in rats; in both cases, this resulted in behavioral improvement in addition to nigrostriatal rescue. In the Str, there was also an increase in angiogenesis and astroglial proliferation (Yasuhara et al., 2004, Yasuhara et al., 2005, Yasuhara, Date, 2007). Embryonic DAN treated with VEGF-C showed increased survival compared to controls, and intrastriatal injections of VEGF-C into Parkinsonian rats showed behavioral improvement, minor amelioration in nigrostriatal populations in Str and SNpc, and slight or no increase in angiogenesis in Str depending on dosage. In intact brains, VEGF-C injection led to an increase in astrocyte and microglia number (Piltonen et al., 2011). It was shown that VEGF-A and VEGF-C were secreted by hVM1 clone 32 cells *in vitro* and it is therefore plausible that *in vivo*, these factors participated in the rescue of TH+ nerve terminals in the Str and TH+ cells in the SNpc of adult hNSC-transplanted mice. Neither VEGF-A or VEGF-C

increased angiogenesis but they could have contributed to glial proliferation in adult hNSC-transplanted mice as shown via GFAP immunostaining increase. Moreover, VEGF released by transplanted cells also could have contributed to SGZ neurogenesis improvement in adult mice, and could have played a role in increased GDNF levels *in vitro* as VEGF can upregulate GDNF expression (Yasuhara, Date, 2007).

The chemokine MCP-1 is a two-faced factor as it has been shown to have both detrimental and beneficial effects. It activates microglia and guides them to site of injury and is also involved in cell death. In addition, MCP-1 contributes to microglial activation and migration, and promotes angiogenesis (Fuzzati-Armentero, Cerri & Blandini, 2019, Kalkonde et al., 2007, Kempuraj et al., 2016, Liu et al., 2019, Pallet et al., 2012, Pawitan, 2014, Wang et al., 2014). Although MCP-1 influences DAn, genetic knockout of MCP-1 or both MCP-1 and its receptor did not prevent MPTP-induced DAn degeneration (Guyon et al., 2009, Kalkonde et al., 2007, Liu et al., 2019). In this study, hVM1 clone 32 cell transplantation did not lead to an increase in angiogenesis in either adult or middle-aged Parkinsonian mice. However, there was an increase in microglia in the SNpc of adult mice, so the presence of MCP-1 potentially secreted by the hNSCs *in vivo* could have been contributed to this microglial activation.

Fractalkine inhibits neuroinflammation in the CNS, and induces recovery physiological and functional recovery in Parkinsonian mice (Morganti et al., 2012, Nash et al., 2015, Pabon et al., 2011, Thome, Standaert & Harms, 2015). The importance of FKN and its receptor, CX3CR1, in PD, has been demonstrated through numerous studies. Compared to *CX3CR1*^{+/-} MPTP-treated mice, *CX3CR1*^{-/-} MPTP-treated mice showed exacerbated TH⁺ cell loss and microglial activation in the SNpc (Cardona et al., 2006). Continuous intrastriatal infusion of FKN in Parkinsonian rats led to rescued TH expression and decreased microglial activation in the Str and SNpc (Pabon et al., 2011). Soluble FKN improved motor deficits, increased TH⁺ expression in Str, and rescued NeuN⁺ and TH⁺ cell populations in the SNpc of MPTP-treated mice (Morganti et al., 2012). Overexpression of α -syn in the rat SNpc led to TH and NeuN loss in the SNpc, which was rescued by injection of soluble FKN in the SNpc (Nash et al., 2015). By contrast, overexpression of α -syn in SNpc led to TH expression loss in SNpc of WT mice, but not in *CX3CR1*^{-/-} mice (Thome, Standaert & Harms, 2015). In this study, the prospective release of FKN from hVM1 clone 32 cells could have potentially attenuated microglial reaction in the Hip and contributed to the restoration of TH expression in the Str and SNpc of adult hNSC-transplanted mice.

Stem cell factor is highly expressed by neurons at sites of brain injury and is involved in NSC migration towards these sites (Sun, Lee & Fine, 2004). In 6-OHDA-lesioned rats, NSCs, shown to release mainly SCF but also BDNF *in vitro*, rescued TH+ fibers in the Str and TH+ cells in the SNpc and promoted behavioral improvement, via its anti-apoptotic effects, and increased SVZ neurogenesis. In these same animals, continuous SCF intrastriatal infusion also improved TH+ expression in Str and SNpc, and SVZ neurogenesis, but did not improve all aspects of behavioral dysfunction (Yasuhara et al., 2006). Based on this previous study, in this current study, SCF potentially secreted by hVM1 clone 32 cells *in vivo* could have contributed to nigrostriatal system rescue but did not aid in SVZ neurogenesis.

Currently, the only ongoing clinical trial involving NTFs is a study involving the striatal injection of an AAV vector carrying GDNF in PD patients and results are pending (ClinicalTrials.gov Identifier: NCT01621581) (Kalia, Kalia & Lang, 2015). Encapsulation of cells that are genetically modified to secrete GDNF have demonstrated effective restoration of behavior and the nigrostriatal pathway in various experimental PD models (Akerud et al., 2001, Perez-Bouza et al., 2017, Yasuhara, Date, 2007, Yasuhara et al., 2017). The NTF GDNF was even shown to be beneficial in older animals. In one study, GDNF was injected in the SNpc prior to 6-OHDA in 3, 18, and 24 month-old rats. All of the animals exhibited significant recovery of TH+ cells in the SNpc, and striatal DA and 3,4-Dihydroxyphenylacetic acid levels, however the treatment was more effective in 3 month-old than 24 month-old rats (Fox et al., 2001). Brain-derived neurotrophic factor has been shown to be beneficial in several studies. In MPTP-treated monkeys, BDNF infusion prevented SNpc DAN loss (Tsukahara et al., 1995). Physical exercise is beneficial in PD patients at all stages of the disease, providing control of motor symptoms and an improved quality of life; the basis of this improvement is that physical exercise increases BDNF levels in PD animals and patients (Hirsch et al., 2018). Expression of TH in the Str and SNpc, and motor symptoms, were exacerbated when BDNF TrkB receptors were blocked in the Str of 6-OHDA-lesioned rats (Real et al., 2013). Furthermore, BDNF interacts with DA D3 receptors and can affect their expression. In one study, 12 month-old rats were injected with 6-OHDA and five months later, BDNF was transfected into DAN in the SNpc. Seven months after transfection along with continuous infusion of a DA D3 receptor agonist, these rats showed improved motor behavior and increased TH expression in Str and SNpc compared to PD rats who hadn't received this treatment (Razgado-Hernandez et al., 2015). Therefore, the GDNF and BDNF secreted by hVM1 clone 32 cells could have contributed to rescue of nigrostriatal system in adult hNSC-transplanted mice.

In adult mice, SC-transplanted animals showed a recovery of TH+ fibers at both levels of the Str studied, and of TH+ cells in the SNpc; however, the former was more considerable. In the Str, there were no differences between the control and hNSC-transplanted groups, whereas in the SNpc there were significant differences in TH expression in control and SC-transplanted animals. This could be explained by the fact that the SC transplant was made in the Str, where the cells most likely did not migrate and died, therefore the factors they released were more abundant in the Str than the SNpc, hence the better improvement in Str. Although it is the SNpc that supplies the Str with DA, by transplanting in the Str, one step is skipped in order to directly reinnervate the Str, and as it is a bidirectional communication, both regions of the nigrostriatal pathway show recovery.

It is said that SCs act directly or indirectly by either integrating into the brain or by releasing factors like NTFs, thus leading to improvement (Tam et al., 2014), but it is obvious that in this case, the cells must have been acting indirectly as they were dead by the end of the study. This brings to mind the question that perhaps instead of cells, the CM of cells could be used in infusion studies instead of cells. There have been several studies showing the effects of the injection of CM in experimental PD models. In one study, intrastriatal delivery of CM containing principally SCF and also BDNF did not improve behavioral deficits, restore TH expression in Str and SNpc, or increase SVZ neurogenesis, but the hNSCs secreting these factors did (Yasuhara et al., 2006). Rats treated with 6-OHDA were transplanted in the mfb and VTA with either just rat NSCs or a combination of rat NSCs and rat mesenchymal stem cell-derived CM. The latter group showed increased neurogenesis in the two transplanted regions, more TH+ surviving grafted cells, a larger diffusion of transplanted NSCs, and greater behavioral improvement, compared to rats transplanted with just NSCs (Yao et al., 2016). In another publication, hMSC CM, shown to contain BDNF, GDNF, IL-6, and VEGF, was injected in the Str and SNpc of Parkinsonian rats, and seven weeks post-transplant, there was some behavioral amelioration, and an increase in TH expression in the two treated areas (Teixeira et al., 2017). In a 6-OHDA-lesioned rat model, injection of hNPCs and hNPC CM, which contained BDNF, GDNF, and SCF, were compared; hNPC CM transplant led to better improvement in behavior and TH immunoreactivity in Str and SNpc, seven weeks post-transplant, compared to hNPC grafting (Mendes-Pinheiro et al., 2018). In another study, rat adipose-derived SCs or its CM was intravenously injected into Parkinsonian rats; both groups showed behavioral improvement, DAN rescue in the SNpc, and increased BDNF and NT-3 levels in the Str. The only difference was that rats injected with SCs showed increased NGF striatal levels while CM-injected rats did not (Nakhaeifard et al., 2018). Therefore, successful treatment with CM appears to depend on the content of the secretome, and considering the CM of the differentiated hVM1 clone 32 cells contains GDNF, BDNF, FKN, SCF,

VEGF-A, and VEGF-C (and perhaps other factors not measured), all shown to restore the nigrostriatal system in experimental PD models, it would be interesting to test the aforementioned hNSCs, proliferation CM, and differentiation CM, in an adult MPTP mouse model to see if the infusion of CM would lead to the same, worse, or better effects than the cells alone. Using CM instead of cells would make the transplant preparation and process easier, and would have less ethical issues. Furthermore, CM takes away the concerns of cell survival, integration, and differentiation, as well as immunosuppression. Another option could be to prepare a mix of these factors in their recombinant form that could be manufactured without even using SCs.

In middle-aged mice, grafting of hVM1 clone 32 cells did not rescue TH⁺ fibers in the Str and TH⁺ cells in the SNpc, unlike adult mice. Adult and middle-aged mice had similar basal levels of TH expression in the nigrostriatal pathway and both age groups had approximately the same percentage of decrease of TH expression in the SNpc. However, adult mice showed almost three times more TH⁺ area diminution at the two levels of Str measured. This was surprising as most studies find that middle-aged and aged mice exhibit a more substantial decrease in TH expression in the Str and SNpc as well as striatal DA content, and demonstrate more severe behavioral deficits, when treated with MPTP, compared to adult animals. In addition, older mice do not show recovery, which sometimes occurs in younger mice, and older mice have a higher mortality rate upon MPTP injections compared to younger mice (Date, Felten & Felten, 1990, Guan et al., 2016, Ohashi et al., 2006). In this study, there was a higher mortality rate and behavioral deficits were more severe in time spent in center and stride length shortening, in middle-aged compared to adult mice. However, damage to the Str was more grave in adult compared to middle-aged animals treated with MPTP, which is not consistent with other studies. In all of the literature searched for MPTP treatment in middle-aged and aged mice, none of the studies used the exact same acute MPTP protocol in C57BL/6 mice of the same vendor, and it has been shown that different MPTP protocols lead to different nigrostriatal damage, and that mice of the same strain from different providers show different susceptibility to MPTP (Jackson-Lewis, Przedborski, 2007). Genetics is perhaps playing a role here because older mice have higher lethality when given MPTP so the ones that do survive may have a stronger resistance to MPTP and therefore there is less damage to their nigrostriatal pathway. To mimic CRT in middle-aged and aged mice, the protocol would have to be reworked because the non-significant decrease of striatal nerve terminals does not represent human PD pathology.

The neurotoxin MPTP shows varying behavioral symptoms in mice, with solid, consistent, long-lasting deficits yet to be shown (Blandini, Armentero, 2012, Blesa, Przedborski, 2014, Meredith,

Rademacher, 2011, Rousset et al., 2003, Zhang, Q. S. et al., 2017). Furthermore, it has been demonstrated that MPTP-treated mice can exhibit behavioral recovery or no difference in behavior compared to controls from four days to two months post-injection while maintaining a significantly damaged nigrostriatal system (Huang, D. et al., 2018, Rousset et al., 2003, Schwarting et al., 1999, Zhang, Q. S. et al., 2017). In this study, something similar occurred with nigrostriatal pathway injury in adult and middle-aged MPTP-treated mice, and at experiment completion, there were no differences between any of the groups of any age in distance traveled, time spent grooming and rearing, urination, defecation, and paw overlap. The clearest behavioral changes observed in both age groups were shorter stride length and shorter IL-CL forelimb stride width in MPTP-lesioned mice, the former of which was alleviated by hNSC transplant in middle-aged mice. As well, at four months post-transplant, buffer-treated mice of both age groups spent more time in the center in the open field test, which tended to be reduced in cell-treated mice. Based on the results of this thesis, for future studies done in the same context, other behavioral tests should be applied in addition to stride length and time spent in center measurement.

In middle-aged buffer-treated mice, behavioral deficits were worse but striatal nerve fibers were more abundant compared to adult counterparts who had less TH expression in the Str and less behavioral deficits. This reveals that even when histological structure is better preserved, function of the DA circuitry can be more considerably impaired. Immunostaining of TH to analyze DAN degeneration is not a functional assessment, and in the case of middle-aged mice, it was not able to detect differences between buffer- and cell-treated groups, while the PPT and time spent in center in the OFT were able to do this.

In this thesis, the same protocol of intoxication led to non-comparable lesions in adult and middle-aged mice. One way to better mimic PD pathology could be chronic MPTP treatment in mice with very low doses starting at adult age and transplanting hNSCs at middle-age, when behavioral data shows neurological impairment. However, this is something that is complicated due to the intrinsic difficulty of working with MPTP, a neurotoxin harmful to humans as well. The administration of 6-OHDA remains safer but does not provide whole-body DA degeneration. In this case, for the sake of comparability, the best approach was using this protocol, but like any other, there were pitfalls.

Norepinephrine plays a compensatory role in MPTP-treated mice, but its levels vary depending on the study. In one study, NE levels increased after striatal DA depletion, and there were no behavioral deficits (Zhang, Q. S. et al., 2017). In another study, NE depletion in Str in a MPTP model led to no

changes in distance moved or number of rears, and less grooming (Luchtman, Shao & Song, 2009). Damage to the NE system occurs in PD patients (Zhang, Q. S. et al., 2017), so perhaps these NE level inconsistencies are in the MPTP model only. A more defined compensatory mechanism that occurs in experimental PD models as well as in PD patients is the increase in DA metabolite ratios 3,4-Dihydroxyphenylacetic acid/DA and Homovanillic acid/DA in the Str, which indicate DA turnover (Luchtman, Shao & Song, 2009, Zhang, Q. S. et al., 2017). This compensation leads to lack of behavioral deficits (Rousselet et al., 2003, Zhang, Q. S. et al., 2017). Depletion of DA in the prefrontal cortex has been shown to increase hyperactivity and decrease anxiety, and this hyperactivity is due to disinhibition and attention deficit (Rousselet et al., 2003). Hyperactivity could be explained by increased NE levels in the Str (Zhang, Q. S. et al., 2017). Attention deficit and impulsivity occur in some PD patients (Kehagia et al., 2014, Nieouillon, 2002, Nombela et al., 2014). Hyperactivity, as measured by time spent in the center in the OFT, was observed in buffer-treated mice at four months post-transplant in adult and middle-aged mice, while control and hNSC-treated animals tended to spend less time in the center. Some studies allude to the fact that healthy mice exhibit thigmotaxis, spending less time in the center, which is what occurred in this thesis, but more than anything, it is important to stress the fact that adult and middle-aged control and SC-treated mice spent less time in the center compared to buffer-treated animals. This emphasizes that transplant with hVM1 clone 32 cells rescued this hyperactivity in both age groups studied.

Control astroglial populations were double in middle-aged mice compared to adults in both Str and SNp, confirming a non-pathological, basal increase in inflammation due only to age. In adult mice, astrocytes in the Str only increased upon SC-transplantation, especially on the side of transplantation while in middle-aged animals, there were no significant differences between any of the groups. In the Str of adult mice, astrocytes react only to cell transplant, and VEGF-A and VEGF-C potentially being secreted *in vivo* by transplanted cells induced glial proliferation, while middle-aged didn't have any reaction. In the SNpc of adult mice, there was no astroglial reaction to MPTP while microglia increased in response to MPTP, and in middle-aged mice, there was no reaction of either astrocytes or microglia, except a decreased astroglial population on the side opposite to the transplant. Surprisingly, Iba1+ cell populations increase more upon MPTP lesion in adult compared to middle-aged mice. Detrimental to the transplanted cells or not, inflammation did not negatively affect the transplant's ability to protect the TH+ cells in the SNpc and TH+ fibers in the Str in adult mice. In a study implementing the acute MPTP protocol in male mice, astroglial and microglial populations in Str were the same as in controls but these glial populations were increased in SNpc compared to controls, more than two months post-MPTP treatment (Huang, D. et al., 2018). Other experimental

CRT studies found no changes in GFAP expression in the Str or SNpc among cell-treated and vehicle-treated Parkinsonian animals (Zuo, F. X. et al., 2015, Zuo, F. et al., 2017), which is in contrast to this thesis.

There are reports that activated glial cells like astrocytes and microglia are generated by insufficient immunosuppression, but all mice were succumbed to a strict immunosuppression regimen that has been used in other studies and the equivalent with these same cells used in Parkinsonian rats, so cell death due to immunosuppression problems is not thought to have occurred. Also, MCs migrating to LNs is a sign of immunosuppression. Adult and middle-aged hNSC-transplanted mice tended to have increased MC density compared to the other experimental groups. However, in terms of amount of total MCs, adult SC-transplanted mice had more compared to buffer-treated animals, which in turn had more than control mice. All middle-aged mice had approximately the same number of MCs in the LNs. Because of the differences between the groups of both ages, it does not seem that MCs migrated to the LNs to aid in immunosuppression. Mast cell populations have not been studied before in *in vivo* PD models let alone CRT studies within the field. A possible explanation for the migration of MCs to the LNs in adult and middle-aged cell-transplanted mice could be that SCF and MCP-1, both involved in MC migration (Collington et al., 2010, da Silva, Jamur & Oliver, 2014, Iemura et al., 1994, Norrby, 2002) and potentially secreted by the hVM1 clone 32 cells *in vivo*, promoted MC population accumulation in the CNS-connected LNs, which were shown to express β -III tubulin, NFL, PSD-95, SYP, and TH. Moreover, MCs did not appear to be contributing to inflammation in the CNS as they were practically not present, they did not aid in transplant tolerance as the graft did not survive, and they did not help promoting angiogenesis, as there were no differences in angiogenesis in the Str and SNpc in any of the groups in both adult and middle-aged mice.

When looking at neurogenesis in the SVZ, NES expression did not change between any of the groups of either age. Expression of Ki-67 in middle-aged controls was a little lower compared to adult equivalents and did not change between any of the groups in either age group, with the exception of buffer-treated middle-aged mice, which tended to have more Ki-67+ cells than age-matched controls and SC-transplanted animals. Expression of neuroblast marker DCX decreased in all adult mice upon treatment with MPTP, to levels similar to those of all middle-aged mice, emphasizing the drastic decrease of neuroblast neurogenesis in the SVZ with increased age. In one study, 6-OHDA-lesioned adult female mice were transplanted with hNSCs, and SVZ changes were studied; transplant restored DA receptor D1, DAT, NeuN, PSD-95, and TH, in the SVZ, which had decreased expression upon 6-OHDA lesion. Expression of Ki-67 was unchanged in control, buffer-treated, and cell-treated

groups, similar to the results in this thesis. Although SVZ neurogenesis was partially rescued and there were behavioral improvements in hNSC-transplanted mice, striatal TH expression was recovered over time in 6-OHDA-lesioned mice and the significant decrease in TH+ cells in SN which was not alleviated by transplant (Zuo, F. et al., 2017). In another publication using 6-OHDA-lesioned rats, hNSCs induced behavioral and nigrostriatal TH expression recovery along with increased neurogenesis as shown via BrdU/DCX double-positive immunostaining in the SVZ compared to buffer-treated animals (Yasuhara et al., 2006).

There was no NSC/NPC neurogenesis occurring in the SGZ of any of the adult or middle-aged mice, but perhaps the more relevant piece of information comes from the immature neuron population in the Hip. In middle-aged mice, there was no neurogenesis, but in the SGZ of adult mice, the neuroblast population decreased in buffer-treated animals and was alleviated by transplant of hVM1 clone 32 cells. Hence, the transplant was capable of restoring hippocampal neurogenesis. Although it has been described that neuroinflammation depletes neurogenesis, increased levels of astrocytes in the Str and increased levels of microglia in the SNpc did not negatively affect neurogenesis. Looking at the SGZ inflammation in adult mice, microglial populations had a tendency to decrease in hNSC-treated mice, suggesting that lower microglia reaction could have contributed to increased neurogenesis. The NTFs BDNF, GDNF, and VEGF, which promote neurogenesis (Shohayeb et al., 2018, van den Berge, van Strien & Hol, 2013, Yang et al., 2008), and FKN, which represses microglia (Morganti et al., 2012, Pabon et al., 2011, Thome, Standaert & Harms, 2015), were secreted by the hVM1 clone 32 cells *in vitro*, possibly leading to the aforementioned occurrences in the Hip *in vivo*. In addition, in adult mice, there was a high correlation between TH expression in the Str and SNpc, and DCX expression in the SGZ, thus supporting the connection between DA and hippocampal neurogenesis.

Reviewing every result concerning the nigrostriatal pathway and behavior from every experimental PD study involving SCs is beyond the scope of this thesis, so the results of this thesis will subsequently be compared to those *in vivo* studies using hNSCs of fetal brain origin. In adult 6-OHDA-lesioned rats, hNSC transplantation led to behavioral improvement, TH expression recovery in the Str and SNpc, and SVZ neurogenesis increase, compared to buffer-treated rats one month post-transplant. Some of the grafted cells survived and expressed MAP2 but not TH, and the cells were shown to secrete mostly SCF and some BDNF, but not GDNF or VEGF, *in vitro* (Yasuhara et al., 2006). In another study, adult MPTP-treated hNSC-transplanted mice were analyzed approximately one month post-transplant. Mice transplanted with SCs showed partial improvement in behavior and slight rescue of TH expression in the nigrostriatal system. Some of the surviving transplanted cells

expressed DCX, Ki-67, and NES, and grafted cells were shown to migrate. In addition, Str and SNpc levels of BDNF and NT-3 increased while those of IL-1 β and TNF α decreased (Zuo, F. X. et al., 2015). Mice of 20 months of age were treated with MPTP and transplanted with murine NSCs above the SN/VTA one week or four weeks later. There were no changes in behavior in any of the groups throughout the experiment, and at three weeks post-transplant there was TH expression recovery in Str and SNpc of SC-transplanted mice. Expression of DAT was restored to almost control-like levels in Str and SNpc. Some surviving grafted cells expressed GDNF, GFAP, NeuN, and TH, but there was no double-staining for any of these markers. Seven weeks post-MPTP lesion, there was no recovery of TH in expression in the Str or SNpc of buffer-transplanted mice (Ourednik et al., 2002).

Comparing this thesis to these aforementioned fetal brain-derived hNSC CRT publications, it is apparent that nigrostriatal system restoration is consistent, but there is no coherent behavioral impairment and/or recovery. Moreover, in these studies, there was graft survival, which did not occur in this thesis. Interestingly, in the study by Ourednik et al., 2002, aged mice did not show striatal TH expression recovery as seen in this thesis. However, they used mostly female mice from a different provider, and a different MPTP protocol, 30 mg/kg twice at a five-hour interval (Ourednik et al., 2002), thus potentially leading to these differences observed in the two studies.

Overall, the work in this thesis demonstrated firstly, that hVM1 clone 32 cells rescue nigrostriatal TH+ populations, but only in adult Parkinsonian mice. Secondly, using the MPTP mouse model, behavioral changes do not always correlate to TH expression changes in the Str and SNpc. Thirdly, increased neuroinflammation and decreased neurogenesis due to aging play a role in less effective CRT in middle-aged mice. This is a proof-of-concept study that CRT can work using hVM1 clone 32 cells in adult mice and that they exert a trophic effect in adult mice with neurogenesis increase, but at one point, based on age, hNSCs are not sufficient to generate these neurotrophic effects because the body is too old, thus stressing the importance of the age of recipient and the stage of PD progression when receiving a transplant.

The hVM1 clone 32 cells support the fact that CRT is a plausible and effective treatment for PD if the timing and environment are adequate. Whether they themselves could be used in clinical trials is another story due to their fetal origin, *v-myc* immortalization, lack of survival in experimental PD mice, and need for immunosuppression. However, the alternative could be using differentiated hVM1 clone 32 CM, maybe even from a lower passage. By doing this, all of the aforementioned issues

would be eliminated except for the former. Likewise, a blend of recombinant factors could be manufactured for infusion without having to use SCs.

Interestingly, some of the factors that potentially generate PD occur naturally during aging, such as neuroinflammation, protein misfolding, and ALP dysfunction (Chai, Lim, 2013, Kalia, Lang, 2015, Sarkar, Raymick & Imam, 2016, Wirdefeldt et al., 2011, Wyss-Coray, 2016) thus re-emphasizing just how much PD is an age-associated disease. Because higher inflammation and lower neurogenesis hamper the effectiveness of CRT, and potentially CM transplant, due to aging, there is a need for multifactorial treatment including anti-inflammatory drugs and neurogenesis enhancers. For example, minocycline, an antibiotic currently in PD clinical trials, decreases inflammation, and taking NSAIDs has been linked to a lower risk of developing PD (De Virgilio et al., 2016, Kalia, Lang, 2015, Lesage, Brice, 2009, Sarkar, Raymick & Imam, 2016). The transfer of blood from one animal to another, from younger to older animals, has been linked to increased neurogenesis in older animals (Castellano et al., 2017, Villeda et al., 2014). After testing for which components were aiding in this process, one of the protein fractions isolated from the blood, so-called GRF6021, is currently in a Phase II clinical trial (ClinicalTrials.gov Identifier: NCT03713957) (The Michael J. Fox Foundation for Parkinson's Research, 2019, U.S. National Library of Medicine, 2019). In addition, dietary supplements like vitamins and fatty acids have been shown to have favorable effects on neurogenesis (Poulose et al., 2017). Thus, in the future, a more complete and effective treatment of PD could be daily medications of anti-inflammatories and neurogenesis enhancers, and multiple CRT and/or CM infusion treatments every few years throughout life. Furthermore, early diagnosis of PD via the discovery of prodromal PD biomarkers could allow for more effective PD treatment because intervention could be done at an earlier point in time with CRT or CM infusion.

In this study, hVM1 clone 32 cells were transplanted in a bilateral PD mouse model, in order to perform a comprehensive study of the fate of these cells and the effects they exert in both adult and middle-aged mice. To our knowledge, there has yet to be a more complete study of the effect of hNSCs derived from fetal brain, let alone any type of SC used in CRT, in older or even adult MPTP-lesioned mice. This thesis not only explored experimental PD in two age groups, but within these two age groups, analyzed nigrostriatal TH expression, behavior, inflammation, angiogenesis, and neurogenesis.

CONCLUSIONS

1. The hVM1 clone 32 cells are fetal-derived human neural stem cells that, upon differentiation *in vitro*, exhibit A9 dopaminergic neuron characteristics and secrete trophic factors GDNF, BDNF, VEGF-A, VEGF-C, SCF, FKN, and MCP-1.
2. Administration of MPTP leads to different degrees of dopaminergic neurodegeneration and behavioral impairment in adult and middle-aged mice. Although hVM1 clone 32 cells are dead by month four post-grafting, they rescue nigrostriatal TH+ populations in adult Parkinsonian mice, an effect that could potentially be mediated by the secretion of neurotrophic factors *in vivo* as seen *in vitro*.
3. Differences in age account for a distinct response to the same MPTP protocol, and in order to better mimic human Parkinson's disease pathology, a different protocol needs to be applied to middle-aged mice to obtain more severe nigrostriatal damage.
4. Behavioral changes in adult and middle-aged MPTP-treated mice compared to controls are detected by hyperactivity in the open field test and reduced stride length in the paw print test. Hyperactivity tends to be lowered by hVM1 clone 32 cell transplant in both age groups four months post-transplant, and stride length is recuperated in stem cell-transplanted middle-aged mice.
5. Astroglial proliferation in the striatum and augmented microglial population in the substantia nigra pars compacta of human neural stem cell-treated adult mice do not impede nigrostriatal system amelioration due to hVM1 clone 32 cell transplant.
6. Grafting of hVM1 clone 32 cells in adult and middle-aged MPTP-lesioned mice leads to mast cell migration to the superficial cervical lymph nodes.
7. Angiogenesis in the striatum and substantia nigra pars compacta is not affected by age, MPTP, or neural stem cell transplantation.
8. In adult mice, hVM1 clone 32 transplantation does not rescue neurogenesis in the subventricular zone in terms of NES, Ki-67, or DCX expression, but does restore neurogenesis in the subgranular zone, which is accompanied by a decrease in microglia. Expression of TH in the striatum and substantia nigra pars compacta is correlated to this hippocampal neurogenesis.

9. Cell replacement therapy in middle-aged MPTP-lesioned mice is less effective due to concomitant increased basal neuroinflammation and decreased neurogenesis due to aging.

CONCLUSIONES

1. Las células hVM1 clon 32 son células madre neurales humanas de origen fetal que, en diferenciación *in vitro*, muestran características de neuronas dopaminérgicas A9 y secretan los factores tróficos GDNF, BDNF, VEGF-A, VEGF-C, SCF, FKN, y MCP-1.
2. La administración de MPTP resulta en una pérdida de TH y en alteraciones de comportamiento diferentes en ratones adultos que de mediana edad. Aunque a los cuatro meses del trasplante las células hVM1 clon 32 han muerto, en ratones adultos parkinsonianos se observa que también han protegido las poblaciones TH positivas nigroestriadas, un efecto potencialmente mediado por la secreción de factores neurotróficos *in vivo* como se observa *in vitro*.
3. La respuesta al protocolo de MPTP es diferente en función de la edad del ratón, por lo que para lograr una mejor reproducción de la patología humana de la enfermedad de Parkinson, habría que aplicar un protocolo distinto en ratones de mediana edad que dé lugar a una lesión nigroestriada mayor.
4. Los ratones adultos y de mediana edad tratados con MPTP muestran cambios comportamentales en comparación con controles con hiperactividad en el test de campo abierto y reducción de la zancada en el test de deambulación. En animales trasplantados con células hVM1 clon 32, la hiperactividad tiende a reducirse en ambos grupos de edad y la zancada se normaliza en ratones de mediana edad.
5. En ratones adultos tratados con células hVM1 clon 32, la proliferación astrogliar en el estriado y el aumento en la población microglial en la sustancia negra parte compacta no impiden que el trasplante induzca una mejora global del sistema nigroestriado.
6. El injerto de células hVM1 clon 32 en ratones adultos y de mediana edad tratados con MPTP promueve la migración de mastocitos a los nodos linfáticos cervicales superficiales.
7. La angiogénesis en el estriado y la sustancia negra parte compacta no está afectada por la edad, el MPTP, ni el trasplante de células madre neurales.

8. En ratones adultos, el trasplante de células hVM1 clon 32 no restaura la neurogénesis en la zona subventricular, en términos de expresión de NES, Ki-67, o DCX, pero sí en la zona subgranular, donde se acompaña de una disminución de la población microglial. La expresión de TH en el estriado y la sustancia negra parte compacta está correlacionada con esta neurogénesis hipocampal.

9. La terapia de reemplazo celular es menos efectiva en ratones de mediana edad lesionados con MPTP debido a la neuroinflamación basal aumentada y la neurogénesis disminuida propias del envejecimiento.

REFERENCES

- Abraham, S.N. & St John, A.L. 2010, "Mast cell-orchestrated immunity to pathogens", *Nature reviews.Immunology*, vol. 10, no. 6, pp. 440-452.
- Akerud, P., Canals, J.M., Snyder, E.Y. & Arenas, E. 2001, "Neuroprotection through delivery of glial cell line-derived neurotrophic factor by neural stem cells in a mouse model of Parkinson's disease", *The Journal of neuroscience : the official journal of the Society for Neuroscience*, vol. 21, no. 20, pp. 8108-8118.
- Akerud, P., Holm, P.C., Castelo-Branco, G., Sousa, K., Rodriguez, F.J. & Arenas, E. 2002, "Persephin-overexpressing neural stem cells regulate the function of nigral dopaminergic neurons and prevent their degeneration in a model of Parkinson's disease", *Molecular and cellular neurosciences*, vol. 21, no. 2, pp. 205-222.
- Allen, S.J., Watson, J.J., Shoemark, D.K., Barua, N.U. & Patel, N.K. 2013, "GDNF, NGF and BDNF as therapeutic options for neurodegeneration", *Pharmacology & therapeutics*, vol. 138, no. 2, pp. 155-175.
- Andersson, E.R., Salto, C., Villaescusa, J.C., Cajanek, L., Yang, S., Bryjova, L., Nagy, I.I., Vainio, S.J., Ramirez, C., Bryja, V. & Arenas, E. 2013, "Wnt5a cooperates with canonical Wnts to generate midbrain dopaminergic neurons in vivo and in stem cells", *Proceedings of the National Academy of Sciences of the United States of America*, vol. 110, no. 7, pp. E602-10.
- Ang, S.L. 2006, "Transcriptional control of midbrain dopaminergic neuron development", *Development (Cambridge, England)*, vol. 133, no. 18, pp. 3499-3506.
- Appay, V. & Rowland-Jones, S.L. 2001, "RANTES: a versatile and controversial chemokine", *Trends in immunology*, vol. 22, no. 2, pp. 83-87.
- Apple, D.M., Solano-Fonseca, R. & Kokovay, E. 2017, "Neurogenesis in the aging brain", *Biochemical pharmacology*, vol. 141, pp. 77-85.
- Arenas, E. 2014, "Wnt signaling in midbrain dopaminergic neuron development and regenerative medicine for Parkinson's disease", *Journal of molecular cell biology*, vol. 6, no. 1, pp. 42-53.
- Arimoto, T., Choi, D.Y., Lu, X., Liu, M., Nguyen, X.V., Zheng, N., Stewart, C.A., Kim, H.C. & Bing, G. 2007, "Interleukin-10 protects against inflammation-mediated degeneration of dopaminergic neurons in substantia nigra", *Neurobiology of aging*, vol. 28, no. 6, pp. 894-906.
- Aspelund, A., Antila, S., Proulx, S.T., Karlsen, T.V., Karaman, S., Detmar, M., Wiig, H. & Alitalo, K. 2015, "A dural lymphatic vascular system that drains brain interstitial fluid and macromolecules", *The Journal of experimental medicine*, vol. 212, no. 7, pp. 991-999.
- Baloh, R.H., Tansey, M.G., Lampe, P.A., Fahrner, T.J., Enomoto, H., Simburger, K.S., Leitner, M.L., Araki, T., Johnson, E.M., Jr & Milbrandt, J. 1998, "Artemin, a novel member of the GDNF ligand family, supports peripheral and central neurons and signals through the GFRalpha3-RET receptor complex", *Neuron*, vol. 21, no. 6, pp. 1291-1302.
- Banisadr, G., Gosselin, R.D., Mechighel, P., Kitabgi, P., Rostene, W. & Parsadaniantz, S.M. 2005, "Highly regionalized neuronal expression of monocyte chemoattractant protein-1 (MCP-

- 1/CCL2) in rat brain: evidence for its colocalization with neurotransmitters and neuropeptides", *The Journal of comparative neurology*, vol. 489, no. 3, pp. 275-292.
- Beghdadi, W., Madjene, L.C., Benhamou, M., Charles, N., Gautier, G., Launay, P. & Blank, U. 2011, "Mast cells as cellular sensors in inflammation and immunity", *Frontiers in immunology*, vol. 2, pp. 37.
- Ben Abdallah, N.M., Slomianka, L., Vyssotski, A.L. & Lipp, H.P. 2010, "Early age-related changes in adult hippocampal neurogenesis in C57 mice", *Neurobiology of aging*, vol. 31, no. 1, pp. 151-161.
- Benabid, A.L., Chabardes, S., Mitrofanis, J. & Pollak, P. 2009, "Deep brain stimulation of the subthalamic nucleus for the treatment of Parkinson's disease", *The Lancet.Neurology*, vol. 8, no. 1, pp. 67-81.
- Benner, E.J., Banerjee, R., Reynolds, A.D., Sherman, S., Pisarev, V.M., Tsiperson, V., Nemachek, C., Ciborowski, P., Przedborski, S., Mosley, R.L. & Gendelman, H.E. 2008, "Nitrated alpha-synuclein immunity accelerates degeneration of nigral dopaminergic neurons", *PloS one*, vol. 3, no. 1, pp. e1376.
- Bjorklund, A. & Lindvall, O. 2017, "Replacing Dopamine Neurons in Parkinson's Disease: How did it happen?", *Journal of Parkinson's disease*, vol. 7, no. s1, pp. S21-S31.
- Blandini, F. & Armentero, M.T. 2012, "Animal models of Parkinson's disease", *The FEBS journal*, vol. 279, no. 7, pp. 1156-1166.
- Blesa, J. & Przedborski, S. 2014, "Parkinson's disease: animal models and dopaminergic cell vulnerability", *Frontiers in neuroanatomy*, vol. 8, pp. 155.
- Bolon, B. & Graham, D.G. 2011, *Appendixes: Ready References of Neurobiology Knowledge*.
- Borta, A. & Hoglinger, G.U. 2007, "Dopamine and adult neurogenesis", *Journal of neurochemistry*, vol. 100, no. 3, pp. 587-595.
- Braak, H., Ghebremedhin, E., Rub, U., Bratzke, H. & Del Tredici, K. 2004, "Stages in the development of Parkinson's disease-related pathology", *Cell and tissue research*, vol. 318, no. 1, pp. 121-134.
- Burkhard, P., Dominici, P., Borri-Voltattorni, C., Jansonius, J.N. & Malashkevich, V.N. 2001, "Structural insight into Parkinson's disease treatment from drug-inhibited DOPA decarboxylase", *Nature structural biology*, vol. 8, no. 11, pp. 963-967.
- Caballero, B., Sherman, S.J. & Falk, T. 2017, "Insights into the Mechanisms Involved in Protective Effects of VEGF-B in Dopaminergic Neurons", *Parkinson's disease*, vol. 2017, pp. 4263795.
- Cardona, A.E., Pioro, E.P., Sasse, M.E., Kostenko, V., Cardona, S.M., Dijkstra, I.M., Huang, D., Kidd, G., Dombrowski, S., Dutta, R., Lee, J.C., Cook, D.N., Jung, S., Lira, S.A., Littman, D.R. & Ransohoff, R.M. 2006, "Control of microglial neurotoxicity by the fractalkine receptor", *Nature neuroscience*, vol. 9, no. 7, pp. 917-924.

- Carvalho, M.M., Campos, F.L., Coimbra, B., Pego, J.M., Rodrigues, C., Lima, R., Rodrigues, A.J., Sousa, N. & Salgado, A.J. 2013, "Behavioral characterization of the 6-hydroxidopamine model of Parkinson's disease and pharmacological rescuing of non-motor deficits", *Molecular neurodegeneration*, vol. 8, pp. 14-1326-8-14.
- Castellano, J.M., Mosher, K.I., Abbey, R.J., McBride, A.A., James, M.L., Berdnik, D., Shen, J.C., Zou, B., Xie, X.S., Tingle, M., Hinkson, I.V., Angst, M.S. & Wyss-Coray, T. 2017, "Human umbilical cord plasma proteins revitalize hippocampal function in aged mice", *Nature*, vol. 544, no. 7651, pp. 488-492.
- Chai, C. & Lim, K.L. 2013, "Genetic insights into sporadic Parkinson's disease pathogenesis", *Current Genomics*, vol. 14, no. 8, pp. 486-501.
- Chandra, G., Roy, A., Rangasamy, S.B. & Pahan, K. 2017, "Induction of Adaptive Immunity Leads to Nigrostriatal Disease Progression in MPTP Mouse Model of Parkinson's Disease", *Journal of immunology (Baltimore, Md.: 1950)*, vol. 198, no. 11, pp. 4312-4326.
- Chaturvedi, R.K., Shukla, S., Seth, K. & Agrawal, A.K. 2006, "Nerve growth factor increases survival of dopaminergic graft, rescue nigral dopaminergic neurons and restores functional deficits in rat model of Parkinson's disease", *Neuroscience letters*, vol. 398, no. 1-2, pp. 44-49.
- Chaudhuri, K.R. & Schapira, A.H. 2009, "Non-motor symptoms of Parkinson's disease: dopaminergic pathophysiology and treatment", *The Lancet.Neurology*, vol. 8, no. 5, pp. 464-474.
- Chauhan, N.B., Siegel, G.J. & Lee, J.M. 2001, "Depletion of glial cell line-derived neurotrophic factor in substantia nigra neurons of Parkinson's disease brain", *Journal of chemical neuroanatomy*, vol. 21, no. 4, pp. 277-288.
- Collington, S.J., Hallgren, J., Pease, J.E., Jones, T.G., Rollins, B.J., Westwick, J., Austen, K.F., Williams, T.J., Gurish, M.F. & Weller, C.L. 2010, "The role of the CCL2/CCR2 axis in mouse mast cell migration in vitro and in vivo", *Journal of immunology (Baltimore, Md.: 1950)*, vol. 184, no. 11, pp. 6114-6123.
- Conductier, G., Blondeau, N., Guyon, A., Nahon, J.L. & Rovere, C. 2010, "The role of monocyte chemoattractant protein MCP1/CCL2 in neuroinflammatory diseases", *Journal of neuroimmunology*, vol. 224, no. 1-2, pp. 93-100.
- Contin, M. & Martinelli, P. 2010, "Pharmacokinetics of levodopa", *Journal of neurology*, vol. 257, no. Suppl 2, pp. S253-61.
- Cooke, M.J., Vulic, K. & Shoichet, M.S. 2010, "Design of biomaterials to enhance stem cell survival when transplanted into the damaged central nervous system", *Soft Matter*, vol. 6, no. 20, pp. 4988-4998.
- Courtois, E.T., Castillo, C.G., Seiz, E.G., Ramos, M., Bueno, C., Liste, I. & Martinez-Serrano, A. 2010, "In vitro and in vivo enhanced generation of human A9 dopamine neurons from neural stem cells by Bcl-XL", *The Journal of biological chemistry*, vol. 285, no. 13, pp. 9881-9897.

- Cyron, D. 2016, "Mental Side Effects of Deep Brain Stimulation (DBS) for Movement Disorders: The Futility of Denial", *Frontiers in integrative neuroscience*, vol. 10, pp. 17.
- da Silva, E.Z., Jamur, M.C. & Oliver, C. 2014, "Mast cell function: a new vision of an old cell", *The journal of histochemistry and cytochemistry : official journal of the Histochemistry Society*, vol. 62, no. 10, pp. 698-738.
- Date, I., Felten, D.L. & Felten, S.Y. 1990, "Long-term effect of MPTP in the mouse brain in relation to aging: neurochemical and immunocytochemical analysis", *Brain research*, vol. 519, no. 1-2, pp. 266-276.
- Davis, S.M., Collier, L.A., Goodwin, S., Lukins, D.E., Powell, D.K. & Pennypacker, K.R. 2019, "Efficacy of leukemia inhibitory factor as a therapeutic for permanent large vessel stroke differs among aged male and female rats", *Brain research*, vol. 1707, pp. 62-73.
- Daynac, M., Morizur, L., Chicheportiche, A., Mouthon, M.A. & Boussin, F.D. 2016, "Age-related neurogenesis decline in the subventricular zone is associated with specific cell cycle regulation changes in activated neural stem cells", *Scientific reports*, vol. 6, pp. 21505.
- De Virgilio, A., Greco, A., Fabbrini, G., Inghilleri, M., Rizzo, M.I., Gallo, A., Conte, M., Rosato, C., Ciniglio Appiani, M. & de Vincentiis, M. 2016, "Parkinson's disease: Autoimmunity and neuroinflammation", *Autoimmunity reviews*, vol. 15, no. 10, pp. 1005-1011.
- Dutta, S. & Sengupta, P. 2016, "Men and mice: Relating their ages", *Life Sciences*, vol. 152, pp. 244-248.
- Duty, S. & Jenner, P. 2011, "Animal models of Parkinson's disease: a source of novel treatments and clues to the cause of the disease", *British journal of pharmacology*, vol. 164, no. 4, pp. 1357-1391.
- Ekdahl, C.T., Claasen, J.H., Bonde, S., Kokaia, Z. & Lindvall, O. 2003, "Inflammation is detrimental for neurogenesis in adult brain", *Proceedings of the National Academy of Sciences of the United States of America*, vol. 100, no. 23, pp. 13632-13637.
- Emgard, M., Hallin, U., Karlsson, J., Bahr, B.A., Brundin, P. & Blomgren, K. 2003, "Both apoptosis and necrosis occur early after intracerebral grafting of ventral mesencephalic tissue: a role for protease activation", *Journal of neurochemistry*, vol. 86, no. 5, pp. 1223-1232.
- Emgard, M., Karlsson, J., Hansson, O. & Brundin, P. 1999, "Patterns of cell death and dopaminergic neuron survival in intrastriatal nigral grafts", *Experimental neurology*, vol. 160, no. 1, pp. 279-288.
- Ermine, C.M., Wright, J.L., Frausin, S., Kauhausen, J.A., Parish, C.L., Stanic, D. & Thompson, L.H. 2018, "Modelling the dopamine and noradrenergic cell loss that occurs in Parkinson's disease and the impact on hippocampal neurogenesis", *Hippocampus*, vol. 28, no. 5, pp. 327-337.
- Falk, T., Gonzalez, R.T. & Sherman, S.J. 2010, "The yin and yang of VEGF and PEDF: multifaceted neurotrophic factors and their potential in the treatment of Parkinson's Disease", *International journal of molecular sciences*, vol. 11, no. 8, pp. 2875-2900.

- Falk, T., Yue, X., Zhang, S., McCourt, A.D., Yee, B.J., Gonzalez, R.T. & Sherman, S.J. 2011, "Vascular endothelial growth factor-B is neuroprotective in an in vivo rat model of Parkinson's disease", *Neuroscience letters*, vol. 496, no. 1, pp. 43-47.
- Falk, T., Zhang, S. & Sherman, S.J. 2009, "Vascular endothelial growth factor B (VEGF-B) is up-regulated and exogenous VEGF-B is neuroprotective in a culture model of Parkinson's disease", *Molecular neurodegeneration*, vol. 4, pp. 49-1326-4-49.
- Fox, C.M., Gash, D.M., Smoot, M.K. & Cass, W.A. 2001, "Neuroprotective effects of GDNF against 6-OHDA in young and aged rats", *Brain research*, vol. 896, no. 1-2, pp. 56-63.
- Fuzzati-Armentero, M.T., Cerri, S. & Blandini, F. 2019, "Peripheral-Central Neuroimmune Crosstalk in Parkinson's Disease: What Do Patients and Animal Models Tell Us?", *Frontiers in neurology*, vol. 10, pp. 232.
- Gonzalez, R., Garitaonandia, I., Crain, A., Poustovoitov, M., Abramihina, T., Noskov, A., Jiang, C., Morey, R., Laurent, L.C., Elsworth, J.D., Snyder, E.Y., Redmond, D.E., Jr & Semechkin, R. 2015, "Proof of concept studies exploring the safety and functional activity of human parthenogenetic-derived neural stem cells for the treatment of Parkinson's disease", *Cell transplantation*, vol. 24, no. 4, pp. 681-690.
- Gu, S., Huang, H., Bi, J., Yao, Y. & Wen, T. 2009, "Combined treatment of neurotrophin-3 gene and neural stem cells is ameliorative to behavior recovery of Parkinson's disease rat model", *Brain research*, vol. 1257, pp. 1-9.
- Guan, Q., Wang, M., Chen, H., Yang, L., Yan, Z. & Wang, X. 2016, "Aging-related 1-methyl-4-phenyl-1,2,3,6-tetrahydropyridine-induced neurochemical and behavioral deficits and redox dysfunction: improvement by AK-7", *Experimental gerontology*, vol. 82, pp. 19-29.
- Guyon, A., Skrzydelski, D., De Giry, I., Rovere, C., Conductier, G., Trocello, J.M., Dauge, V., Kitabgi, P., Rostene, W., Nahon, J.L. & Melik Parsadaniantz, S. 2009, "Long term exposure to the chemokine CCL2 activates the nigrostriatal dopamine system: a novel mechanism for the control of dopamine release", *Neuroscience*, vol. 162, no. 4, pp. 1072-1080.
- Hallett, P.J., Cooper, O., Sadi, D., Robertson, H., Mendez, I. & Isacson, O. 2014, "Long-term health of dopaminergic neuron transplants in Parkinson's disease patients", *Cell reports*, vol. 7, no. 6, pp. 1755-1761.
- Herculano-Houzel, S., Mota, B. & Lent, R. 2006, "Cellular scaling rules for rodent brains", *Proceedings of the National Academy of Sciences of the United States of America*, vol. 103, no. 32, pp. 12138-12143.
- Hirsch, M.A., van Wegen, E.E.H., Newman, M.A. & Heyn, P.C. 2018, "Exercise-induced increase in brain-derived neurotrophic factor in human Parkinson's disease: a systematic review and meta-analysis", *Translational neurodegeneration*, vol. 7, pp. 7-018-0112-1. eCollection 2018.
- Huang, D., Wang, Z., Tong, J., Wang, M., Wang, J., Xu, J., Bai, X., Li, H., Huang, Y., Wu, Y., Ma, Y., Yu, M. & Huang, F. 2018, "Long-term Changes in the Nigrostriatal Pathway in the MPTP Mouse Model of Parkinson's Disease", *Neuroscience*, vol. 369, pp. 303-313.

- Huang, J., Zhu, C., Zhang, P., Zhu, Q., Liu, Y., Zhu, Z., Wang, M., Li, W., Yang, G., Dong, N., Liu, J., Chen, L., Zhang, Y., Yang, R., Deng, L., Fan, J., Wang, X., Liu, J., Ma, B., Fu, Q. & Wu, K. 2013, "S100+ cells: a new neuro-immune cross-talkers in lymph organs", *Scientific reports*, vol. 3, pp. 1114.
- Iancu, R., Mohapel, P., Brundin, P. & Paul, G. 2005, "Behavioral characterization of a unilateral 6-OHDA-lesion model of Parkinson's disease in mice", *Behavioural brain research*, vol. 162, no. 1, pp. 1-10.
- Iemura, A., Tsai, M., Ando, A., Wershil, B.K. & Galli, S.J. 1994, "The c-kit ligand, stem cell factor, promotes mast cell survival by suppressing apoptosis", *The American journal of pathology*, vol. 144, no. 2, pp. 321-328.
- Jackson, S.J., Andrews, N., Ball, D., Bellantuono, I., Gray, J., Hachoumi, L., Holmes, A., Latcham, J., Petrie, A., Potter, P., Rice, A., Ritchie, A., Stewart, M., Strepka, C., Yeoman, M. & Chapman, K. 2017, "Does age matter? The impact of rodent age on study outcomes", *Laboratory animals*, vol. 51, no. 2, pp. 160-169.
- Jackson-Lewis, V. & Przedborski, S. 2007, "Protocol for the MPTP mouse model of Parkinson's disease", *Nature protocols*, vol. 2, no. 1, pp. 141-151.
- Jin, K., Mao, X.O., Cottrell, B., Schilling, B., Xie, L., Row, R.H., Sun, Y., Peel, A., Childs, J., Gendeh, G., Gibson, B.W. & Greenberg, D.A. 2004, "Proteomic and immunochemical characterization of a role for stathmin in adult neurogenesis", *FASEB journal : official publication of the Federation of American Societies for Experimental Biology*, vol. 18, no. 2, pp. 287-299.
- Jin, K., Sun, Y., Xie, L., Batteur, S., Mao, X.O., Smelick, C., Logvinova, A. & Greenberg, D.A. 2003, "Neurogenesis and aging: FGF-2 and HB-EGF restore neurogenesis in hippocampus and subventricular zone of aged mice", *Aging cell*, vol. 2, no. 3, pp. 175-183.
- Joe, E.H., Choi, D.J., An, J., Eun, J.H., Jou, I. & Park, S. 2018, "Astrocytes, Microglia, and Parkinson's Disease", *Experimental neurobiology*, vol. 27, no. 2, pp. 77-87.
- Johann, V., Schiefer, J., Sass, C., Mey, J., Brook, G., Kruttgen, A., Schlangen, C., Bernreuther, C., Schachner, M., Dihne, M. & Kosinski, C.M. 2007, "Time of transplantation and cell preparation determine neural stem cell survival in a mouse model of Huntington's disease", *Experimental brain research*, vol. 177, no. 4, pp. 458-470.
- Jones, M.K., Nair, A. & Gupta, M. 2019, "Mast Cells in Neurodegenerative Disease", *Frontiers in cellular neuroscience*, vol. 13, pp. 171.
- Jovanovic, V.M., Salti, A., Tilleman, H., Zega, K., Jukic, M.M., Zou, H., Friedel, R.H., Prakash, N., Blaess, S., Edenhofer, F. & Brodski, C. 2018, "BMP/SMAD Pathway Promotes Neurogenesis of Midbrain Dopaminergic Neurons In Vivo and in Human Induced Pluripotent and Neural Stem Cells", *The Journal of neuroscience : the official journal of the Society for Neuroscience*, vol. 38, no. 7, pp. 1662-1676.

- Kalia, L.V., Kalia, S.K. & Lang, A.E. 2015, "Disease-modifying strategies for Parkinson's disease", *Movement disorders : official journal of the Movement Disorder Society*, vol. 30, no. 11, pp. 1442-1450.
- Kalia, L.V. & Lang, A.E. 2015, "Parkinson's disease", *Lancet (London, England)*, vol. 386, no. 9996, pp. 896-912.
- Kalkonde, Y.V., Morgan, W.W., Sigala, J., Maffi, S.K., Condello, C., Kuziel, W., Ahuja, S.S. & Ahuja, S.K. 2007, "Chemokines in the MPTP model of Parkinson's disease: absence of CCL2 and its receptor CCR2 does not protect against striatal neurodegeneration", *Brain research*, vol. 1128, no. 1, pp. 1-11.
- Kehagia, A.A., Housden, C.R., Regenthal, R., Barker, R.A., Muller, U., Rowe, J., Sahakian, B.J. & Robbins, T.W. 2014, "Targeting impulsivity in Parkinson's disease using atomoxetine", *Brain : a journal of neurology*, vol. 137, no. Pt 7, pp. 1986-1997.
- Kempuraj, D., Thangavel, R., Fattal, R., Pattani, S., Yang, E., Zaheer, S., Santillan, D.A., Santillan, M.K. & Zaheer, A. 2016, "Mast Cells Release Chemokine CCL2 in Response to Parkinsonian Toxin 1-Methyl-4-Phenyl-Pyridinium (MPP(+))", *Neurochemical research*, vol. 41, no. 5, pp. 1042-1049.
- Kim, S., Kwon, S.H., Kam, T.I., Panicker, N., Karuppagounder, S.S., Lee, S., Lee, J.H., Kim, W.R., Kook, M., Foss, C.A., Shen, C., Lee, H., Kulkarni, S., Pasricha, P.J., Lee, G., Pomper, M.G., Dawson, V.L., Dawson, T.M. & Ko, H.S. 2019, "Transneuronal Propagation of Pathologic alpha-Synuclein from the Gut to the Brain Models Parkinson's Disease", *Neuron*, vol. 103, no. 4, pp. 627-641.e7.
- Kocabicak, E. & Temel, Y. 2013, "Deep brain stimulation of the subthalamic nucleus in Parkinson's disease: surgical technique, tips, tricks and complications", *Clinical neurology and neurosurgery*, vol. 115, no. 11, pp. 2318-2323.
- Kriks, S., Shim, J.W., Piao, J., Ganat, Y.M., Wakeman, D.R., Xie, Z., Carrillo-Reid, L., Auyeung, G., Antonacci, C., Buch, A., Yang, L., Beal, M.F., Surmeier, D.J., Kordower, J.H., Tabar, V. & Studer, L. 2011, "Dopamine neurons derived from human ES cells efficiently engraft in animal models of Parkinson's disease", *Nature*, vol. 480, no. 7378, pp. 547-551.
- Lesage, S. & Brice, A. 2009, "Parkinson's disease: from monogenic forms to genetic susceptibility factors", *Human molecular genetics*, vol. 18, no. R1, pp. R48-59.
- Li, W., Englund, E., Widner, H., Mattsson, B., van Westen, D., Latt, J., Rehncrona, S., Brundin, P., Bjorklund, A., Lindvall, O. & Li, J.Y. 2016, "Extensive graft-derived dopaminergic innervation is maintained 24 years after transplantation in the degenerating parkinsonian brain", *Proceedings of the National Academy of Sciences of the United States of America*, vol. 113, no. 23, pp. 6544-6549.
- Lim, J., Bang, Y. & Choi, H.J. 2018, "Abnormal hippocampal neurogenesis in Parkinson's disease: relevance to a new therapeutic target for depression with Parkinson's disease", *Archives of Pharmacal Research*, vol. 41, no. 10, pp. 943-954.

- Lindholm, P., Voutilainen, M.H., Lauren, J., Peranen, J., Leppanen, V.M., Andressoo, J.O., Lindahl, M., Janhunen, S., Kalkkinen, N., Timmusk, T., Tuominen, R.K. & Saarma, M. 2007, "Novel neurotrophic factor CDNF protects and rescues midbrain dopamine neurons in vivo", *Nature*, vol. 448, no. 7149, pp. 73-77.
- Lindsberg, P.J., Strbian, D. & Karjalainen-Lindsberg, M.L. 2010, "Mast cells as early responders in the regulation of acute blood-brain barrier changes after cerebral ischemia and hemorrhage", *Journal of cerebral blood flow and metabolism : official journal of the International Society of Cerebral Blood Flow and Metabolism*, vol. 30, no. 4, pp. 689-702.
- Ling, Z.D., Potter, E.D., Lipton, J.W. & Carvey, P.M. 1998, "Differentiation of mesencephalic progenitor cells into dopaminergic neurons by cytokines", *Experimental neurology*, vol. 149, no. 2, pp. 411-423.
- Liss, B. & Striessnig, J. 2019, "The Potential of L-Type Calcium Channels as a Drug Target for Neuroprotective Therapy in Parkinson's Disease", *Annual Review of Pharmacology and Toxicology*, vol. 59, pp. 263-289.
- Liu, J.Q., Chu, S.F., Zhou, X., Zhang, D.Y. & Chen, N.H. 2019, "Role of chemokines in Parkinson's disease", *Brain research bulletin*, vol. 152, pp. 11-18.
- Lotharius, J., Barg, S., Wiekop, P., Lundberg, C., Raymon, H.K. & Brundin, P. 2002, "Effect of mutant alpha-synuclein on dopamine homeostasis in a new human mesencephalic cell line", *The Journal of biological chemistry*, vol. 277, no. 41, pp. 38884-38894.
- Louveau, A., Smirnov, I., Keyes, T.J., Eccles, J.D., Rouhani, S.J., Peske, J.D., Derecki, N.C., Castle, D., Mandell, J.W., Lee, K.S., Harris, T.H. & Kipnis, J. 2015, "Structural and functional features of central nervous system lymphatic vessels", *Nature*, vol. 523, no. 7560, pp. 337-341.
- Lu, L.F., Lind, E.F., Gondek, D.C., Bennett, K.A., Gleeson, M.W., Pino-Lagos, K., Scott, Z.A., Coyle, A.J., Reed, J.L., Van Snick, J., Strom, T.B., Zheng, X.X. & Noelle, R.J. 2006, "Mast cells are essential intermediaries in regulatory T-cell tolerance", *Nature*, vol. 442, no. 7106, pp. 997-1002.
- Luchtman, D.W., Shao, D. & Song, C. 2009, "Behavior, neurotransmitters and inflammation in three regimens of the MPTP mouse model of Parkinson's disease", *Physiology & Behavior*, vol. 98, no. 1-2, pp. 130-138.
- Luo, J., Daniels, S.B., Lenington, J.B., Notti, R.Q. & Conover, J.C. 2006, "The aging neurogenic subventricular zone", *Aging cell*, vol. 5, no. 2, pp. 139-152.
- Macdonald, P.A. & Monchi, O. 2011, "Differential effects of dopaminergic therapies on dorsal and ventral striatum in Parkinson's disease: implications for cognitive function", *Parkinson's disease*, vol. 2011, pp. 572743.
- Marxreiter, F., Regensburger, M. & Winkler, J. 2013, "Adult neurogenesis in Parkinson's disease", *Cellular and molecular life sciences : CMLS*, vol. 70, no. 3, pp. 459-473.
- Mendes-Pinheiro, B., Teixeira, F.G., Anjo, S.I., Manadas, B., Behie, L.A. & Salgado, A.J. 2018, "Secretome of Undifferentiated Neural Progenitor Cells Induces Histological and Motor

- Improvements in a Rat Model of Parkinson's Disease", *Stem cells translational medicine*, vol. 7, no. 11, pp. 829-838.
- Meredith, G.E. & Rademacher, D.J. 2011, "MPTP mouse models of Parkinson's disease: an update", *Journal of Parkinson's disease*, vol. 1, no. 1, pp. 19-33.
- Morganti, J.M., Nash, K.R., Grimmig, B.A., Ranjit, S., Small, B., Bickford, P.C. & Gemma, C. 2012, "The soluble isoform of CX3CL1 is necessary for neuroprotection in a mouse model of Parkinson's disease", *The Journal of neuroscience : the official journal of the Society for Neuroscience*, vol. 32, no. 42, pp. 14592-14601.
- Muller, H.W., Junghans, U. & Kappler, J. 1995, "Astroglial neurotrophic and neurite-promoting factors", *Pharmacology & therapeutics*, vol. 65, no. 1, pp. 1-18.
- Nakhaeifard, M., Haji Ghasem Kashani, M., Goudarzi, I. & Rezaei, A. 2018, "Conditioned Medium Protects Dopaminergic Neurons in Parkinsonian Rats", *Cell journal*, vol. 20, no. 3, pp. 348-354.
- Nash, K.R., Moran, P., Finneran, D.J., Hudson, C., Robinson, J., Morgan, D. & Bickford, P.C. 2015, "Fractalkine over expression suppresses alpha-synuclein-mediated neurodegeneration", *Molecular therapy : the journal of the American Society of Gene Therapy*, vol. 23, no. 1, pp. 17-23.
- Nieouillon, A. 2002, "Dopamine and the regulation of cognition and attention", *Progress in neurobiology*, vol. 67, no. 1, pp. 53-83.
- Niethammer, M., Feigin, A. & Eidelberg, D. 2012, "Functional neuroimaging in Parkinson's disease", *Cold Spring Harbor perspectives in medicine*, vol. 2, no. 5, pp. a009274.
- Nombela, C., Rittman, T., Robbins, T.W. & Rowe, J.B. 2014, "Multiple modes of impulsivity in Parkinson's disease", *PloS one*, vol. 9, no. 1, pp. e85747.
- Norrby, K. 2002, "Mast cells and angiogenesis", *APMIS : Acta Pathologica, Microbiologica, et Immunologica Scandinavica*, vol. 110, no. 5, pp. 355-371.
- Ohashi, S., Mori, A., Kurihara, N., Mitsumoto, Y. & Nakai, M. 2006, "Age-related severity of dopaminergic neurodegeneration to MPTP neurotoxicity causes motor dysfunction in C57BL/6 mice", *Neuroscience letters*, vol. 401, no. 1-2, pp. 183-187.
- Ourednik, J., Ourednik, V., Lynch, W.P., Schachner, M. & Snyder, E.Y. 2002, "Neural stem cells display an inherent mechanism for rescuing dysfunctional neurons", *Nature biotechnology*, vol. 20, no. 11, pp. 1103-1110.
- Pabon, M.M., Bachstetter, A.D., Hudson, C.E., Gemma, C. & Bickford, P.C. 2011, "CX3CL1 reduces neurotoxicity and microglial activation in a rat model of Parkinson's disease", *Journal of neuroinflammation*, vol. 8, pp. 9-2094-8-9.
- Pallet, N., Dieude, M., Cailhier, J. & Hebert, M. 2012, "The molecular legacy of apoptosis in transplantation", *American journal of transplantation : official journal of the American Society*

of Transplantation and the American Society of Transplant Surgeons, vol. 12, no. 6, pp. 1378-1384.

- Park, H.J., Shin, J.Y., Lee, B.R., Kim, H.O. & Lee, P.H. 2012, "Mesenchymal stem cells augment neurogenesis in the subventricular zone and enhance differentiation of neural precursor cells into dopaminergic neurons in the substantia nigra of a parkinsonian model", *Cell transplantation*, vol. 21, no. 8, pp. 1629-1640.
- Patel, N.K., Bunnage, M., Plaha, P., Svendsen, C.N., Heywood, P. & Gill, S.S. 2005, "Intrapataminal infusion of glial cell line-derived neurotrophic factor in PD: a two-year outcome study", *Annals of Neurology*, vol. 57, no. 2, pp. 298-302.
- Pawitan, J.A. 2014, "Prospect of stem cell conditioned medium in regenerative medicine", *BioMed research international*, vol. 2014, pp. 965849.
- Perez-Bouza, A., Di Santo, S., Seiler, S., Meyer, M., Anderegg, L., Huber, A., Guzman, R. & Widmer, H.R. 2017, "Simultaneous Transplantation of Fetal Ventral Mesencephalic Tissue and Encapsulated Genetically Modified Cells Releasing GDNF in a Hemi-Parkinsonian Rat Model of Parkinson's Disease", *Cell transplantation*, vol. 26, no. 9, pp. 1572-1581.
- Perez-Navarro, E., Canudas, A.M., Akerund, P., Alberch, J. & Arenas, E. 2000, "Brain-derived neurotrophic factor, neurotrophin-3, and neurotrophin-4/5 prevent the death of striatal projection neurons in a rodent model of Huntington's disease", *Journal of neurochemistry*, vol. 75, no. 5, pp. 2190-2199.
- Phani, S., Loike, J.D. & Przedborski, S. 2012, "Neurodegeneration and inflammation in Parkinson's disease", *Parkinsonism & related disorders*, vol. 18 Suppl 1, pp. S207-9.
- Piltonen, M., Planken, A., Leskela, O., Myohanen, T.T., Hanninen, A.L., Auvinen, P., Alitalo, K., Andressoo, J.O., Saarma, M. & Mannisto, P.T. 2011, "Vascular endothelial growth factor C acts as a neurotrophic factor for dopamine neurons in vitro and in vivo", *Neuroscience*, vol. 192, pp. 550-563.
- Pluchino, S., Muzio, L., Imitola, J., Deleidi, M., Alfaro-Cervello, C., Salani, G., Porcheri, C., Brambilla, E., Cavasinni, F., Bergamaschi, A., Garcia-Verdugo, J.M., Comi, G., Khoury, S.J. & Martino, G. 2008, "Persistent inflammation alters the function of the endogenous brain stem cell compartment", *Brain : a journal of neurology*, vol. 131, no. Pt 10, pp. 2564-2578.
- Poulose, S.M., Miller, M.G., Scott, T. & Shukitt-Hale, B. 2017, "Nutritional Factors Affecting Adult Neurogenesis and Cognitive Function", *Advances in nutrition (Bethesda, Md.)*, vol. 8, no. 6, pp. 804-811.
- Pretze, M., Wangler, C. & Wangler, B. 2014, "6-[18F]fluoro-L-DOPA: a well-established neurotracer with expanding application spectrum and strongly improved radiosyntheses", *BioMed research international*, vol. 2014, pp. 674063.
- Rafuse, V.F., Soundararajan, P., Leopold, C. & Robertson, H.A. 2005, "Neuroprotective properties of cultured neural progenitor cells are associated with the production of sonic hedgehog", *Neuroscience*, vol. 131, no. 4, pp. 899-916.

- Ramos-Moreno, T., Castillo, C.G. & Martinez-Serrano, A. 2012, "Long term behavioral effects of functional dopaminergic neurons generated from human neural stem cells in the rat 6-OH-DA Parkinson's disease model. Effects of the forced expression of BCL-X(L)", *Behavioural brain research*, vol. 232, no. 1, pp. 225-232.
- Ramos-Moreno, T., Lendinez, J.G., Pino-Barrio, M.J., Del Arco, A. & Martinez-Serrano, A. 2012, "Clonal human fetal ventral mesencephalic dopaminergic neuron precursors for cell therapy research", *PloS one*, vol. 7, no. 12, pp. e52714.
- Razgado-Hernandez, L.F., Espadas-Alvarez, A.J., Reyna-Velazquez, P., Sierra-Sanchez, A., Anaya-Martinez, V., Jimenez-Estrada, I., Bannon, M.J., Martinez-Fong, D. & Aceves-Ruiz, J. 2015, "The transfection of BDNF to dopamine neurons potentiates the effect of dopamine D3 receptor agonist recovering the striatal innervation, dendritic spines and motor behavior in an aged rat model of Parkinson's disease", *PloS one*, vol. 10, no. 2, pp. e0117391.
- Real, C.C., Ferreira, A.F., Chaves-Kirsten, G.P., Torrao, A.S., Pires, R.S. & Britto, L.R. 2013, "BDNF receptor blockade hinders the beneficial effects of exercise in a rat model of Parkinson's disease", *Neuroscience*, vol. 237, pp. 118-129.
- Redmond, D.E., Jr, Bjugstad, K.B., Teng, Y.D., Ourednik, V., Ourednik, J., Wakeman, D.R., Parsons, X.H., Gonzalez, R., Blanchard, B.C., Kim, S.U., Gu, Z., Lipton, S.A., Markakis, E.A., Roth, R.H., Elsworth, J.D., Sladek, J.R., Jr, Sidman, R.L. & Snyder, E.Y. 2007, "Behavioral improvement in a primate Parkinson's model is associated with multiple homeostatic effects of human neural stem cells", *Proceedings of the National Academy of Sciences of the United States of America*, vol. 104, no. 29, pp. 12175-12180.
- Regensburger, M., Prots, I. & Winner, B. 2014, "Adult hippocampal neurogenesis in Parkinson's disease: impact on neuronal survival and plasticity", *Neural plasticity*, vol. 2014, pp. 454696.
- Rentzos, M., Nikolaou, C., Andreadou, E., Paraskevas, G.P., Rombos, A., Zoga, M., Tsoutsou, A., Boufidou, F., Kapaki, E. & Vassilopoulos, D. 2009, "Circulating interleukin-10 and interleukin-12 in Parkinson's disease", *Acta Neurologica Scandinavica*, vol. 119, no. 5, pp. 332-337.
- Ridet, J.L., Malhotra, S.K., Privat, A. & Gage, F.H. 1997, "Reactive astrocytes: cellular and molecular cues to biological function", *Trends in neurosciences*, vol. 20, no. 12, pp. 570-577.
- Ronnberg, E., Calounova, G. & Pejler, G. 2012, "Mast cells express tyrosine hydroxylase and store dopamine in a serglycin-dependent manner", *Biological chemistry*, vol. 393, no. 1-2, pp. 107-112.
- Rousselet, E., Joubert, C., Callebert, J., Parain, K., Tremblay, L., Orioux, G., Launay, J.M., Cohen-Salmon, C. & Hirsch, E.C. 2003, "Behavioral changes are not directly related to striatal monoamine levels, number of nigral neurons, or dose of parkinsonian toxin MPTP in mice", *Neurobiology of disease*, vol. 14, no. 2, pp. 218-228.
- Sampaio, T.B., Savall, A.S., Gutierrez, M.E.Z. & Pinton, S. 2017, "Neurotrophic factors in Alzheimer's and Parkinson's diseases: implications for pathogenesis and therapy", *Neural regeneration research*, vol. 12, no. 4, pp. 549-557.

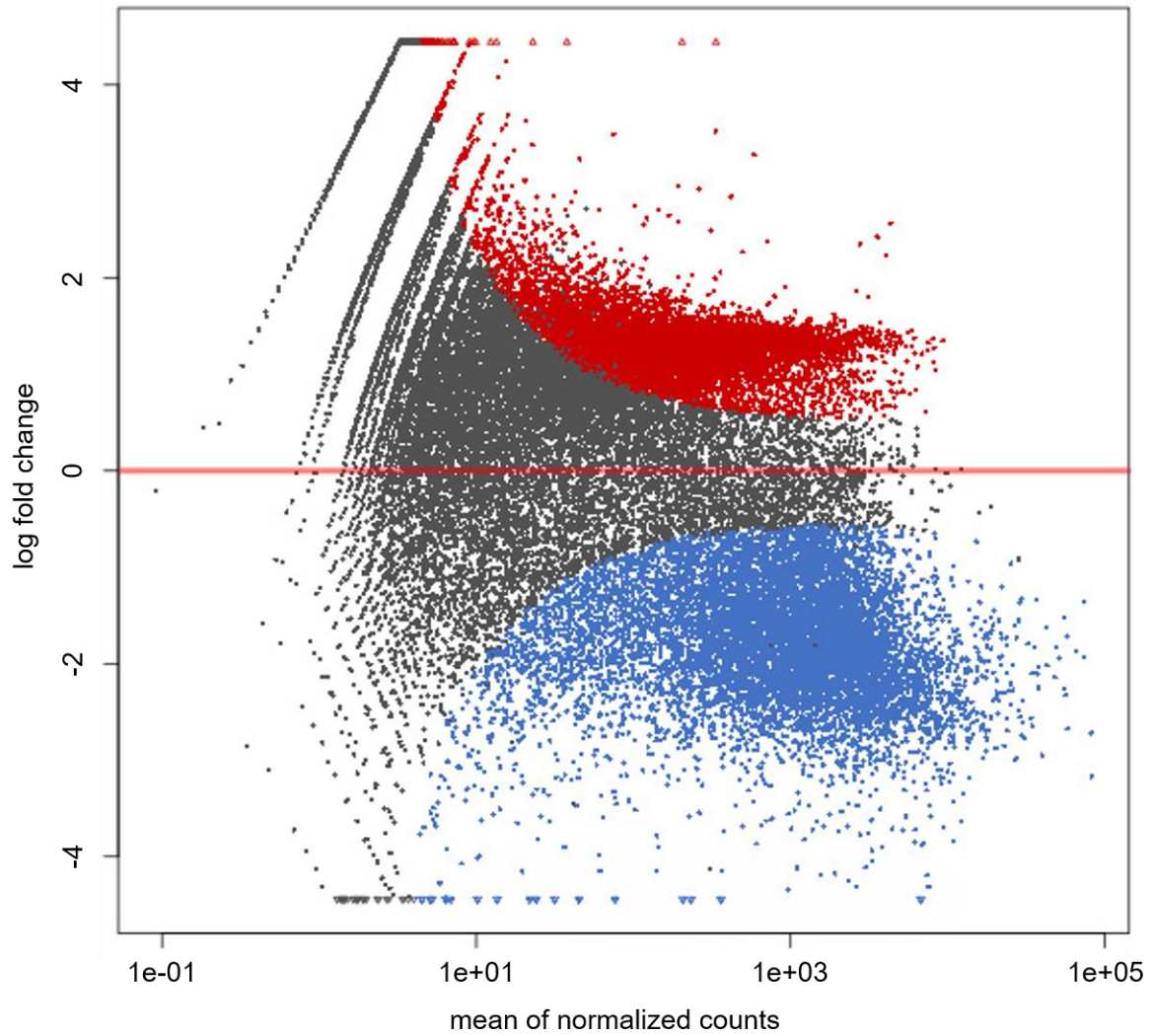
- Sarkar, S., Raymick, J. & Imam, S. 2016, "Neuroprotective and Therapeutic Strategies against Parkinson's Disease: Recent Perspectives", *International journal of molecular sciences*, vol. 17, no. 6, pp. 10.3390/ijms17060904.
- Sarnat, H.B. 2013, "Clinical neuropathology practice guide 5-2013: markers of neuronal maturation", *Clinical neuropathology*, vol. 32, no. 5, pp. 340-369.
- Schwarting, R.K., Sedelis, M., Hofele, K., Auburger, G.W. & Huston, J.P. 1999, "Strain-dependent recovery of open-field behavior and striatal dopamine deficiency in the mouse MPTP model of Parkinson's disease", *Neurotoxicity research*, vol. 1, no. 1, pp. 41-56.
- Sedelis, M., Schwarting, R.K. & Huston, J.P. 2001, "Behavioral phenotyping of the MPTP mouse model of Parkinson's disease", *Behavioural brain research*, vol. 125, no. 1-2, pp. 109-125.
- Sengupta, P. 2013, "The Laboratory Rat: Relating Its Age With Human's", *International journal of preventive medicine*, vol. 4, no. 6, pp. 624-630.
- Shim, J.W. & Madsen, J.R. 2018, "VEGF Signaling in Neurological Disorders", *International journal of molecular sciences*, vol. 19, no. 1, pp. 10.3390/ijms19010275.
- Shohayeb, B., Diab, M., Ahmed, M. & Ng, D.C.H. 2018, "Factors that influence adult neurogenesis as potential therapy", *Translational neurodegeneration*, vol. 7, pp. 4-018-0109-9. eCollection 2018.
- Silver, R. & Curley, J.P. 2013, "Mast cells on the mind: new insights and opportunities", *Trends in neurosciences*, vol. 36, no. 9, pp. 513-521.
- Skaper, S.D., Facci, L. & Giusti, P. 2014, "Mast cells, glia and neuroinflammation: partners in crime?", *Immunology*, vol. 141, no. 3, pp. 314-327.
- Sofroniew, M.V. 2005, "Reactive astrocytes in neural repair and protection", *The Neuroscientist : a review journal bringing neurobiology, neurology and psychiatry*, vol. 11, no. 5, pp. 400-407.
- Stoker, T.B. & Barker, R.A. 2016, "Cell therapies for Parkinson's disease: how far have we come?", *Regenerative medicine*, vol. 11, no. 8, pp. 777-786.
- Stoker, T.B., Blair, N.F. & Barker, R.A. 2017, "Neural grafting for Parkinson's disease: challenges and prospects", *Neural regeneration research*, vol. 12, no. 3, pp. 389-392.
- Stoker, T.B., Torsney, K.M. & Barker, R.A. 2018, "Emerging Treatment Approaches for Parkinson's Disease", *Frontiers in neuroscience*, vol. 12, pp. 693.
- Sullivan, A.M. & Toulouse, A. 2011, "Neurotrophic factors for the treatment of Parkinson's disease", *Cytokine & growth factor reviews*, vol. 22, no. 3, pp. 157-165.
- Sun, L., Lee, J. & Fine, H.A. 2004, "Neuronally expressed stem cell factor induces neural stem cell migration to areas of brain injury", *The Journal of clinical investigation*, vol. 113, no. 9, pp. 1364-1374.

- Takamura, N., Nakagawa, S., Masuda, T., Boku, S., Kato, A., Song, N., An, Y., Kitaichi, Y., Inoue, T., Koyama, T. & Kusumi, I. 2014, "The effect of dopamine on adult hippocampal neurogenesis", *Progress in neuro-psychopharmacology & biological psychiatry*, vol. 50, pp. 116-124.
- Tam, R.Y., Fuehrmann, T., Mitrousis, N. & Shoichet, M.S. 2014, "Regenerative therapies for central nervous system diseases: a biomaterials approach", *Neuropsychopharmacology : official publication of the American College of Neuropsychopharmacology*, vol. 39, no. 1, pp. 169-188.
- Taylor, T.N., Greene, J.G. & Miller, G.W. 2010, "Behavioral phenotyping of mouse models of Parkinson's disease", *Behavioural brain research*, vol. 211, no. 1, pp. 1-10.
- Teixeira, F.G., Carvalho, M.M., Panchalingam, K.M., Rodrigues, A.J., Mendes-Pinheiro, B., Anjo, S., Manadas, B., Behie, L.A., Sousa, N. & Salgado, A.J. 2017, "Impact of the Secretome of Human Mesenchymal Stem Cells on Brain Structure and Animal Behavior in a Rat Model of Parkinson's Disease", *Stem cells translational medicine*, vol. 6, no. 2, pp. 634-646.
- The Michael J. Fox Foundation for Parkinson's Research 2019, , *Founded Studies*. Available: <https://www.michaeljfox.org/funded-studies> [2019, August 26, 2019].
- Theoharides, T.C., Alysandratos, K.D., Angelidou, A., Delivanis, D.A., Sismanopoulos, N., Zhang, B., Asadi, S., Vasiadi, M., Weng, Z., Miniati, A. & Kalogeromitros, D. 2012, "Mast cells and inflammation", *Biochimica et biophysica acta*, vol. 1822, no. 1, pp. 21-33.
- Thome, A.D., Standaert, D.G. & Harms, A.S. 2015, "Fractalkine Signaling Regulates the Inflammatory Response in an alpha-Synuclein Model of Parkinson Disease", *PLoS one*, vol. 10, no. 10, pp. e0140566.
- Tian, Y.Y., Tang, C.J., Wang, J.N., Feng, Y., Chen, X.W., Wang, L., Qiao, X. & Sun, S.G. 2007, "Favorable effects of VEGF gene transfer on a rat model of Parkinson disease using adeno-associated viral vectors", *Neuroscience letters*, vol. 421, no. 3, pp. 239-244.
- Tome, D., Fonseca, C.P., Campos, F.L. & Baltazar, G. 2017, "Role of Neurotrophic Factors in Parkinson's Disease", *Current pharmaceutical design*, vol. 23, no. 5, pp. 809-838.
- Tonnesen, J., Seiz, E.G., Ramos, M., Lindvall, O., Martinez-Serrano, A. & Kokaia, M. 2010, "Functional properties of the human ventral mesencephalic neural stem cell line hVM1", *Experimental neurology*, vol. 223, no. 2, pp. 653-656.
- Troncoso-Escudero, P., Parra, A., Nassif, M. & Vidal, R.L. 2018, "Outside in: Unraveling the Role of Neuroinflammation in the Progression of Parkinson's Disease", *Frontiers in neurology*, vol. 9, pp. 860.
- Tsukahara, T., Takeda, M., Shimohama, S., Ohara, O. & Hashimoto, N. 1995, "Effects of brain-derived neurotrophic factor on 1-methyl-4-phenyl-1,2,3,6-tetrahydropyridine-induced parkinsonism in monkeys", *Neurosurgery*, vol. 37, no. 4, pp. 733-9; discussion 739-41.
- U.S. National Library of Medicine 2019, , *ClinicalTrials.gov*. Available: <https://clinicaltrials.gov/> [2019, August 26].

- van den Berge, S.A., van Strien, M.E. & Hol, E.M. 2013, "Resident adult neural stem cells in Parkinson's disease--the brain's own repair system?", *European journal of pharmacology*, vol. 719, no. 1-3, pp. 117-127.
- Villa, A., Liste, I., Courtois, E.T., Seiz, E.G., Ramos, M., Meyer, M., Juliusson, B., Kusk, P. & Martinez-Serrano, A. 2009, "Generation and properties of a new human ventral mesencephalic neural stem cell line", *Experimental cell research*, vol. 315, no. 11, pp. 1860-1874.
- Villeda, S.A., Plambeck, K.E., Middeldorp, J., Castellano, J.M., Mosher, K.I., Luo, J., Smith, L.K., Bieri, G., Lin, K., Berdnik, D., Wabl, R., Udeochu, J., Wheatley, E.G., Zou, B., Simmons, D.A., Xie, X.S., Longo, F.M. & Wyss-Coray, T. 2014, "Young blood reverses age-related impairments in cognitive function and synaptic plasticity in mice", *Nature medicine*, vol. 20, no. 6, pp. 659-663.
- Wang, Q., Ren, J., Morgan, S., Liu, Z., Dou, C. & Liu, B. 2014, "Monocyte chemoattractant protein-1 (MCP-1) regulates macrophage cytotoxicity in abdominal aortic aneurysm", *PLoS one*, vol. 9, no. 3, pp. e92053.
- Wenning, G.K., Odin, P., Morrish, P., Rehncrona, S., Widner, H., Brundin, P., Rothwell, J.C., Brown, R., Gustavii, B., Hagell, P., Jahansahi, M., Sawle, G., Bjorklund, A., Brooks, D.J., Marsden, C.D., Quinn, N.P. & Lindvall, O. 1997, "Short- and long-term survival and function of unilateral intrastriatal dopaminergic grafts in Parkinson's disease", *Annals of Neurology*, vol. 42, no. 1, pp. 95-107.
- Wirdefeldt, K., Adami, H.O., Cole, P., Trichopoulos, D. & Mandel, J. 2011, "Epidemiology and etiology of Parkinson's disease: a review of the evidence", *European journal of epidemiology*, vol. 26 Suppl 1, pp. S1-58.
- Wulfing, C. & Gunther, H.S. 2015, "Dendritic cells and macrophages neurally hard-wired in the lymph node", *Scientific reports*, vol. 5, pp. 16866.
- Wyss-Coray, T. 2016, "Ageing, neurodegeneration and brain rejuvenation", *Nature*, vol. 539, no. 7628, pp. 180-186.
- Xia, N., Zhang, P., Fang, F., Wang, Z., Rothstein, M., Angulo, B., Chiang, R., Taylor, J. & Reijo Pera, R.A. 2016, "Transcriptional comparison of human induced and primary midbrain dopaminergic neurons", *Scientific reports*, vol. 6, pp. 20270.
- Xiao, N. & Le, Q.T. 2016, "Neurotrophic Factors and Their Potential Applications in Tissue Regeneration", *Archivum Immunologiae et Therapiae Experimentalis*, vol. 64, no. 2, pp. 89-99.
- Yang, P., Arnold, S.A., Habas, A., Hetman, M. & Hagg, T. 2008, "Ciliary neurotrophic factor mediates dopamine D2 receptor-induced CNS neurogenesis in adult mice", *The Journal of neuroscience : the official journal of the Society for Neuroscience*, vol. 28, no. 9, pp. 2231-2241.
- Yao, Y., Huang, C., Gu, P. & Wen, T. 2016, "Combined MSC-Secreted Factors and Neural Stem Cell Transplantation Promote Functional Recovery of PD Rats", *Cell transplantation*, vol. 25, no. 6, pp. 1101-1113.

- Yasuhara, T. & Date, I. 2007, "Intracerebral transplantation of genetically engineered cells for Parkinson's disease: toward clinical application", *Cell transplantation*, vol. 16, no. 2, pp. 125-132.
- Yasuhara, T., Kameda, M., Sasaki, T., Tajiri, N. & Date, I. 2017, "Cell Therapy for Parkinson's Disease", *Cell transplantation*, vol. 26, no. 9, pp. 1551-1559.
- Yasuhara, T., Matsukawa, N., Hara, K., Yu, G., Xu, L., Maki, M., Kim, S.U. & Borlongan, C.V. 2006, "Transplantation of human neural stem cells exerts neuroprotection in a rat model of Parkinson's disease", *The Journal of neuroscience : the official journal of the Society for Neuroscience*, vol. 26, no. 48, pp. 12497-12511.
- Yasuhara, T., Shingo, T., Kobayashi, K., Takeuchi, A., Yano, A., Muraoka, K., Matsui, T., Miyoshi, Y., Hamada, H. & Date, I. 2004, "Neuroprotective effects of vascular endothelial growth factor (VEGF) upon dopaminergic neurons in a rat model of Parkinson's disease", *The European journal of neuroscience*, vol. 19, no. 6, pp. 1494-1504.
- Yasuhara, T., Shingo, T., Muraoka, K., Kameda, M., Agari, T., Wen Ji, Y., Hayase, H., Hamada, H., Borlongan, C.V. & Date, I. 2005, "Neurorescue effects of VEGF on a rat model of Parkinson's disease", *Brain research*, vol. 1053, no. 1-2, pp. 10-18.
- Zhang, J. & Jiao, J. 2015, "Molecular Biomarkers for Embryonic and Adult Neural Stem Cell and Neurogenesis", *BioMed research international*, vol. 2015, pp. 727542.
- Zhang, Q.S., Heng, Y., Mou, Z., Huang, J.Y., Yuan, Y.H. & Chen, N.H. 2017, "Reassessment of subacute MPTP-treated mice as animal model of Parkinson's disease", *Acta Pharmacologica Sinica*, vol. 38, no. 10, pp. 1317-1328.
- Zhang, T., Hong, J., Di, T. & Chen, L. 2016, "MPTP Impairs Dopamine D1 Receptor-Mediated Survival of Newborn Neurons in Ventral Hippocampus to Cause Depressive-Like Behaviors in Adult Mice", *Frontiers in molecular neuroscience*, vol. 9, pp. 101.
- Zuo, F., Xiong, F., Wang, X., Li, X., Wang, R., Ge, W. & Bao, X. 2017, "Intrastriatal Transplantation of Human Neural Stem Cells Restores the Impaired Subventricular Zone in Parkinsonian Mice", *Stem cells (Dayton, Ohio)*, vol. 35, no. 6, pp. 1519-1531.
- Zuo, F.X., Bao, X.J., Sun, X.C., Wu, J., Bai, Q.R., Chen, G., Li, X.Y., Zhou, Q.Y., Yang, Y.F., Shen, Q. & Wang, R.Z. 2015, "Transplantation of Human Neural Stem Cells in a Parkinsonian Model Exerts Neuroprotection via Regulation of the Host Microenvironment", *International journal of molecular sciences*, vol. 16, no. 11, pp. 26473-26492.

APPENDIX I



Supplementary Figure 1: Manhattan plot of differentially expressed genes of hVM1 clone 32 cells in proliferation and differentiation conditions. In red are genes that were increased in differentiation with a q-value < 0.05 , in blue are genes that were increased in proliferation with a q-value < 0.05 , and in grey are genes that had a q-value > 0.05 .

Category	Gene symbol	Gene ID	Fold change	q-value
NSCs/NPCs	<i>SOX21</i>	ENSG00000125285	-3.61	4.59E-28
	<i>SOX1</i>	ENSG00000182968	-3.55	4.29E-18
	<i>SFRP2</i>	ENSG00000145423	-3.44	3.37E-27
	<i>FZD9</i>	ENSG00000188763	-3.16	1.71E-08
	<i>HES5</i>	ENSG00000197921	-2.90	0.0442
	<i>METRN</i>	ENSG00000103260	-2.71	1.61E-16
	<i>GNL3</i>	ENSG00000163938	-2.39	4.76E-09
	<i>TRAF4</i>	ENSG00000076604	-2.33	5.01E-13
	<i>SLC2A1</i>	ENSG00000117394	-2.26	2.55E-13
	<i>NR2F1</i>	ENSG00000175745	-2.02	4.56E-09
	<i>SMARCA4</i>	ENSG00000127616	-1.97	6.43E-11
	<i>CTNNB1</i>	ENSG00000168036	-1.94	2.54E-08
	<i>ACVR2B</i>	ENSG00000114739	-1.93	2.28E-08
	<i>NEPRO</i>	ENSG00000163608	-1.60	0.000530
	<i>CDH2</i>	ENSG00000170558	-1.59	3.96E-06
	<i>GATA2</i>	ENSG00000179348	-1.58	0.00198
	<i>NFE2L2</i>	ENSG00000116044	-1.55	6.33E-06
	<i>FIBP</i>	ENSG00000172500	-1.50	2.92E-05
	<i>ZIC1</i>	ENSG00000152977	-1.50	4.02E-05
	<i>NOTCH2</i>	ENSG00000134250	-1.43	6.85E-06
	<i>MSI1</i>	ENSG00000135097	-1.40	2.92E-05
	<i>SOX11</i>	ENSG00000176887	-1.28	8.31E-05
	<i>MTURN</i>	ENSG00000180354	-1.23	0.000305
	<i>MSI2</i>	ENSG00000153944	-1.19	0.000343
	<i>RXRA</i>	ENSG00000186350	-1.19	0.000331
	<i>ACVR1B</i>	ENSG00000135503	-0.97	0.00380
	<i>TNC</i>	ENSG00000041982	-0.96	0.00423
	<i>SLAIN1</i>	ENSG00000139737	-0.90	0.0134
	<i>NPDC1</i>	ENSG00000107281	-0.87	0.0318
	<i>ABCG2</i>	ENSG00000118777	1.04	5.90E-03
	<i>INHBA</i>	ENSG00000122641	1.09	0.0369
	<i>ROR2</i>	ENSG00000169071	1.11	0.00118
	<i>CDH1</i>	ENSG00000039068	1.19	0.00137
	<i>OCN</i>	ENSG00000197822	1.27	0.00426
	<i>ACVR1C</i>	ENSG00000123612	1.27	0.00280
	<i>RUNX1</i>	ENSG00000159216	1.28	0.000334
	<i>PAX3</i>	ENSG00000135903	1.34	0.00209
	<i>INSC</i>	ENSG00000188487	1.43	0.00044
<i>PAX6</i>	ENSG00000007372	1.61	0.00313	
Mature neurons	<i>SYN2</i>	ENSG00000157152	0.81	0.0192
	<i>GAP43</i>	ENSG00000172020	0.89	0.0143
	<i>NRXN1</i>	ENSG00000179915	0.90	0.0250
	<i>MAPT</i>	ENSG00000186868	0.98	0.00922
	<i>NRXN2</i>	ENSG00000110076	0.98	0.00815
	<i>NAV1</i>	ENSG00000134369	1.00	0.0103
	<i>SYT6</i>	ENSG00000134207	1.01	0.00975
	<i>SYNPO</i>	ENSG00000171992	1.05	0.00389
	<i>SYNPO2</i>	ENSG00000172403	1.16	0.000840
	<i>SHANK2</i>	ENSG00000162105	1.17	0.00106
	<i>NAV3</i>	ENSG00000067798	1.18	0.000838
	<i>NEXMIF</i>	ENSG00000050030	1.19	0.000838
	<i>SV2B</i>	ENSG00000185518	1.23	0.000633
	<i>SYT2</i>	ENSG00000143858	1.23	0.00140

Category	Gene symbol	Gene ID	Fold change	q-value
	<i>SYNPR</i>	ENSG00000163630	1.27	0.000453
	<i>PSD-93</i>	ENSG00000150672	1.27	0.000465
	<i>SV2C</i>	ENSG00000122012	1.29	0.000276
	<i>NELL2</i>	ENSG00000184613	1.34	0.000277
	<i>NCAM2</i>	ENSG00000154654	1.34	0.000786
	<i>SYN3</i>	ENSG00000185666	1.35	0.000266
	<i>SYT9</i>	ENSG00000170743	1.36	0.000173
	<i>CDH12</i>	ENSG00000154162	1.37	0.000515
	<i>NELL1</i>	ENSG00000165973	1.38	0.000183
	<i>SNAP91</i>	ENSG00000065609	1.41	0.000680
	<i>NEGR1</i>	ENSG00000172260	1.41	0.000328
	<i>SYT16</i>	ENSG00000139973	1.43	9.69E-05
	<i>NRG1</i>	ENSG00000157168	1.44	0.000154
	<i>NRXN3</i>	ENSG00000021645	1.46	0.000119
	<i>ELAVL4</i>	ENSG00000162374	1.57	9.45E-05
	<i>SYT13</i>	ENSG00000019505	1.66	0.000346
	<i>SYT10</i>	ENSG00000110975	1.77	0.000396
	<i>NPY</i>	ENSG00000122585	2.29	0.0186
	<i>SYT4</i>	ENSG00000132872	2.75	2.36E-07
	<i>APOE</i>	ENSG00000130203	2.92	7.57E-13
NTFs and their receptors	<i>FGF18</i>	ENSG00000156427	1.07	0.0328
	<i>FGF10</i>	ENSG00000070193	1.19	0.00779
	<i>FGF13</i>	ENSG00000129682	1.19	0.000565
	<i>FGF12</i>	ENSG00000114279	1.25	0.000510
	<i>FGF5</i>	ENSG00000138675	1.38	0.00949
	<i>NDNF</i>	ENSG00000173376	1.48	0.00201
	<i>FGF23</i>	ENSG00000118972	1.60	0.0148
Astrocytes/Radial glia	<i>BIRC5</i>	ENSG00000089685	-2.30	5.95E-11
	<i>GJA1</i>	ENSG00000152661	-1.29	0.000957
	<i>GAP43</i>	ENSG00000172020	0.89	0.0143
	<i>NDRG2</i>	ENSG00000165795	0.89	0.0237
Oligodendrocytes	<i>ERBB3</i>	ENSG00000065361	0.98	0.0471
	<i>NFASC</i>	ENSG00000163531	1.24	0.00125
	<i>PLP1</i>	ENSG00000123560	1.28	0.00462
	<i>MYT1</i>	ENSG00000196132	1.31	0.000399
	<i>CNTNAP2</i>	ENSG00000174469	1.37	0.000296
	<i>NRG1</i>	ENSG00000157168	1.44	0.000154
Serotonergic neurons	<i>HMCES</i>	ENSG00000183624	-1.93	1.36E-08
	<i>HTR7</i>	ENSG00000148680	0.92	0.00936
	<i>HTR5BP</i>	ENSG00000125631	0.99	0.0274
	<i>HTR2C</i>	ENSG00000147246	1.23	0.00434
	<i>HTR3B</i>	ENSG00000149305	1.24	0.00501
	<i>HTR1E</i>	ENSG00000168830	1.24	0.00140
	<i>HTR2A</i>	ENSG00000102468	1.25	0.00252
	<i>HTR5A</i>	ENSG00000157219	1.26	0.0339
	<i>HTR4</i>	ENSG00000164270	1.38	0.000280
	<i>DDC</i>	ENSG00000132437	1.53	0.00556
	<i>HTR6</i>	ENSG00000158748	1.67	0.0143
	<i>HTR1F</i>	ENSG00000179097	2.27	0.0356
GABAergic neurons	<i>GABRG2</i>	ENSG00000113327	1.14	0.00235
	<i>SLC6A13</i>	ENSG00000010379	1.14	0.0289
	<i>GABRA6</i>	ENSG00000145863	1.16	0.00215
	<i>GABRA2</i>	ENSG00000151834	1.17	0.00178

Category	Gene symbol	Gene ID	Fold change	q-value
	<i>GABRR3</i>	ENSG00000183185	1.18	0.00629
	<i>GABRG1</i>	ENSG00000163285	1.21	0.00305
	<i>GADI1</i>	ENSG00000128683	1.22	0.00578
	<i>GABRB3</i>	ENSG00000166206	1.25	0.00024
	<i>SLC6A12</i>	ENSG00000111181	1.27	0.0263
	<i>GABRQ</i>	ENSG00000268089	1.27	0.0114
	<i>GABRG3</i>	ENSG00000182256	1.27	0.00039
	<i>GABRA1</i>	ENSG00000022355	1.33	0.00727
	<i>GABRBI</i>	ENSG00000163288	1.36	0.00023
	<i>GAD2</i>	ENSG00000136750	1.38	0.00396
	<i>GABRR1</i>	ENSG00000146276	1.39	0.00738
	<i>GABRP</i>	ENSG00000094755	1.40	0.0123
	<i>GABRA3</i>	ENSG00000011677	1.42	0.000305
	<i>GABRB2</i>	ENSG00000145864	1.50	3.36E-05
	<i>GABRA4</i>	ENSG00000109158	1.54	0.000342
Glutamatergic neurons	<i>SLC1A3</i>	ENSG00000079215	-1.65	5.29E-06
	<i>SLC17A5</i>	ENSG00000119899	-1.11	0.00152
	<i>GRIP2</i>	ENSG00000144596	-1.03	0.00359
	<i>GRIK5</i>	ENSG00000105737	0.85	0.04465
	<i>GRIN3A</i>	ENSG00000198785	1.11	0.00241
	<i>SLC1A1</i>	ENSG00000106688	1.19	0.00230
	<i>GRIA2</i>	ENSG00000120251	1.19	0.000862
	<i>SLC17A4</i>	ENSG00000146039	1.24	0.00784
	<i>GRIK1</i>	ENSG00000171189	1.26	0.00106
	<i>GRID1</i>	ENSG00000182771	1.28	0.000107
	<i>SLC17A3</i>	ENSG00000124564	1.28	0.00229
	<i>GRIK4</i>	ENSG00000149403	1.31	0.000520
	<i>GRM8</i>	ENSG00000179603	1.33	0.000194
	<i>GRIK3</i>	ENSG00000163873	1.35	0.000180
	<i>GRIK2</i>	ENSG00000164418	1.37	0.000320
	<i>GRID2</i>	ENSG00000152208	1.39	0.000176
	<i>GRM5</i>	ENSG00000168959	1.40	0.000299
	<i>GRM1</i>	ENSG00000152822	1.40	0.000283
	<i>GRM7</i>	ENSG00000196277	1.45	9.91E-05
	<i>SLC17A8</i>	ENSG00000179520	1.47	0.000680
	<i>GRIN2A</i>	ENSG00000183454	1.53	5.24E-05
	<i>GRM3</i>	ENSG00000198822	1.57	6.06E-05
Cholinergic neurons	<i>CHRNA6</i>	ENSG00000147434	1.28	0.0101
	<i>CHRNA1</i>	ENSG00000138435	1.37	0.0264
	<i>CHRNB4</i>	ENSG00000117971	1.51	0.00121
	<i>CHRNA2</i>	ENSG00000120903	1.67	0.0157
	<i>SLC5A7</i>	ENSG00000115665	1.78	0.00633
	<i>CHRND</i>	ENSG00000135902	1.88	0.00308
	<i>CHRNA9</i>	ENSG00000174343	2.58	1.16E-09
Neural plasticity	<i>PLXNA1</i>	ENSG00000114554	-1.96	2.82E-10
	<i>SPOCK2</i>	ENSG00000107742	-1.93	3.48E-10
	<i>PTENP1</i>	ENSG00000237984	-1.69	0.00264
	<i>PTEN</i>	ENSG00000171862	-1.60	8.11E-06
	<i>SEMA3A</i>	ENSG00000075213	-1.54	7.88E-06
	<i>SEMA3E</i>	ENSG00000170381	-1.43	5.22E-05
	<i>SNCAIP</i>	ENSG00000064692	-0.91	0.01437
	<i>ULK4</i>	ENSG00000168038	0.65	0.0433
	<i>SPOCK1</i>	ENSG00000152377	0.70	0.0349

Category	Gene symbol	Gene ID	Fold change	q-value
	<i>SEMA3D</i>	ENSG00000153993	0.99	0.00812
	<i>NAV1</i>	ENSG00000134369	0.10	0.0103
	<i>SYNPO</i>	ENSG00000171992	1.05	0.00389
	<i>SRGAP1</i>	ENSG00000196935	1.17	0.00548
	<i>NAV3</i>	ENSG00000067798	1.18	0.00084
	<i>UNC5C</i>	ENSG00000182168	1.19	0.00080
	<i>RASGRF2</i>	ENSG00000113319	1.20	0.00309
	<i>ASTN2</i>	ENSG00000148219	1.25	0.00042
	<i>SEMA3C</i>	ENSG00000075223	1.27	0.00116
	<i>STMN2</i>	ENSG00000104435	1.28	0.00711
	<i>TENM2</i>	ENSG00000145934	1.28	0.00042
	<i>DCC</i>	ENSG00000187323	1.30	0.00033
	<i>ASTN1</i>	ENSG00000152092	1.31	0.00067
	<i>SLIT3</i>	ENSG00000184347	1.37	0.00046
	<i>SPOCK3</i>	ENSG00000196104	1.42	0.00076
	<i>SLITRK6</i>	ENSG00000184564	1.73	0.0159
	<i>UNCX</i>	ENSG00000164853	3.09	0.0350
Proliferation and cell cycle	<i>SFRP2</i>	ENSG00000145423	-3.44	3.37E-27
	<i>ZWINT</i>	ENSG00000122952	-3.24	1.36E-17
	<i>PCNA</i>	ENSG00000132646	-3.18	4.02E-17
	<i>GMNN</i>	ENSG00000112312	-3.07	3.34E-15
	<i>CENPE</i>	ENSG00000138778	-3.04	5.73E-15
	<i>PLK4</i>	ENSG00000142731	-2.98	1.05E-15
	<i>PLK1</i>	ENSG00000166851	-2.97	4.64E-21
	<i>CDC25A</i>	ENSG00000164045	-2.87	1.60E-16
	<i>MAD2L1</i>	ENSG00000164109	-2.84	1.22E-14
	<i>ANAPC13</i>	ENSG00000129055	-2.79	1.99E-12
	<i>MDM2</i>	ENSG00000135679	-2.76	1.02E-13
	<i>BCCIP</i>	ENSG00000107949	-2.75	2.29E-11
	<i>MPHOSPH10</i>	ENSG00000124383	-2.74	2.59E-12
	<i>BUB1</i>	ENSG00000169679	-2.74	6.33E-15
	<i>KNSTRN</i>	ENSG00000128944	-2.73	1.49E-13
	<i>ASPM</i>	ENSG00000066279	-2.68	4.88E-13
	<i>SPC24</i>	ENSG00000161888	-2.68	7.26E-14
	<i>INCENP</i>	ENSG00000149503	-2.66	5.34E-17
	<i>NDC80</i>	ENSG00000080986	-2.64	7.50E-11
	<i>MCM10</i>	ENSG00000065328	-2.59	5.26E-13
	<i>NUP107</i>	ENSG00000111581	-2.57	4.56E-11
	<i>ANAPC7</i>	ENSG00000196510	-2.55	2.49E-12
	<i>E2F1</i>	ENSG00000101412	-2.55	1.62E-13
	<i>KNL1</i>	ENSG00000137812	-2.55	4.72E-11
	<i>MPHOSPH6</i>	ENSG00000135698	-2.54	9.99E-12
	<i>NET1</i>	ENSG00000173848	-2.53	5.92E-13
	<i>RFC5</i>	ENSG00000111445	-2.51	4.56E-11
	<i>CENPM</i>	ENSG00000100162	-2.51	1.31E-11
	<i>PALB2</i>	ENSG00000083093	-2.46	4.70E-11
	<i>PLK3</i>	ENSG00000173846	-2.43	2.28E-10
	<i>TICRR</i>	ENSG00000140534	-2.41	4.60E-10
	<i>SKA3</i>	ENSG00000165480	-2.38	1.04E-10
	<i>RFC2</i>	ENSG00000049541	-2.37	3.86E-12
	<i>ESPL1</i>	ENSG00000135476	-2.36	9.14E-13
	<i>BUB1B</i>	ENSG00000156970	-2.34	3.03E-09
	<i>RFC4</i>	ENSG00000163918	-2.33	1.97E-09

Category	Gene symbol	Gene ID	Fold change	q-value
	<i>CENPJ</i>	ENSG00000151849	-2.33	3.61E-10
	<i>CDT1</i>	ENSG00000167513	-2.33	4.70E-11
	<i>PIMREG</i>	ENSG00000129195	-2.31	8.64E-11
	<i>NUF2</i>	ENSG00000143228	-2.31	1.76E-08
	<i>DSNI</i>	ENSG00000149636	-2.30	1.75E-09
	<i>ESCO2</i>	ENSG00000171320	-2.29	9.90E-10
	<i>CCSAP</i>	ENSG00000154429	-2.28	2.99E-10
	<i>CENPF</i>	ENSG00000117724	-2.28	1.64E-09
	<i>RPA2</i>	ENSG00000117748	-2.27	4.48E-10
	<i>SPDL1</i>	ENSG00000040275	-2.25	6.12E-10
	<i>CENPU</i>	ENSG00000151725	-2.24	8.48E-09
	<i>MZT1</i>	ENSG00000204899	-2.22	3.40E-10
	<i>E2F4</i>	ENSG00000205250	-2.21	5.29E-11
	<i>SHCBP1</i>	ENSG00000171241	-2.20	8.85E-10
	<i>CDK1</i>	ENSG00000170312	-2.19	2.14E-07
	<i>ANAPC1</i>	ENSG00000153107	-2.18	1.45E-09
	<i>BUB3</i>	ENSG00000154473	-2.17	3.72E-10
	<i>MIS12</i>	ENSG00000167842	-2.17	3.78E-08
	<i>PDS5A</i>	ENSG00000121892	-2.17	4.72E-10
	<i>CNTROB</i>	ENSG00000170037	-2.16	1.15E-09
	<i>CENPW</i>	ENSG00000203760	-2.11	4.11E-08
	<i>ZWILCH</i>	ENSG00000174442	-2.10	5.10E-08
	<i>CENPA</i>	ENSG00000115163	-2.10	5.71E-10
	<i>ANAPC15</i>	ENSG00000110200	-2.09	3.59E-06
	<i>SKA1</i>	ENSG00000154839	-2.09	1.15E-08
	<i>CCNE1</i>	ENSG00000105173	-2.09	6.39E-08
	<i>MZT2B</i>	ENSG00000152082	-2.08	1.42E-08
	<i>DNA2</i>	ENSG00000138346	-2.07	1.60E-08
	<i>SMU1</i>	ENSG00000122692	-2.06	4.93E-08
	<i>WAPL</i>	ENSG00000062650	-2.06	6.92E-09
	<i>MPHOSPH8</i>	ENSG00000196199	-2.04	1.93E-08
	<i>NUSAP1</i>	ENSG00000137804	-2.03	1.94E-07
	<i>BAP1</i>	ENSG00000163930	-2.01	4.67E-10
	<i>ZW10</i>	ENSG00000086827	-2.01	7.14E-08
	<i>NOC3L</i>	ENSG00000173145	-2.01	1.61E-06
	<i>RAD21</i>	ENSG00000164754	-1.98	1.25E-08
	<i>KNTC1</i>	ENSG00000184445	-1.96	1.250E-07
	<i>RFC1</i>	ENSG00000035928	-1.96	3.41E-07
	<i>BRCA2</i>	ENSG00000139618	-1.94	8.48E-08
	<i>PRCC</i>	ENSG00000143294	-1.93	9.86E-10
	<i>MAU2</i>	ENSG00000129933	-1.92	2.76E-09
	<i>BRAP</i>	ENSG00000089234	-1.91	1.57E-07
	<i>MOB1A</i>	ENSG00000114978	-1.91	2.28E-08
	<i>CENPH</i>	ENSG00000153044	-1.91	4.68E-07
	<i>MPHOSPH9</i>	ENSG00000051825	-1.90	2.65E-07
	<i>RPA1</i>	ENSG00000132383	-1.89	9.55E-10
	<i>ANAPC5</i>	ENSG00000089053	-1.89	5.34E-08
	<i>E2F2</i>	ENSG00000007968	-1.89	1.51E-08
	<i>CENPQ</i>	ENSG00000031691	-1.88	3.92E-06
	<i>BRCA1</i>	ENSG00000012048	-1.86	1.32E-07
	<i>MPLKIP</i>	ENSG00000168303	-1.85	3.80E-07
	<i>AC083899.1</i>	ENSG00000204745	-1.83	7.22E-07
	<i>CDK10</i>	ENSG00000185324	-1.83	5.38E-07

Category	Gene symbol	Gene ID	Fold change	q-value
	<i>CENPK</i>	ENSG00000123219	-1.82	1.12E-05
	<i>CENPO</i>	ENSG00000138092	-1.79	1.17E-06
	<i>MAD2L2</i>	ENSG00000116670	-1.76	1.50E-05
	<i>ATM</i>	ENSG00000149311	-1.76	2.04E-06
	<i>PLK2</i>	ENSG00000145632	-1.75	5.31E-07
	<i>CDK2AP1</i>	ENSG00000111328	-1.74	2.03E-08
	<i>RFC3</i>	ENSG00000133119	-1.74	6.95E-07
	<i>SKA2</i>	ENSG00000182628	-1.71	6.76E-06
	<i>ANAPC2</i>	ENSG00000176248	-1.69	6.74E-06
	<i>RTF2</i>	ENSG00000022277	-1.66	1.24E-05
	<i>CENPC</i>	ENSG00000145241	-1.66	9.53E-06
	<i>ERICD</i>	ENSG00000280303	-1.65	0.0314
	<i>SUGT1</i>	ENSG00000165416	-1.64	8.44E-06
	<i>GSPT2</i>	ENSG00000189369	-1.64	7.33E-05
	<i>ANAPC4</i>	ENSG00000053900	-1.64	1.28E-05
	<i>ESCO1</i>	ENSG00000141446	-1.63	3.03E-05
	<i>AC125232.1</i>	ENSG00000231259	-1.62	2.45E-04
	<i>ANAPC16</i>	ENSG00000166295	-1.60	1.59E-05
	<i>EAPP</i>	ENSG00000129518	-1.60	6.02E-05
	<i>DSCC1</i>	ENSG00000136982	-1.60	7.06E-05
	<i>ANAPC11</i>	ENSG00000141552	-1.59	1.28E-05
	<i>CENPL</i>	ENSG00000120334	-1.58	2.89E-05
	<i>BARD1</i>	ENSG00000138376	-1.58	5.25E-06
	<i>E2F3</i>	ENSG00000112242	-1.56	8.86E-07
	<i>PDS5B</i>	ENSG00000083642	-1.55	6.76E-06
	<i>CDK7</i>	ENSG00000134058	-1.55	7.33E-05
	<i>MZT2A</i>	ENSG00000173272	-1.55	2.33E-05
	<i>BRAT1</i>	ENSG00000106009	-1.53	4.64E-06
	<i>SPC25</i>	ENSG00000152253	-1.46	1.59E-05
	<i>SKP1</i>	ENSG00000113558	-1.45	5.73E-05
	<i>GAK</i>	ENSG00000178950	-1.43	2.28E-05
	<i>CCNB1IP1</i>	ENSG00000100814	-1.38	0.000220
	<i>MTBP</i>	ENSG00000172167	-1.33	0.000510
	<i>CSPP1</i>	ENSG00000104218	-1.33	0.000210
	<i>SFRP1</i>	ENSG00000104332	-1.33	0.0000700
	<i>NSL1</i>	ENSG00000117697	-1.33	0.000230
	<i>G2E3</i>	ENSG00000092140	-1.32	0.000370
	<i>NIPBL</i>	ENSG00000164190	-1.31	0.0000700
	<i>SWI5</i>	ENSG00000175854	-1.28	0.00118
	<i>CDKN2C</i>	ENSG00000123080	-1.26	0.00223
	<i>INCA1</i>	ENSG00000196388	-1.25	0.00493
	<i>NUMA1</i>	ENSG00000137497	-1.19	0.000210
	<i>SPICE1</i>	ENSG00000163611	-1.14	0.00450
	<i>BRIP1</i>	ENSG00000136492	-1.05	0.00359
	<i>CDK6</i>	ENSG00000105810	-1.00	0.00190
	<i>CTC1</i>	ENSG00000178971	-0.97	0.00855
	<i>CENPI</i>	ENSG00000102384	-0.97	0.00792
	<i>MOB1B</i>	ENSG00000173542	-0.89	0.0101
	<i>NPDC1</i>	ENSG00000107281	-0.88	0.0318
	<i>MAD1L1</i>	ENSG00000002822	-0.81	0.0148
	<i>BTG4</i>	ENSG00000137707	0.91	0.0268
	<i>SAMSN1</i>	ENSG00000155307	1.21	0.00212
	<i>RAD21L1</i>	ENSG00000244588	1.29	0.0264

Category	Gene symbol	Gene ID	Fold change	q-value
	<i>CCNA1</i>	ENSG00000133101	1.46	0.0448
	<i>AC092651.1</i>	ENSG00000230395	5.02	0.00570
Other	<i>SNCA</i>	ENSG00000145335	1.27	0.00360
	<i>LRRK2</i>	ENSG00000188906	1.30	0.000569

Supplementary Table 1: Extended list of differentially expressed genes of hVM1 clone 32 cells in proliferation and differentiation conditions. In blue, genes upregulated in division, and in red, genes upregulated in differentiation.

APPENDIX II